

THE ROLE OF NUCLEAR FACTOR-KAPPA B (NF- $\kappa$ B) IN THE REGULATION  
OF LUNG INFLAMMATION

By

Michael Brett Everhart

Dissertation

Submitted to the Faculty of the  
Graduate School of Vanderbilt University  
in partial fulfillment of the requirements  
for the degree of

DOCTOR OF PHILOSOPHY

in

Cell and Developmental Biology

December, 2004

Nashville, Tennessee

Approved:

Professor Timothy S. Blackwell

Professor Lynn M. Matrisian

Professor Ann W. Richmond

Professor Virginia L. Shepherd

Professor Jin Chen

To Aubrey

## ACKNOWLEDGEMENTS

I owe a tremendous debt of gratitude to all those who supported me through my time at Vanderbilt. I would like to thank Tim Blackwell for providing an avenue for me to continue my graduate career. I hope you enjoyed being my mentor as much as I enjoyed being your first Graduate Student. You have been a constant source of support both scientifically and personally. I have learned much from you and will always be grateful for my experiences in your lab.

I would like to thank all of those who have helped me to achieve my goals. Everyone in the Blackwell Laboratory.....Ornella Zioa, Wei Han, Dong-Sheng Cheng, William Lawson, Vasily Polosukhin, George Stathopoulos. These are the people that had to listen to everything from “where is the....” to “how do you”. Sometimes it is the small things that mean so much. I would like to thank Kirk Lane and Tom Blackwell for the many discussions both scientific and political. I must also thank Fiona Yull and the members of her laboratory, Bo Li, Taylor Sherrill, Melissa Arutiunov, for their unending work in the mouse facility. I would also like to thank John Christman and Ruxana Sadikot for their support. I would also like to extend my thanks to everyone in the Division of Allergy, Pulmonary, and Critical Care Medicine for taking me in and making me feel at home.

I would like to thank each of my committee members, Dr. Lynn Matrisian, Dr. Ann Richmond, Dr. Virginia Shepherd, and Dr. Jin Chen for their constant encouragement and support. I would especially like to thank Lynn for being there during the most difficult times.

I would not be where I am today without my parents and my brother. Thank you mom and dad for providing an environment which enabled me to think, learn, laugh, and love. Thank you Todd for being a role model and source of inspiration.

Most of all, I would like to thank my best friend and partner Aubrey. You are a constant source of love and support. I will be eternally grateful for your patience and sacrifice. Thank you for making this a wonderful stage of our lives. I look forward to the next. Also, I would like to thank my children, Tanner, Shadow, Satchel, and Phoenix. Aubrey, thank you for reminding me what is truly important in this world.

## TABLE OF CONTENTS

	Page
DEDICATION.....	ii
ACKNOWLEDGEMENTS.....	iii
LIST OF TABLES.....	viii
LIST OF FIGURES.....	ix
LIST OF ABBREVIATIONS.....	xii

### Chapter

#### I. INTRODUCTION

Nuclear Factor-kappa B (NF- $\kappa$ B) Transcription Factor Family.....	1
NF- $\kappa$ B Dependent Gene Regulation.....	5
The Biology of NF- $\kappa$ B.....	7
NF- $\kappa$ B in Innate Immunity.....	8
Role of Macrophages in NF- $\kappa$ B Dependent Lung Inflammation.....	11
Detection Methods of NF- $\kappa$ B Activation <i>In vivo</i> .....	12
HLL Transgenic Reporter Mouse Model.....	12
Bioluminescence Imaging.....	15

#### II. MATERIALS AND METHODS

Animals.....	19
Bioluminescence.....	19
Bone Marrow Derived Macrophages.....	20
Cell Culture and Cell Lines.....	20
Co-culture.....	21
Extraction of Cytoplasmic and Nuclear Proteins.....	21
Fetal Liver Transplantation.....	22
Fluorescence Activated Cell Sorting.....	23
Histology and Immunohistochemistry.....	24
Lipopolysaccharide Administration.....	25
Liposomal Clodronate.....	26
Luciferase Assay.....	26
Microscopy.....	27
Neutrophil Quantification.....	27
<i>Pseudomonas aeruginosa</i> Administration.....	27

<i>Pseudomonas aeruginosa</i> Lung Colony Counts.....	28
Statistical Analysis.....	28
Transfection.....	28
Western Blots.....	29

### III. RESULTS

#### GENERATION OF NF- $\kappa$ B TRANSGENIC REPORTER MOUSE MODEL

Introduction.....	31
Results	
NGL Construct Design.....	33
<i>In vitro</i> Detection of NF- $\kappa$ B Activity by Luciferase Assay and GFP Fluorescence Microscopy.....	34
NF- $\kappa$ B Transgenic Reporter Mouse Generation .....	35
GFP/Luciferase Protein Half-life.....	37
LPS Model of Lung Inflammation	
Intraperitoneal Administration of LPS.....	38
Administration of LPS by Intraperitoneal Osmotic Pump.....	41
Intratracheal Administration of LPS.....	44
<i>Pseudomonas aeruginosa</i> Model of Lung Inflammation.....	47
Detection of Lung NF- $\kappa$ B Activity by <i>Ex vivo</i> GFP Fluorescence Imaging.....	49
Detection of NF- $\kappa$ B Activity in Bronchoalveolar Lavage Cells FACS after IT LPS.....	50
Summary.....	52
Future Directions.....	53

#### KINETICS OF ALVEOLAR MACROPHAGE REPOPULATION FOLLOWING FETAL LIVER TRANSPLANTATION

Introduction.....	54
Results	
Kinetics of Peripheral Blood Monocyte Reconstitution.....	56
Fixation Affects the Detection of GFP by Fluorescence Microscopy And Immunohistochemistry.....	59

Identification of Donor Macrophages in the Lung by Fluorescence Microscopy.....	61
Quantification of Donor Alveolar Macrophage Repopulation in the Lung by Immunohistochemistry and Tissue Cell Counts.....	62
Quantification of Donor Alveolar Macrophage Repopulation in the Lung by Brochoalveolar Lavage Macrophage FACS Analysis.....	63
Investigation of Alveolar Macrophage Function in FLT Chimeras.....	65
Summary.....	66

## ROLE OF ALVEOLAR MACROPHAGE $\text{I}\kappa\text{B-}\alpha$ AND p50 IN THE REGULATION OF LUNG INFLAMMATION

Introduction.....	69
Results	
Generation of Fetal Liver Transplant Chimeras.....	72
Wild-type FLT Chimeras.....	72
$\text{I}\kappa\text{B-}\alpha^{-/+}$ FLT Chimeras.....	74
$\text{I}\kappa\text{B-}\alpha^{-/-}$ FLT Chimeras.....	77
p50 <sup>-/-</sup> FLT Chimeras.....	80
Bioluminescence Correlates with Tissue Luciferase Activity.....	81
NF- $\kappa$ B Regulation in $\text{I}\kappa\text{B-}\alpha^{-/+}$ and p50 <sup>-/-</sup> Bone Marrow Derived Macrophages.....	82
NF- $\kappa$ B in Macrophage/Epithelium Communication.....	85
Summary.....	86
Future Directions.....	89
IV: Discussion.....	90
Appendix	
A. Publications.....	97
REFERENCES.....	98

## LIST OF TABLES

Table	Page
1. Pro-inflammatory Molecules Regulated by NF- $\kappa$ B.....	5

## LIST OF FIGURES

Figure	Page
1. Diagram of Rel and I $\kappa$ B Family Members.....	2
2. NF- $\kappa$ B Signal Transduction Pathway.....	4
3. Diagram of HLL Reporter Construct.....	13
4. Luciferase Activity in Organs of HLL Mice After IP and Inhaled LPS.....	14
5. Bioluminescence Imaging.....	16
6. Bioluminescence Detection of Luciferase Activity in HLL Mouse after IP LPS.....	17
7. Bioluminescence Imaging of HLL Mice after IP and Inhaled LPS.....	18
8. Diagram of NGL Reporter Construct.....	33
9. Detection of NGL reporter constructs in RAW 267.4 Cells.....	34
10. <i>In vitro</i> Detection of NF- $\kappa$ B Activity in A549 Cells by Fluorescence Microscopy and Luciferase Assay.....	36
11. GFP/Luciferase Protein Half-life in NGL Bone Marrow Derived Macrophages.....	37
12. Bioluminescence Imaging of NGL Mice after IP LPS.....	39
13. Quantification of Photon Counts from NGL Mice after IP, IT, and IP Pump LPS.....	40
14. GFP Immunohistochemistry and H&E Histology of NGL Mice after IP LPS.....	41
15. Quantification of Lung Neutrophils in Tissue Sections.....	42
16. Bioluminescence Imaging of NGL Mice after IP Pump LPS.....	43
17. GFP Immunohistochemistry and H&E Histology of NGL Mice after IP Pump LPS....	44
18. Bioluminescence Imaging of NGL Mice after IT LPS.....	45
19. GFP Immunohistochemistry and H&E Histology of NGL Mice after IT LPS.....	46
20. Bioluminescence Imaging of NGL Mice after IT <i>Pseudomonas aeruginosa</i> .....	47

21. GFP Immunohistochemistry and H&E Histology of NGL Mice after IT <i>Pseudomonas aeruginosa</i> .....	48
22. <i>Ex vivo</i> Detection of GFP Fluorescence from lungs of NGL Mice after IP and IP Pump LPS.....	49
23. Quantification of <i>Ex vivo</i> GFP Fluorescence Photon Counts from NGL Mice after IP and IP Pump LPS.....	50
24. Detection of GFP+ Bronchoalveolar Cells by FACS from NGL Mice after IT LPS.....	51
25. FACS Analysis of Peripheral Blood Cells from Nagy GFP Transgenic Mice.....	57
26. Kinetics of Peripheral Blood Monocyte Reconstitution Following Fetal Liver Transplantation.....	58
27. Affects of Fixation on Detection of GFP by Fluorescence Microscopy.....	59
28. Affects of Fixation on Detection of GFP by Immunohistochemistry.....	60
29. Detection of Donor Macrophages in the Lung by GFP Fluorescence.....	61
30. Detection of Macrophages and Donors Cells in the Lung by CD68 and GFP Immunohistochemistry.....	62
31. Quantification of Total Lung and GFP+ Macrophages by Tissue Cell Counts.....	64
32. Quantification of GFP+ Alveolar Macrophages in Lung Lavage by FACS.....	65
33. Detection of <i>Pseudomonas aeruginosa</i> Clearance in WT and Nagy GFP FLT Chimeras.....	66
34. Bioluminescence Imaging of WT FLT Chimeras.....	73
35. Quantification of Photon Counts in FLT Chimeras.....	74
36. Detection of Lung Inflammation by Histology in WT FLT Chimeras.....	75
37. Quantification of Lung Neutrophils in Tissue Sections.....	75
38. Bioluminescence Imaging of $\text{I}\kappa\text{B-}\alpha^{-/+}$ FLT Chimeras.....	76
39. Detection of Lung Inflammation by Histology in $\text{I}\kappa\text{B-}\alpha^{-/+}$ FLT Chimeras.....	77
40. Bioluminescence Imaging of $\text{I}\kappa\text{B-}\alpha^{-/-}$ FLT Chimeras.....	78

41. Detection of Lung Inflammation by Histology in $\text{I}\kappa\text{B-}\alpha^{-/-}$ FLT Chimeras.....	79
42. Bioluminescence Imaging of $\text{p50}^{-/-}$ FLT Chimeras.....	79
43. Detection of Lung Inflammation by Histology in $\text{p50}^{-/-}$ FLT Chimeras.....	80
44. $\text{p50}^{-/-}$ FLT Chimera Mortality after IP LPS.....	81
45. Detection of Luciferase Activity from WT and $\text{I}\kappa\text{B-}\alpha^{-/+}$ FLT Lungs after IT LPS.....	82
46. Detection of Cytoplasmic $\text{I}\kappa\text{B-}\alpha$ and Nuclear RelA Protein by Western Blot in WT and $\text{I}\kappa\text{B-}\alpha^{-/+}$ BMDM $\Phi$ after LPS.....	83
47. Detection of Cytoplasmic $\text{I}\kappa\text{B-}\alpha$ Protein by Western Blot in WT and $\text{p50}^{-/-}$ BMDM $\Phi$ after LPS.....	84
48. The Role of NF- $\kappa\text{B}$ in Macrophage/Epithelium Communication Using a Co-Culture System.....	85
49. Diagram of the Proposed Role of NF- $\kappa\text{B}$ in the Regulation of Lung Inflammation.....	95

## LIST OF ABBREVIATIONS

NF- $\kappa$ B	Nuclear factor-kappa B
LPS	Lipopolysaccharide
IT	Intratracheal
IP	Intraperitoneal
BMDM $\Phi$	Bone marrow derived macrophage
I $\kappa$ B	Inhibitor of kappa B
IKK	I $\kappa$ B kinase
FLT	Fetal liver transplantation
FACS	Fluorescence activated cell sorting
GFP	Green fluorescent protein
Luc	Luciferase
TNF	Tumor necrosis factor
DOPC	Egg-phosphatidylcholine
PCR	Polymerase chain reaction
DAB	3,3'-diaminobenzidine tetrahydrochloride
cDNA	Complementary DNA
HIV-LTR	Human Immunodeficiency Virus-Long Terminal Repeat
HLL	HIV-LTR Luciferase
IL-1	Interleukin 1
EDTA	Ethylenediaminetetraacetic acid
PMSF	Phenylmethylsulfonyl fluoride

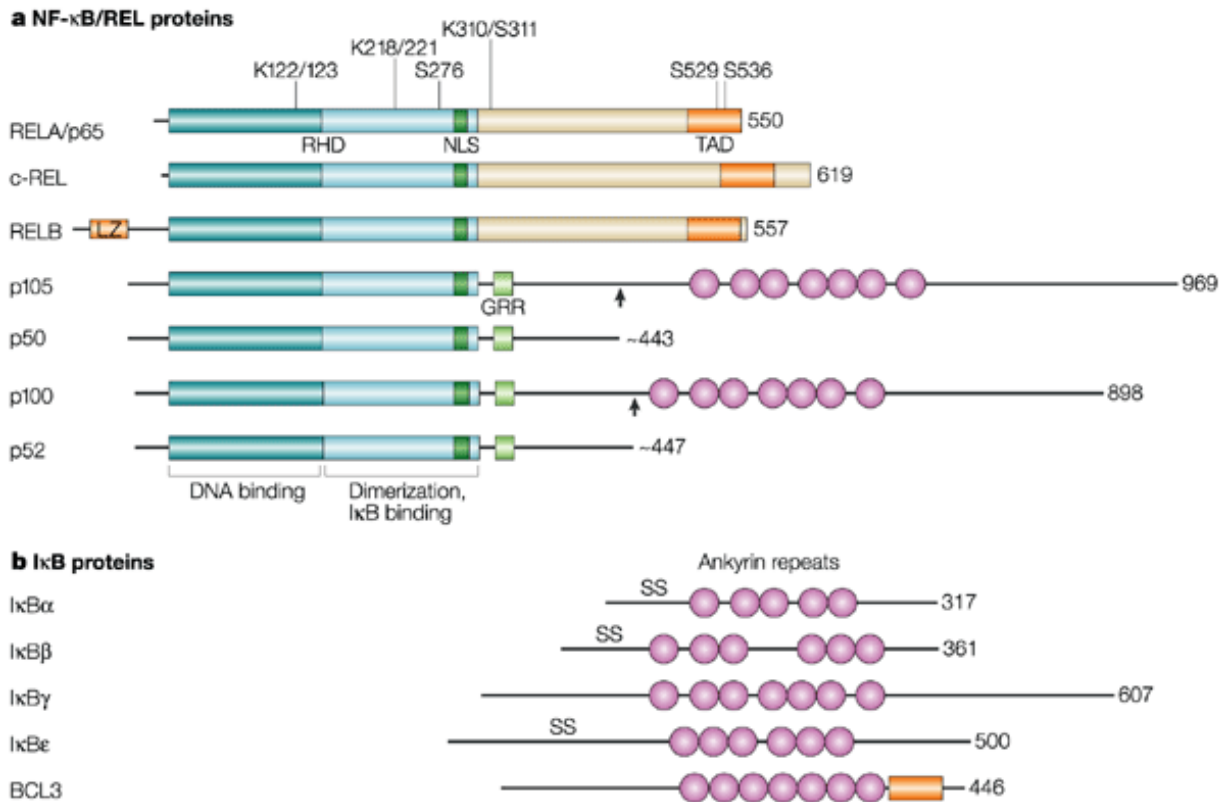
PBS	Phosphate buffered saline
kDa	Kilodalton
M	Molar
SDS-PAGE	Sodium dodecylsulfate polyacrylamide gel electrophoresis
RHD	Rel homology domain
NGL	<u>N</u> F- $\kappa$ B/ <u>G</u> reen fluorescent protein/ <u>L</u> uciferase

## CHAPTER I

### INTRODUCTION

#### **Nuclear Factor-kappa B (NF- $\kappa$ B) Transcription Factor Family**

NF- $\kappa$ B was first identified as a DNA binding activity in the immunoglobulin  $\kappa$  light chain gene major (J-C) intron transcriptional enhancer (Sen, 1986). It was quickly realized that NF- $\kappa$ B was not restricted to B cells, but was ubiquitously expressed in virtually all cell types. The NF- $\kappa$ B transcription factor family is comprised of five members in vertebrate animals: p65/RelA, c-Rel, RelB, NF- $\kappa$ B1 (p50), and NF- $\kappa$ B2 (p52) (Figure 1). The hallmark of the NF- $\kappa$ B family is a conserved 300 amino acid Rel homology domain (RHD) within the amino terminus. The RHD contains the DNA-binding domain, dimerization domain, and nuclear localization sequence (NLS). RelA, RelB, and c-Rel contain a strong transcriptional transactivation domain (TAD) in the carboxy terminus. The TAD coordinates interaction with the basal transcription apparatus, including the TATA-binding protein (TBP), transcription factor IIB, and the p300 and cyclic-AMP-response element (CREB)-binding protein (CBP) co-activators (Blair, 1994; Schmitz, 1995). While p50 and p52 proteins are capable of binding DNA, they are incapable of directly activating transcription for lack of a TAD. Instead, p50 and p52 homodimers can function as transcriptional repressors (Ghosh, 1998). The prototypical NF- $\kappa$ B complex is the RelA/p50 heterodimer. NF- $\kappa$ B activation is accomplished through the formation of multiple combinations of NF- $\kappa$ B homodimers and heterodimers which activate



Chen, L., Greene, W. C. (2004). Shaping the nuclear action of NF- $\kappa$ B. *Nature Review Cell and Molecular Biology*, 5, 392-401.

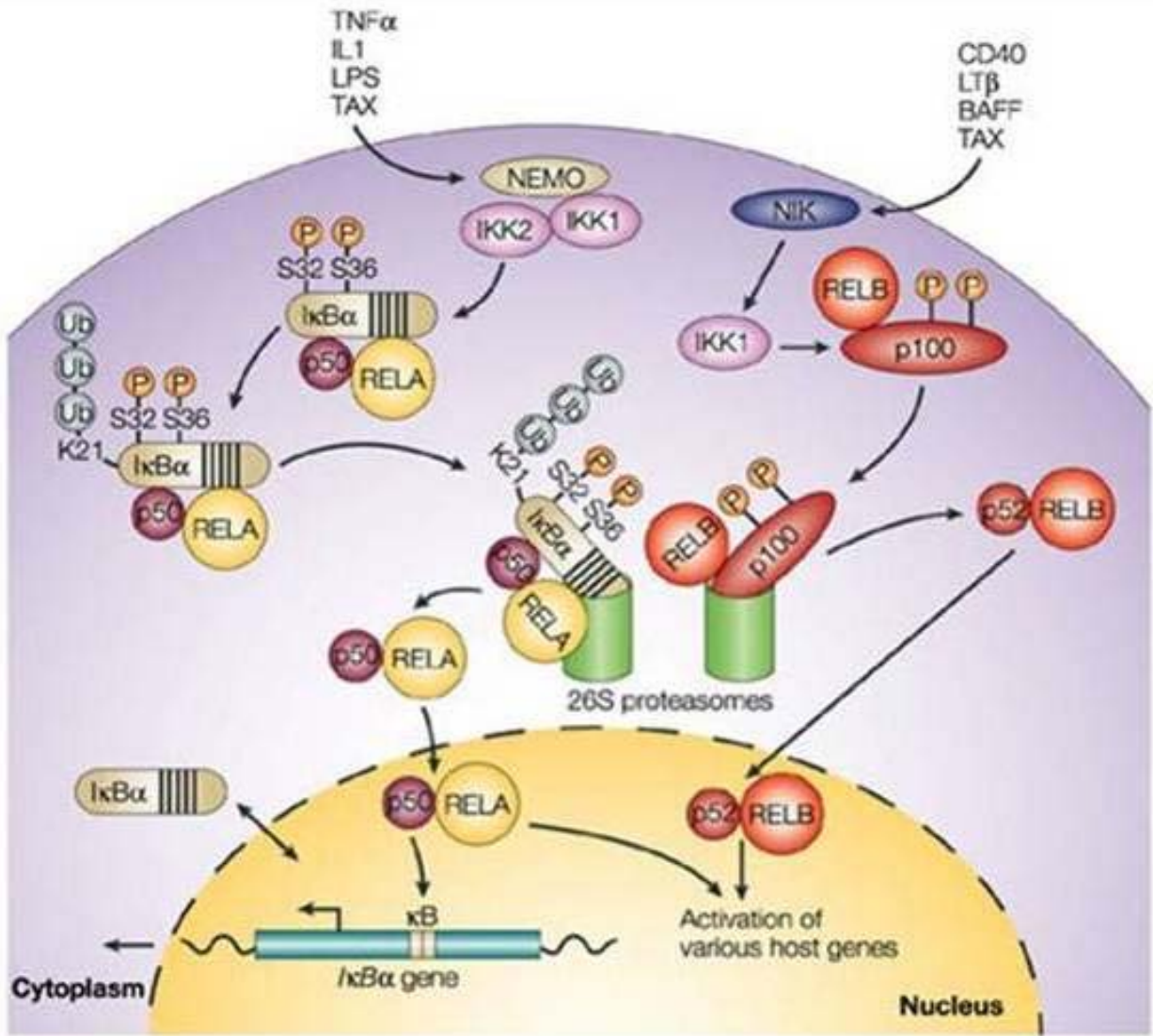
Nature Reviews | Molecular Cell Biology

**Figure 1**

gene transcription by binding to consensus  $\kappa$ B sequences in the promoter elements of NF- $\kappa$ B-regulated genes.

Inhibitors of NF- $\kappa$ B (I $\kappa$ B) were first described as cytoplasmic proteins that inhibit activity of the heterodimeric NF- $\kappa$ B complex (Sen, 1986). The I $\kappa$ Bs are encoded by a small multigene family that currently includes I $\kappa$ B- $\alpha$ , I $\kappa$ B- $\beta$ , I $\kappa$ B- $\epsilon$ , I $\kappa$ B $\gamma$ , and BCL3 (Ghosh, 1998; Verma, 1995). I $\kappa$ Bs are characterized by the presence of five to seven ankyrin motifs which regulate interaction with Rel proteins. Differential sequestration of NF- $\kappa$ B in the cytoplasm has

been described for I $\kappa$ B- $\alpha$  and I $\kappa$ B- $\beta$ . I $\kappa$ B- $\alpha$  masks only one of the nuclear localization signals of an NF- $\kappa$ B dimer and relies on a nuclear export signal to maintain cytoplasmic localization of the complex, allowing shuttling of NF- $\kappa$ B out of the nucleus (Huang, 2000; Malek, 2001). The rapid re-synthesis of I $\kappa$ B- $\alpha$  after NF- $\kappa$ B activation aids in the de-activation of NF- $\kappa$ B through cytoplasmic shuttling of NF- $\kappa$ B dimers (Huang, 2000; Turpin, 1999). I $\kappa$ B- $\beta$ , on the other hand, masks nuclear localization sequences on both NF- $\kappa$ B subunits, inhibiting nuclear import (Malek, 2001). The p50 and p52 NF- $\kappa$ B protein precursors, p105 and p100, also contain ankyrin repeats and can function as inhibitors (Ghosh, 1998). Following cell stimulation, I $\kappa$ Bs are phosphorylated on serine residues in the amino-terminus, targeting them for degradation by the ubiquitin/26S proteasome pathway, thus allowing NF- $\kappa$ B dimers to translocate to the nucleus (Figure 2). The protein kinases that mediate I $\kappa$ B phosphorylation have been identified and are referred to as I $\kappa$ B kinase 1 (IKK1) and I $\kappa$ B kinase 2 (IKK2) (Didonato, 1997; Mercurio, 1997; Regnier, 1997). These kinases exist in a high molecular weight complex with a structural regulatory subunit called IKK $\gamma$ /NEMO (Rothwarf, 1998; Zandi, 1997). Activation of the IKK complex by factors such as TNF $\alpha$  and IL-1, results in phosphorylation of serine residues within the activation loop of IKK1 and IKK2. The activated IKK complex then phosphorylates the I $\kappa$ B proteins on serines 32 and 36 for I $\kappa$ B- $\alpha$  and serines 19 and 23 for I $\kappa$ B- $\beta$ . Phosphorylation of these residues leads to the binding of the  $\beta$ -TrCP-SCF complex, resulting in polyubiquitination of I $\kappa$ B and subsequent degradation by the 26S proteasome (Karin, 2000). Destruction of the I $\kappa$ B enables for the nuclear translocation of the NF- $\kappa$ B dimers. NF- $\kappa$ B binds to decameric enhancer motifs found in the promoters and introns of a variety of genes, including the immunoglobulin  $\kappa$



Chen, L., Greene, W. C. (2004). Shaping the nuclear action of NF- $\kappa$ B. *Nature Review Cell and Molecular Biology*, 5, 392-401.

Figure 2

light chain, the human immunodeficiency virus long terminal repeat, numerous cytokines, chemokines, adhesion molecules, enzymes, and receptors (Fan, 2001; Ghosh, 1998; Siebenlist, 1994; Verma, 1995) (Table 1).

**Table I**

Pro-inflammatory Molecules Regulated by NF- $\kappa$ B

<u>Tumor Necrosis Factor</u>		<u>Colony Stimulating Factors</u>
TNF- $\alpha$		G-CSF
TNF- $\beta$		GM-CSF
<u>Interleukins</u>		<u>Interferons</u>
IL-1 $\beta$		IFN- $\beta$
IL-2		
IL-6		<u>Adhesion Molecules</u>
IL-12		ICAM-1
		E-selectin
		V-CAM
<u>Chemokines</u>		<u>Enzymes</u>
IL-8	Rantes	COX-2
Gro $\alpha$ , $\beta$ , $\gamma$	CINC	Manganese superoxide dismutase
MIP-1	KC	Inducible nitric oxide synthase
MCP-1/JE	MIP-2	

**NF- $\kappa$ B-Dependent Gene Regulation**

The role of NF- $\kappa$ B in the differential regulation of NF- $\kappa$ B-linked genes involves both gene- and cell-specific factors. Recent evidence suggests that NF- $\kappa$ B may regulate distinct sets of genes in particular cell types based on the type and duration of the stimulus. For example, in the murine cell line RAW 267.4, LPS treatment induces NF- $\kappa$ B binding to MIP-2 and MnSOD promoters within 20 minutes, but binding to the IL-6 promoter occurs much later (150 minutes) (Saccini, 2001). These differences in NF- $\kappa$ B promoter binding correlated with mRNA

expression of these genes. In addition to type and duration of stimulus, cell differentiation may influence the types of NF- $\kappa$ B linked cytokines produced. For example, different patterns of NF- $\kappa$ B linked cytokines were expressed in response to LPS treatment from dendritic cells and macrophages derived from the same monocyte precursors (Baltathakis, 2001).

The availability of other transcription factors (AP-1, CREB, C/EBP $\beta$ , STATs) in the microenvironment of specific gene promoters has been shown to influence the profile of NF- $\kappa$ B linked genes expressed following NF- $\kappa$ B nuclear translocation. However, the common denominator of transcriptional activation may lie in the ability to recruit co-activator proteins, which functions to: 1) interface with the basal transcriptional machinery; 2) maintain chromatin in an “open” configuration by directing the acetylation of histones; and 3) stabilize NF- $\kappa$ B interactions with the promoter through modification of RelA (Ashburner, 2001; Chan, 2001; Chen, 2001; Gerritsen, 1997; McManus, 2001; Sheppard, 1999; Vanden Berghe, 1999; Wadgaonkar, 1999). The interaction of NF- $\kappa$ B with CREB-binding protein (CBP) and its functional homolog p300 has been shown to be critical for transcriptional activity (Sheppard, 1999). This interaction maintains chromatin in an “open” configuration through acetyltransferase activity incorporated in p300/CBP or p300/CBP associated factor (p/CAF) (Berger, 1999; Chan, 2001; McManus, 2001). Additional mechanisms of transcriptional regulation include modulation of RelA by phosphorylation or acetylation. Phosphorylation of serine 276 by protein kinase A enhances the ability of RelA to interact with CBP (Zhong, 1998). Phosphorylation of serine 529 in the transactivation domain increases transcriptional activity (Wang, 1998). Also, CBP and p300 acetylate RelA making it inaccessible to I $\kappa$ B- $\alpha$  binding and therefore resistant to inactivation by nuclear-cytoplasmic shuttling (Chen, 2001).

Histone deacetylases (HDACs) appear to function as a counterbalance in the regulation of transcriptional activity of NF- $\kappa$ B. For example, inhibition of class 1 histone deacetylases (HDAC1-3) can prolong and enhance NF- $\kappa$ B transcriptional activity in cultured cells (Ashburner, 2001; Chen, 2001). These data suggest the balance of acetylation:deacetylation at specific promoters can determine transcriptional activity.

The data presented above supports a model of differential NF- $\kappa$ B linked gene expression by intranuclear regulation of NF- $\kappa$ B function through interactions with co-activators and co-repressors. Intranuclear regulation of NF- $\kappa$ B appears to play an important role in defining the cellular phenotype after NF- $\kappa$ B activation.

### **The Biology of NF- $\kappa$ B**

NF- $\kappa$ B activation has been shown to play a critical role in a variety of biological processes. NF- $\kappa$ B is rapidly activated by a wide range of chemically diverse agents and cellular stress conditions, such as lipopolysaccharide (LPS), microbial and viral pathogens, cytokines, and growth factors (Baeuerle, 1996). NF- $\kappa$ B also serves to protect against apoptosis and regulate cell-cycle progression (Foo, 1999). Activation of NF- $\kappa$ B has been reported at sites of inflammation in diverse diseases such as rheumatoid arthritis, inflammatory bowel disease, multiple sclerosis, psoriasis, and asthma. NF- $\kappa$ B has also been shown to play a role in the initiation and maintenance of the oncogenic phenotype (Baldwin, 2001; Haefner, 2002). NF- $\kappa$ B has been studied extensively in innate and adaptive immunity. Mice that lack individual NF- $\kappa$ B proteins demonstrate defects in B- and T-cell proliferation, activation, cytokine production, and isotype switching (Gerondakis, 1998). B-cell defects involving NF- $\kappa$ B include lack of

immunoglobulin class switching, lack of germinal centers, and disruption of splenic micro-architecture. For example, mice deficient in NF- $\kappa$ B1 and NF- $\kappa$ B2 do not produce mature B-cells (Franzoso, 1997). In innate immunity, the importance of NF- $\kappa$ B is reflected by the many NF- $\kappa$ B dependent genes involved in defining the innate immune response (Table 1). The role of NF- $\kappa$ B in the regulation of innate immunity is the focus of this work and will be discussed in more detail below.

### **NF- $\kappa$ B in Innate Immunity**

The NF- $\kappa$ B pathway plays key roles in both adaptive immunity and innate (non-lymphocyte-mediated) immunity in the lungs and other organs. Since many noxious and inflammatory stimuli have been shown to activate NF- $\kappa$ B in the lungs, the NF- $\kappa$ B pathway appears to be a focal point for induction of lung inflammation. *In vivo* activators of NF- $\kappa$ B in the lungs include airway instillation of intact bacteria, LPS, ozone, and silica as well as systemic activators such as sepsis, hemorrhage, and direct liver injury (Blackwell, 1999a; Blackwell, 1999c; Browder, 1999; Haddad, 1996; Mizgerd, 2000; Shenkar, 1996). In addition to activators of NF- $\kappa$ B, the use of relatively non-specific inhibitors of NF- $\kappa$ B in several animal models has proven beneficial (Blackwell, 1996; Bohrer, 1997; Lauzurica, 1999).

Regulation of innate immunity in part is achieved through the recognition of specific patterns of microbial components, especially those of pathogens. A family of pattern recognition receptors has been described, called Toll-like receptors (TLR). To date, at least 10 Toll-like receptors have been described and recognize a variety of ligands (bacterial lipoproteins – TLR2, double stranded RNA – TLR3, lipopolysaccharide – TLR4, flagellin – TLR5 just to name a few). The first mammalian TLR identified (TLR4), was shown to cause induction of genes for several

inflammatory cytokines and costimulatory molecules when overexpressed (Medzhitov, 1997). Shortly after, TLR4 was shown to be involved in the recognition of lipopolysaccharide (LPS), a major component of Gram-negative bacteria. In support of this data, two mouse strains have been shown to be hypo-responsive to LPS (C3H/HeJ has a point mutation in the intracellular region of the *Tlr4* gene leading to the replacement of a conserved proline to histidine and C57BL10/ScCr has a null mutation in the *Tlr4* gene). These mice result in defects in TLR4-signaling and consequent suppression of the response to LPS (Poltorak, 1998). Recognition of LPS by TLR4 requires additional molecules. LPS-binding protein (LBP), present in the serum, binds LPS which is then recognized by CD14, a glycosylphosphatidylinositol-anchored molecule. Another protein, MD-2, was identified as a molecule that associates with the extracellular portion of TLR4 and enhances LPS responsiveness. Signaling for TLR4 has been shown to be homologous to that of the IL-1R family. Both TLR and IL-1R interact with an adaptor protein MyD88, which contains a Toll/IL-1 receptor (TIR) domain in its C-terminus and a death domain (DD) in its N-terminus. MyD88 associates with the receptor through TIR domain interaction. Upon stimulation, MyD88 recruits the serine/threonine kinase IL-1R-associated kinase (IRAK) via DD interaction. After IRAK phosphorylation, tumor necrosis factor receptor (TNFR)-associated factor (TRAF6) is recruited leading to activation of two distinct signaling pathways, JNK and NF- $\kappa$ B (Takeda, 2004). While MyD88 has been shown to be important for the production of inflammatory genes in response to LPS, a MyD88-independent pathway has also been described. TRIF (TICAM-1), a TIR-domain containing adaptor, can mediate activation of NF- $\kappa$ B in the absence of MyD88. Studies have shown that TRIF is required for early and late NF- $\kappa$ B responses and IRF-3 responses, but not JNK (Hayden, 2004). TLR4 has been identified in a variety of cell types. In addition to a host of inflammatory

cells (macrophage/monocytes, neutrophils, mast cells, lymphocytes, and dendritic cells), TLR4 expression has been identified in epithelium and epithelium (Iwasaki, 2004; Muir, 2004).

The role of the NF- $\kappa$ B pathway in proper immune system function is reflected in studies involving NF- $\kappa$ B and I $\kappa$ B knockout mice. RelA or IKK2 deficiency results in embryonic lethality secondary to liver apoptosis (Beg, 1995b). Liver apoptosis in RelA deficient mice appears to be TNF-mediated as demonstrated by the production of viable pups in RelA/TNF type I receptor double knockout mice (Alcama, 2001). Although the phenotype of liver apoptosis can be avoided in these mice, immune defects persist in continued susceptibility to infections and death only a few weeks after birth from pneumonia and bacteremia (Alcama, 2001). I $\kappa$ B- $\alpha$  deficient mice are apparently normal at birth, but die within 7-10 days (Beg, 1995a; 2000; Klement, 1996). Enhanced granulopoiesis, severe dermatitis, and increased TNF- $\alpha$  in the skin are present at the time of death. Not all known NF- $\kappa$ B dependent genes are upregulated in I $\kappa$ B- $\alpha$ -deficient cells, implicating additional transcriptional regulators in the activation of some NF- $\kappa$ B target genes. Also, changes in the nuclear levels of NF- $\kappa$ B are cell type dependent. For example, thymocytes and splenocytes exhibit increased nuclear RelA/p50 and p50 homodimers while NF- $\kappa$ B complexes in embryonic fibroblasts are unchanged. However, NF- $\kappa$ B activation in these fibroblasts results in prolonged nuclear localization of NF- $\kappa$ B, implicating I $\kappa$ B- $\alpha$  in the post-induction repression of NF- $\kappa$ B activity. Although p50-deficient mice develop normally and exhibit no histopathological changes, defects in B lymphocyte function and altered susceptibility to infection are observed (Sha, 1995). p50-deficient mice are more susceptible to *Listeria monocytogenes* and *Streptococcus pneumoniae*, respond normally to *Haemophilus influenzae*, and are more resistant to murine encephalomyocarditis virus.

## **Role of Macrophages in NF- $\kappa$ B-Dependent Lung Inflammation**

The relative contribution of specific cell types in the overall NF- $\kappa$ B dependent inflammatory response in the lungs is uncertain; however there is evidence that alveolar macrophages play a critical role in initiating lung inflammation. Early studies using a rat lung inflammation model of airway LPS administration demonstrated two distinct peaks of NF- $\kappa$ B activation (Blackwell, 1999b; Blackwell, 1999d). The initial peak was detected in alveolar macrophages obtained by lung lavage 15-30 minutes after LPS treatment and returned to baseline by 30-60 minutes. The second peak was detected in immigrating neutrophils and lung parenchyma 2-4 hours after LPS. The appearance of TNF- $\alpha$  and IL-1 $\beta$  RNA was detected at the same time as macrophage NF- $\kappa$ B activation, suggesting macrophages were the source of these cytokines.

An alternative approach to delineating the importance of alveolar macrophages in regulating lung inflammation is the selective elimination of macrophages by treatment with liposomal clodronate. Liposomal clodronate induces apoptosis in macrophages but not in other cell types (Broug-Holub, 1997; van Rooijen, 1994a). Lentsch et al. reported that NF- $\kappa$ B activation in lung tissue, cytokine gene expression, and neutrophilic influx were blocked by macrophage depletion in an immune complex model of lung inflammation (Lentsch, 1999). Our group has performed macrophage depletion studies by administering clodronate via intratracheal (IT) and/or intravenous (IV) routes, demonstrating 90% alveolar macrophage depletion 48 hours after treatment by IT + IV route (Koay, 2002). After aerosolized LPS challenge, neutrophilic alveolitis was attenuated by 80% in clodronate treated mice compared to empty liposome treated controls. Reduced neutrophil influx was associated with impaired activation of NF- $\kappa$ B in lung tissue, lower concentrations of TNF- $\alpha$  in lung lavage fluid, and decreased MIP-2 in lung

homogenate. Similarly in a systemic inflammatory model (IP injection of *E. coli* LPS), lung NF- $\kappa$ B activation and neutrophilic alveolitis were markedly reduced in clodronate treated mice. These studies suggest that early NF- $\kappa$ B activation in alveolar macrophages induces the production of pro-inflammatory mediators that promote the activation of NF- $\kappa$ B in other lung cell types and subsequent neutrophilic immigration.

### **Detection Methods for NF- $\kappa$ B Activation *In vivo***

Traditionally, *in vivo* NF- $\kappa$ B activation in mouse models has been elucidated using electrophoretic mobility shift assays (EMSA) or western blots. The fundamental nature of these methods leads to some important limitations. EMSA and western blots are semi-quantitative, evaluate NF- $\kappa$ B activation at a single time point, and do not specifically address the functional mechanism of gene transcription. In tissues, a dilution effect may obscure the ability to detect NF- $\kappa$ B activation if the signal originates in a cell population which represents a minority of the total organ.

### **HLL Transgenic Reporter Mouse Model**

To quantitatively evaluate NF- $\kappa$ B-dependent transcriptional activity over time and examine the consequences of NF- $\kappa$ B activation in multiple organs *in vivo*, a transgenic reporter mouse model was developed in which the *Photinus* luciferase cDNA is driven by the proximal 250 bases of the 5' human immunodeficiency virus (HIV-1) long terminal repeat (LTR) [referred to as HLL mice (HIV-LTR Luciferase)] (Figure 3). The HIV-LTR contains a TATA box, two NF- $\kappa$ B motifs between -82 and -103, and three Sp1 boxes between -46 and -78 (Kingman, 1996; Kretzschmar, 1992; Nabel, 1987). NF- $\kappa$ B activation has been shown to be absolutely required

for transcriptional regulation of the HIV-LTR in primary cell culture experiments (Alcami, 1995).

HLL mice have been used extensively in the Blackwell laboratory to evaluate the time- and dose-dependent, organ-specific pattern of luciferase expression as a surrogate marker for

## HLL HIV-LTR Luciferase

- Promoter – proximal 250 bases of the 5' human immunodeficiency virus (HIV-1) long terminal repeat (LTR) driving the expression of the *Photinus* luciferase cDNA

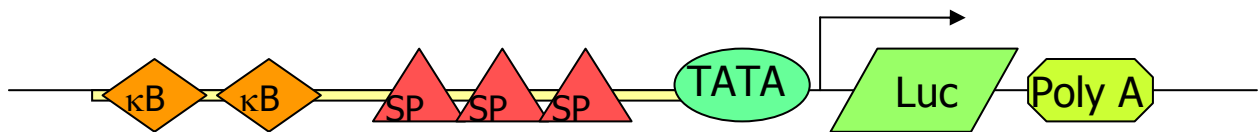


Figure 3

NF- $\kappa$ B activation in several models of lung and systemic inflammation. For example, in a model of systemic (single IP dose) *E. coli* LPS inflammation, NF- $\kappa$ B dependent gene transcription is transiently activated in multiple organs and different organs require different thresholds for NF- $\kappa$ B activation (Blackwell, 2000). The increased expression of mRNA for a variety of NF- $\kappa$ B regulated cytokines mirrored the induction of luciferase activity in lung tissue. Also, a close correlation between neutrophil chemoattractant chemokine KC and luciferase activity was detected in lung tissue homogenates. In addition to cytokine and chemokine production, neutrophil accumulation in alveolar spaces only occurred when NF- $\kappa$ B activation in the lung was achieved. These data support the mechanistic model that local NF- $\kappa$ B activation and production of pro-inflammatory mediators are required for coordinating neutrophil immigration.

The HLL mouse model has also been used to study the differential activation of NF- $\kappa$ B in various organs after either aerosolized or intraperitoneal LPS (Yull, 2003). Figure 4 demonstrates NF- $\kappa$ B- dependent luciferase activity (measured by tissue luciferase assay) in the major organs of the thorax (A) and abdomen (B) 4 hours after treatment with either aerosolized

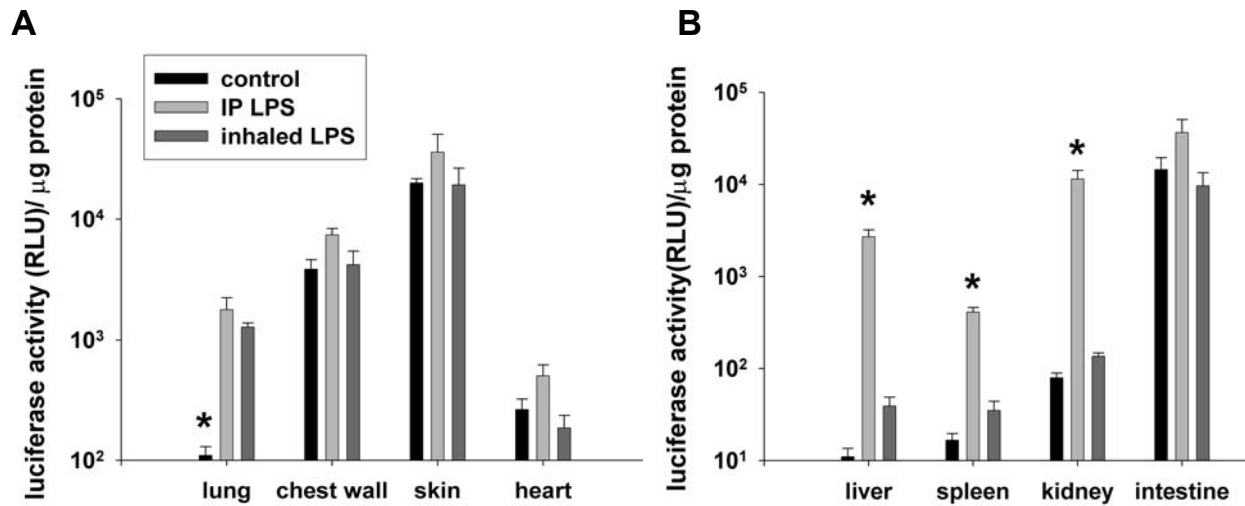


Figure 4: Luciferase activity in various organs of HLL mice at baseline (control) and after treatment with IP or inhaled LPS. NF- $\kappa$ B inducibility was achieved in the liver, spleen, and kidney after IP LPS. Only the lung displayed NF- $\kappa$ B inducibility after IP and inhaled LPS.  $P < 0.05$

or IP LPS. While chest wall and skin have substantially higher basal luciferase activity than lung, no induction is observed after LPS treatment. The lung, however, displays marked up-regulation of luciferase activity after both aerosolized and IP LPS challenge. In the abdomen, high basal levels of luciferase are observed in intestine, bladder, and peritoneum. Inducible luciferase activity is observed in liver, spleen, and kidney after IP LPS but not aerosolized LPS. Aerosolized LPS results in the induction of NF- $\kappa$ B luciferase activity in the lung specifically, whereas IP LPS results in the induction of NF- $\kappa$ B luciferase activity in multiple organs. These

data demonstrate the utility of these transgenic reporter mice in defining the pattern of NF- $\kappa$ B activation in response to specific stimuli and that inducible luciferase activity in the thorax after LPS challenge is localized to the lung.

### **Bioluminescence Imaging**

The process of bioluminescence is the emission of visible light from a living organism mediated by an enzyme-catalyzed reaction of molecular oxygen with a light-emitting substrate (Figure 5). A variety of bioluminescent systems have been identified in nature, each requiring a specific enzyme (luciferase) and substrate (luciferin), with the most recognizable system being from the American firefly *Photinus pyralis*. Bioluminescence imaging involves the expression of the luciferase enzyme *in vivo* as a molecular reporter. This technology has been utilized to monitor transgene expression (Benaron, 1997; Contag, 2000; Contag, 1997), infectious disease progression (Francis, 2000; Francis, 2001; Rocchetta, 2001), tumor growth and metastasis (Edinger, 2002; Rehemtulla, 2000), and transplantation (Koransky, 2001; Tang, 2003). Early experiments by Contag et al. demonstrated that light emission from *Photinus* luciferase generated in internal organs of a mouse was detectable from an external vantage point (Contag, 1995; Contag, 1996). In collaboration with Dr. Duco Jansen (Biomedical Engineering, Vanderbilt University), we have developed a methodology for bioluminescence imaging of HLL mice by measuring *Photinus* luciferase activity in intact, living mice. The bioluminescence apparatus consists of an intensified charged coupled device (ICCD) camera and computer software program that allows for visualization of bioluminescence by producing a pseudo-color image and quantification of photon counts over a standardized area of the mouse (Figure 5). The advantages of this technology over more tradition methods include the ability to use each mouse

as its own control and the ability to perform multiple measurements after treatment in each mouse.

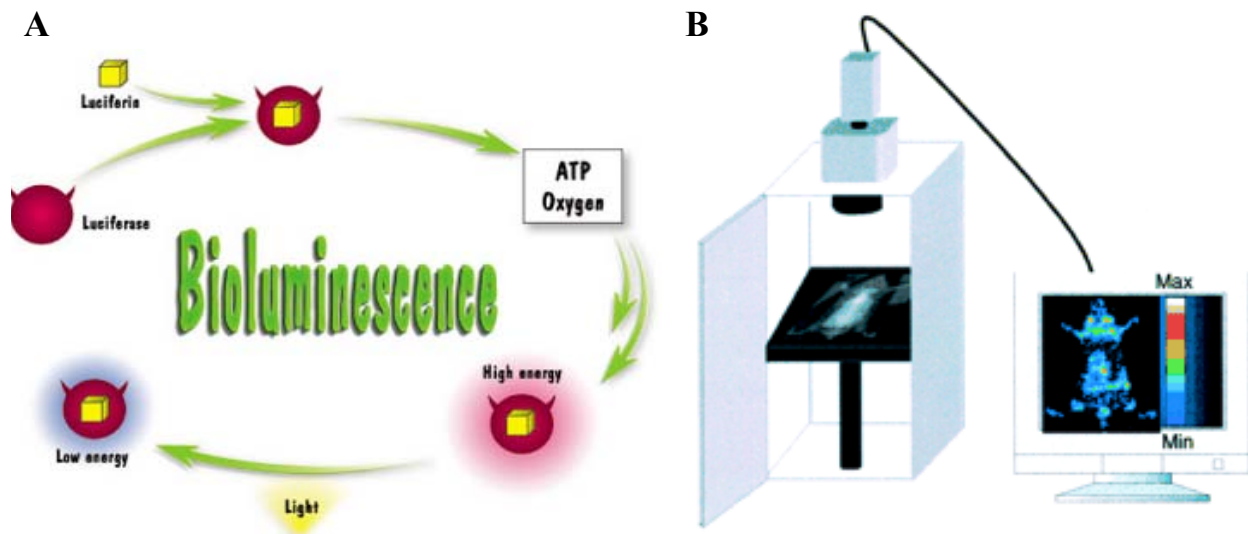


Figure 5: A) Bioluminescence is the emission of visible light from a living organism mediated by an enzyme-catalyzed reaction of molecular oxygen with a light-emitting substrate. B) The bioluminescence apparatus consists of an intensified charged coupled device (ICCD) camera and computer software program that allows for visualization of bioluminescence by producing a pseudo-color image and quantification of photon counts over a standardized area of the mouse.

In developing bioluminescence imaging in the HLL transgenic reporter mouse model, the kinetics of luciferin administration and the correlation of photon emission with tissue luciferase activity have been determined. Figure 6, shows the time course of LPS-induced luciferase activity in a single HLL mouse (Yull, 2003). After a single dose of 3  $\mu\text{g/g}$  IP LPS, basal bioluminescence was predominantly observed in the head and abdomen. Luciferase activity from the thorax increases to a peak between 4 and 8 hours after LPS, returning to baseline by 24 hours. To demonstrate that the inducible luciferase activity in the thorax originates from the

lung, skin flap excision experiments were performed after either inhaled or IP LPS (Figure 7A) (Yull, 2003). HLL mice were treated with aerosolized LPS (8 ml of a 1 mg/ml solution over 30 minutes) or IP LPS (3  $\mu$ g/g) and imaged after 4 hours. A skin flap excision was performed over

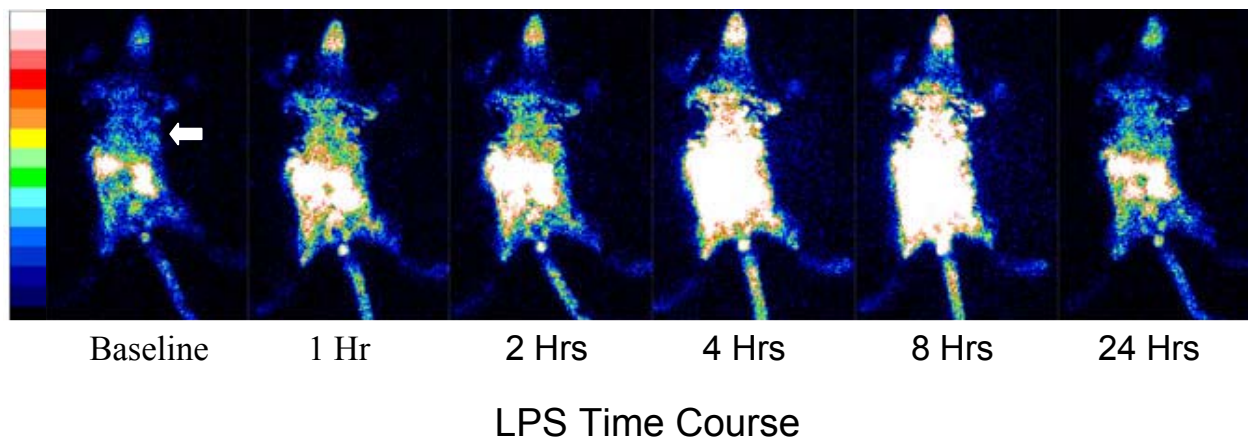


Figure 6: Bioluminescent detection of luciferase activity in HLL mice at baseline and 1, 2, 4, 8, 24 hours after IP LPS. Luciferin was given by IP injection 30 minutes prior to each image. Scale for pseudocolor image corresponding to photon detection is shown to left (white is highest emission). Arrow points to thorax.

the right lung and photon counts were recorded over the right (skin removed) and left (skin intact) lungs. Photon emission increased 4-fold over the left (skin intact) lung after IP and inhaled LPS (Figure 7B). When the skin was removed over the right lung, baseline photon emission was substantially reduced, suggesting high basal luciferase activity in the skin. The relative induction over the right lung (skin removed) was much greater (25-fold), implying the inducible luciferase activity was primarily from the lung. Taken together, these studies demonstrate the power of bioluminescence imaging for detection of NF- $\kappa$ B dependent gene expression in HLL reporter mice. This methodology allows for the quantification of lung NF- $\kappa$ B activity over time in intact, living mice.

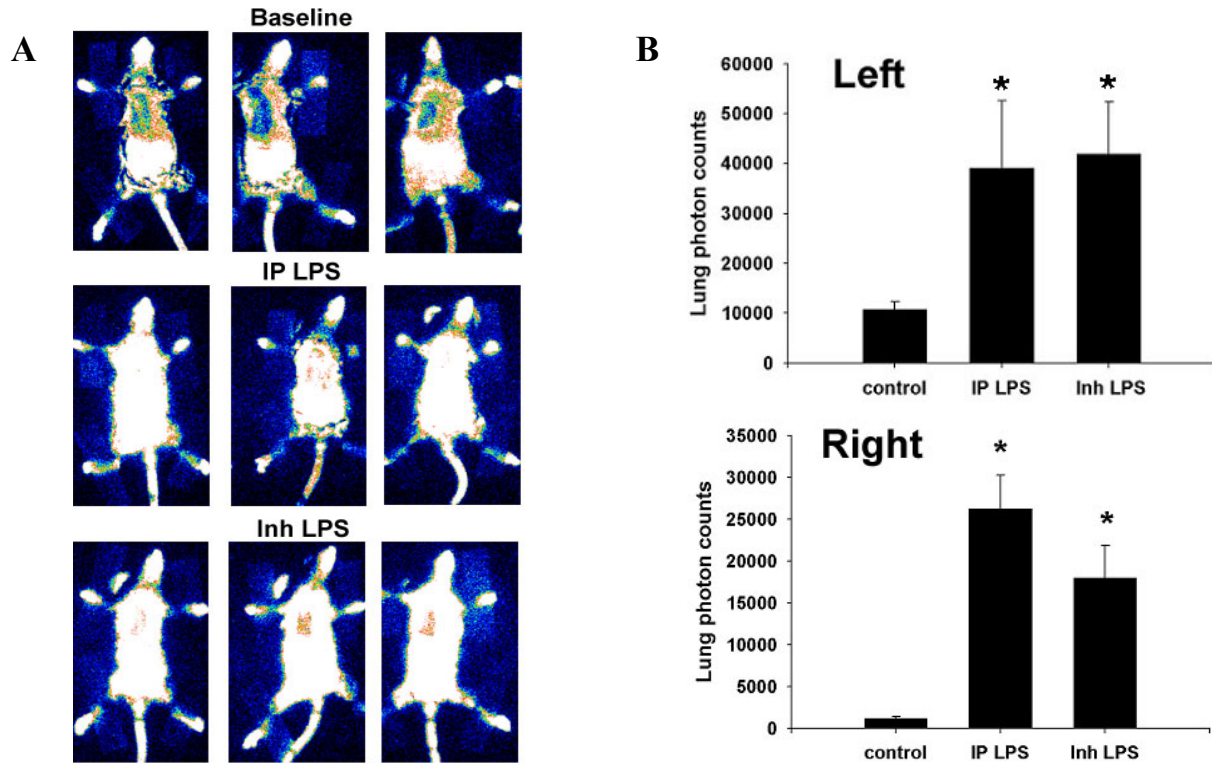


Figure 7: A) Bioluminescent imaging of HLL mice at baseline and after treatment with IP or inhaled LPS. A skin flap excision was performed over the right thorax. B) Photon emission was quantified from the thorax over the right (skin flap excised) and left (skin intact) lungs.

## CHAPTER II

### MATERIALS AND METHODS

#### **Animals**

Transgenic TgN(GFPU)5Nagy mice (referred to as Nagy GFP) were obtained from Dr. Brigid Hogan (Duke University). Nagy GFP transgenic mice ubiquitously express GFP under the control of a CMV immediate early enhancer coupled to a chicken  $\beta$ -actin promoter and first intron. Nagy GFP mice were used as donors in Fetal Liver Transplantation experiments. Wild-type mice (B6;129 background) were obtained from Jackson Laboratory (Bar Harbor, ME). Wild-type mice were used as recipients in FLT experiments.

Mice deficient for p105/p50 (B6;129 – Nfkb1[tmiBal]) were obtained from Jackson Laboratory (Bar Harbor, ME). Mice deficient for I $\kappa$ B- $\alpha$  (2000) were obtained from Fiona Yull (Vanderbilt University). HLL mice were generated by Dr. Yull (Vanderbilt University).

#### **Bioluminescence**

Mice were anesthetized and shaved over the chest before imaging. Luciferin (1 mg/mouse in 100  $\mu$ l isotonic saline) was administered by i.v. injection, and mice were imaged with an intensified charge-coupled device (ICCD) camera (model C2400-32 Hamamatsu, Bridgewater, NJ). This system consists of an image intensifier coupled to an 8-bit charge-coupled device camera, allowing for 256 intensity levels for each pixel. For the duration of photon counting, mice were placed inside a light tight box that housed the camera. Light emission from the mouse was detected as photon counts by the ICCD camera and customized

image processing hardware and software (Hamamatsu, Bridgewater, NJ). The imaging duration (3 min) was selected to avoid saturation of the camera during image acquisition. Quantitative analysis was performed by defining standard area over the mid lung zone and determining the total integrated photon intensity over the area of interest. For presentation, a 4-bit (16 intensity levels) digital false-color photon emission image was generated for each captured image according to the same false-color scale.

### **Bone Marrow Derived Macrophages**

Bone marrow derived macrophages were cultured as follows: mice were euthanized by CO<sub>2</sub> inhalation and femurs isolated by surgical resection. The bone marrow was collected by flushing the femurs with media (DMEM, 10% LCM, 10% FBS, Penicillin/Streptomycin) using a 27 gauge needle and syringe. After a single cell suspension was achieved by repeated pipeting, the cells were transferred to a 150 mm plate and placed at 37<sup>0</sup>C. After six days, the media was removed and BMDMΦ cells washed once with PBS. The cells were lifted by addition of cold PBS/5 mM EDTA for 15 minutes at 4<sup>0</sup>C. Cells were re-plated (DMEM, 10% FBS, Penicillin/Streptomycin) and experiments performed starting on day 7 after culture.

### **Cell Culture and Cell Lines**

RAW 267.4 cells were obtained from American Type Culture Collection (ATCC, Manassas, VA) and were maintained in Dulbecco's Modified Eagle's medium (DMEM) supplemented with 10% fetal bovine serum, 1% L-glutamine, penicillin (100 U/ml) and streptomycin (100 U/ml) (Gibco BRL, Gaithersburg, MD). A549 cells were obtained from ATCC and were maintained in F12K Kaighn's Modification (ATCC) supplemented with 10%

FBS, 1% L-glutamine, and P/S. BMDM $\Phi$  were maintained in DMEM supplemented with 10% fetal bovine serum (Hyclone, Logan, UT), 10% LCM media, 1% L-glutamine, and P/S.

### **Co-culture**

Co-culture experiments were performed in an apparatus that allows for cell-cell communication via the culture media. BMDM $\Phi$  from WT, I $\kappa$ B- $\alpha^{-/+}$ , and p50 $^{-/-}$  mice were cultured as described in the Bone Marrow-Derived Macrophage section. A549 cells were transiently transfected with the 8x NGL construct using Superfect as described in the Transfection section below. The experiments were performed as follows: Day 1 – bone marrow harvested and placed into culture, Day 5 – A549 cells plated into bottom well of co-culture plates, Day 6 – A549 cells transfected with 8x NGL construct and BMDM $\Phi$  plated into upper well of co-culture plates, Day 7 – 5  $\mu$ g/ml LPS added to each co-culture well and 4 hour time point collected and detected by luciferase assay, Day 8 – 24 hour time point collected and luciferase detected, Day 9 – 48 hour time point collected and luciferase detected.

### **Extraction of Cytoplasmic and Nuclear Proteins**

Tissue nuclear proteins were extracted from whole-lung tissue by the method of Deryckere and Gannon (Deryckere, 1994). Briefly, 50 to 100 mg of tissue was mechanically homogenized in liquid nitrogen, to which 4 ml of buffer A (150 mM NaCl, 10 mM HEPES [pH 7.9], 0.6% [vol/vol] NF-40, 0.2 M EDTA, 0.1 M phenylmethylsulfonyl fluoride) was added. The homogenate was transferred to a 15 ml Falcon tube and centrifuged at 850 x g in a tabletop centrifuge for 30 sec to remove cellular debris. The supernatant was then transferred to a 50 ml Falcon tube and incubated on ice for 5 min prior to being centrifuged for 10 min at 3,500 x g.

Supernatant was collected as a cytoplasmic extract. The pellet was resuspended in 300  $\mu$ l of buffer B (sterile water, 25% [vol/vol] glycerol, 20 mM HEPES [pH 7.9], 5 M NaCl, 1 M MgCl<sub>2</sub>, 0.2 M EDTA, 0.1 M phenylmethylsulfonyl fluoride, 1 M dithiothreitol, 10 mg of benzamide per ml, 1 mg of pepstatin per ml, 1 mg of leupeptin per ml, 1 mg of aprotinin per ml) and incubated on ice for 30 min. Following centrifugation at 14,000 rpm in an Eppendorf microcentrifuge for 2 min, the supernatant was collected as the nuclear extract and frozen at -70<sup>0</sup>C. Protein concentrations in nuclear and cytoplasmic extracts were determined using the Bradford assay (Bradford, 1976).

### **Fetal Liver Transplantation**

Fetal liver transplant (FLT) experiments were performed as follows. Timed matings were set up with donor mice and females checked on consecutive days until vaginal plugs were observed. On day E14.5, pregnant females were euthanized by CO<sub>2</sub> inhalation, and the uterus surgically removed. Fetuses were separated using forceps and placed into culture media (RPMI 1640, Invitrogen, Carlsbad, CA). Embryonic livers were removed with the aid of a dissecting microscope, pooled into an Eppendorf tube containing 1ml RPMI, and stored on ice. Single cell suspensions were prepared by drawing cells through needles of decreasing bore size (18, 23, 25 gauge). Recipient mice were lethally irradiated using a <sup>137</sup>cesium gamma source by giving a split dose of 800 rads followed 3 hours later by 400 rads. After irradiation, 2 x 10<sup>6</sup> donor cells were injected intravenously via tail vein. To diminish infection, mice were maintained on antibiotics (polymyxin B and neomycin) for two weeks after FLT and acidified water (pH 2.7) for the duration of the experiment.

## Fluorescence Activated Cell Sorting

### Fetal Liver Transplantation Studies

Peripheral blood samples (0.5 ml) were collected and placed in a polystyrene tube containing 0.1 ml 0.5 M EDTA (pH 8.0) at room temperature. The samples were washed with 3 ml of 1X Fluorescence activated cell sorting (FACS) Buffer (PBS with 1% bovine serum albumin) and centrifuged at 300 x g for 15 minutes at room temperature. After resuspending in 50  $\mu$ l PBS, 4  $\mu$ l Fc block (Pharmingen, San Diego, CA) was added and the mixture stored on ice for 10 minutes. To label monocytes, 2  $\mu$ l CD11b-PE and 2  $\mu$ l Gr-1-APC (Pharmingen, San Diego, CA) was added and the mixture stored on ice for 10 minutes. Ten milliliters of lysis buffer (8.29 g  $\text{NH}_4\text{Cl}$ , 1 g  $\text{KHCO}_3$ , 37.2 mg  $\text{Na}_2\text{EDTA}$  per liter  $\text{H}_2\text{O}$ , pH 7.4) was added to lyse red blood cells. Subsequently, cells were centrifuged at 300 x g for 15 minutes at room temperature, washed with 5 ml FACS buffer, and resuspended in 3 ml FACS buffer for analysis. FACS was then performed using standard protocols using a Becton Dickinson FACScan flow cytometer. For bronchoalveolar lavage (BAL), samples were collected in saline and placed on ice. Lavage cells were pelleted at 300 x g for 15 minutes. After resuspending in 50  $\mu$ l PBS, 4  $\mu$ l Fc block (Pharmingen, San Diego, CA) was added and the mixture incubated on ice for 10 minutes. To label macrophages, 2  $\mu$ l of CD11b-PE (Pharmingen, San Diego, CA) was added and the mixture stored on ice for 10 minutes. Cells were then washed with PBS and resuspended in 200  $\mu$ l FACS buffer for analysis.

### NGL Brochoalveolar Lavage

Bronchoalveolar lavage cells from the lung were collected by lung lavage with 3 aliquots of 1 ml PBS. The samples were washed with 3 ml of FACS buffer (PBS with 1% bovine serum albumin) and centrifuged at 300 x g for 15 minutes at room temperature. The supernatant was removed and the cells resuspended in 300 µl FACS buffer for analysis.

## **Histology and Immunohistochemistry**

### Histology

Lungs were removed en bloc after tracheal ligation, preserved in 10% neutral buffered formalin for 24 hours at 4<sup>0</sup>C, and subsequently embedded in paraffin. Lung tissue sections (5 micron) were prepared in the Mouse Pathology Core Facility (Kelly Parman, Vanderbilt University). H&E stains were performed using a standard protocol.

### CD68 and GFP Immunohistochemistry

To collect lung tissue, mice were perfused with 20 ml saline and lungs inflated with 1ml 10% neutral buffered formalin (NBF). Lungs were stored in NBF overnight at 4<sup>0</sup>C and then paraffin embedded. Five micron sections were cut and placed on charged slides. Following paraffin removal, sections were rehydrated and placed in heated Target Retrieval Solution, High pH (DakoCytomation, Carpinteria, CA) for 20 minutes. Endogenous peroxidase was quenched with 0.03% hydrogen peroxide and samples were treated with casein-based protein blocking solution (DakoCytomation, Carpinteria, CA) prior to primary antibody addition. Tissues were incubated with goat anti-CD68 1:500 (Santa Cruz Biotechnology, Inc, Santa Cruz, CA) or rabbit anti-GFP 1:200 (Clontech, Palo Alto, CA) for 30 minutes. Sections without primary antibody

served as negative controls. The Vectastain ABC Elite (Vector Laboratories, Inc, Burlingame, CA) System and DAB+ (DakoCytomation, Carpinteria, CA) were used with CD68 antibodies and rabbit Envision+ System, HRP/DAB+ (DakoCytomation, Carpinteria, CA) were used with GFP antibodies to produce localized, visible staining. Slides then were lightly counterstained with Mayer's hematoxylin, dehydrated, and coverslipped.

Quantification of total lung macrophages and GFP positive alveolar macrophages was performed on serial sections immunostained with GFP and CD68 antibodies. Sections were visualized under 400x magnification and digital pictures of ten serial, non-overlapping fields were taken using Magnifire SP software (Optronics, Goleta, CA). The number of GFP positive and CD68 positive cells per field was recorded. The results were verified by blinded analysis from a second observer.

### **Lipopolysaccharide Administration**

Gram-negative *Escherichia coli* lipopolysaccharide (LPS serotype 055:B5) was obtained from Sigma (St. Louis, MO). A working solution of LPS was made by resuspending 1 mg LPS in 10 ml sterile PBS. For intraperitoneal injections, a single dose of 3  $\mu$ g LPS per gram body weight was administered. For intratracheal injections, 75  $\mu$ g LPS was administered. For IP osmotic pump, a priming dose of 3  $\mu$ g LPS per gram body weight was administered IP, followed by implantation of osmotic pump (Alzet, Alza Corporation, Palo Alto, CA) in the peritoneal cavity. Mice were anesthetized and the osmotic pump surgically implanted into the peritoneal space using sterile technique. The pump delivered 8  $\mu$ g LPS (8  $\mu$ l) per hour for 24 hours.

## **Liposomal Clodronate**

Liposomal encapsulation of clodronate (dichloromethylene diphosphate) was performed as previously described (van Rooijen, 1994a). Briefly, a mixture of 8 mg cholesterol (Sigma, St. Louis, MO) and 86 mg egg-phosphatidylcholine (DOPC, Avanti, Alabaster, AL) was dissolved in chloroform and then evaporated under nitrogen. Chloroform was further removed by placing under low vacuum in a speedvac Savant concentrator (Holbrook, NY). The clodronate solution was prepared by dissolving 1.2 g of dichloromethylene diphosphonic acid (Sigma, St. Louis, MO) in 5 ml of sterile PBS. The clodronate solution (5 ml) was added to the liposome preparation and mixed thoroughly. The solution was sonicated and centrifuged at 10,000 x g for 1 hour at 4<sup>0</sup>C. The liposome pellet was removed, resuspended in 5 ml PBS, and centrifuged at 10,000 x g for 1 hour at 4<sup>0</sup>C. Liposomes were removed, resuspended in 5 ml PBS, and used within 48 hours. A single dose of liposomal clodronate was administered via intratracheal injection 6 weeks following FLT.

## **Luciferase Assay**

### Cultured Cells

Luciferase assay was performed using a standard protocol. Briefly, cells were washed once with PBS. Cell lysis was achieved by adding 100 µl of Passive Lysis Buffer (Promega, Madison, WI) with gentle agitation for 10 minutes. Cells were collected using a cell scraper and transferred to an Eppendorf tube on ice. The samples were centrifuged at 13,000 rpm at 4<sup>0</sup>C for 5 minutes. Ten µl of supernatant was used to measure luciferase activity in a luminometer.

## Tissue

Lungs were removed en bloc and homogenized in 1 ml of Passive Lysis Buffer using a dounce homogenizer. The samples were transferred to an Eppendorf tube and centrifuged at 13,000 rpm at 4<sup>0</sup>C for 5 minutes. Ten µl of supernatant was used to measure luciferase activity in a luminometer.

## **Microscopy**

All tissue sections were prepared by the Mouse Pathology Core facility (Kelly Parman, Vanderbilt University). Microscopy was performed using an Olympus (Melville, NY) microscope. Digital images were captured using a digital camera and Magnifire SP software (Optronics, Goleta, CA).

## **Neutrophil Quantification**

To quantify lung inflammation *in vivo*, neutrophils were counted on H&E stained lung tissue sections and recorded. For each slide, neutrophils were counted in 10 non-overlapping high power fields on H&E stained lung tissue sections. For each mouse, 3 slides were counted with 3 or more mice included in each treatment group. The data is presented as the number of neutrophils per high power field.

## ***Pseudomonas aeruginosa* Administration**

*Pseudomonas aeruginosa* (strain PA103) was streaked onto trypticase soy agar plates (TSA) and grown in a deferrated dialysates of tripticase soy broth supplemented with 10mM nitriлотriacetic acid (Sigma, St. Louis, MO), 1% glycerol, and 100mM monosodium glutamate at

33<sup>0</sup>C for 1-3 hours in shaking incubator. Cultures were centrifuged at 8500 x g for 5 minutes and the bacterial pellet washed twice in Ringers lactate. The bacteria were diluted to the appropriate number of colony forming units (CFU) per ml in Ringers lactate solution as determined by spectrophotometer. The bacterial concentration was confirmed by diluting the samples and plating the known dilution on sheep blood agar plates. *Pseudomonas* (10<sup>6</sup> cfu) was administered by IT injection.

### ***Pseudomonas aeruginosa* Lung Colony Counts**

The lungs were removed aseptically and placed in 3 ml of sterile saline. The lungs were then homogenized in a tissue homogenizer in a vented hood under sterile conditions. Serial dilutions of the homogenates were prepared and 10 µl of each dilution were plated in soy base blood agar plates (BD, Sparks, MD). The plates were incubated for 18 hours at 37<sup>0</sup>C and the number of colonies counted and recorded.

### **Statistical Analysis**

To assess differences among groups, analyses were performed with GraphPad Instat (GraphPad Software, San Diego, CA) using a one-way analysis of variance (ANOVA) test (p values < 0.05 were considered significant).

### **Transfection**

Transient transfection experiments were performed using Superfect (Qiagen, Valencia, CA) as recommended by the manufacturer. Briefly, the cells were washed once with PBS. The DNA/liposome complex was prepared by resuspending the DNA constructs in serum-free media.

Superfect reagent was then added and allowed to incubate at room temperature for 10-15 minutes. Next, serum-containing media was added to the DNA/liposome complex solution, mixed gently, and placed on the cells for 4 hours at 37<sup>0</sup>C. The DNA/liposome solution was removed and the cells washed once with PBS. Serum-containing media was then added to the cells and placed at 37<sup>0</sup>C overnight. Experiments were then performed the next day.

### **Western Blots**

Nuclear and cytoplasmic proteins from tissue extracts were quantified by Bradford assay and 25 to 50 µg of protein was mixed with an equal volume of 2X sample buffer (containing 0.1% sodium dodecylsulfate (SDS) and 2-mercaptoethanol) and boiled for 5 min. Denatured proteins were separated by electrophoresis on an SDS-polyacrylamide gel along with molecular weight markers and standards. Proteins were transferred to an Immobilon-P (Millipore, Bedford MS) membrane in a mixture of 25 mM Tris base, 192 mM glycine, and 5% [vol/vol] methanol (pH 8.2) at 100 V for 1 hour. Nonspecific binding was blocked by soaking the membrane in phosphate-buffered saline (PBS)-5% nonfat dried milk-0.05% Tween 20 overnight at 4<sup>0</sup>C. Immunoreactive proteins were detected by incubating the filter with specific antibodies to RelA 1:500 (Santa Cruz Biotechnology, Inc.), IκB-α 1:500 (Santa Cruz Biotechnology, Inc.), for 1 hour at room temperature with constant agitation. Nonspecific binding was washed away by rinsing the filter in PBS containing 0.05% Tween 20. The filters were incubated with horseradish peroxidase-conjugated goat anti-rabbit immunoglobulin G (Santa Cruz Biotechnology, Inc.) diluted 1:5,000 in Blotto (Tween-PBS-5% nonfat dried milk) for an hour at room temperature with constant agitation. The filter was washed three times for 10 min with

Tween-PBS. To develop the image, filters were treated with Renaissance Western blot luminescent reagent (NEN, DuPont) for 5 min and exposed to Biomax film for 3 to 10 min.

## CHAPTER III

### RESULTS

#### GENERATION OF NF- $\kappa$ B TRANSGENIC REPORTER MOUSE MODEL

##### **Introduction**

The NF- $\kappa$ B transcription factor family has been shown to play a key role in innate immunity in the lung by regulating acute inflammation through transcriptional control of a variety of pro-inflammatory genes including cytokines, chemokines, adhesion molecules, and enzymes. However, a detailed understanding of the function of the NF- $\kappa$ B pathway in individual lung cell types *in vivo* is critical for appropriately targeting therapeutic interventions that modulate NF- $\kappa$ B. While the HLL transgenic reporter mouse model has provided valuable information regarding NF- $\kappa$ B activation *in vivo*, we have been unable to localize NF- $\kappa$ B-dependent luciferase production to specific cells or regions within the lung by immunohistochemistry or *in situ* hybridization.

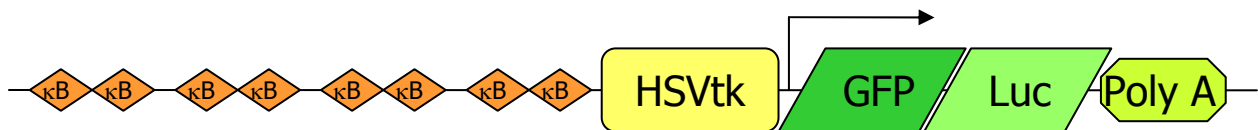
In order to dissect the role of NF- $\kappa$ B in specific lung cell types in the context of an integrated NF- $\kappa$ B dependent inflammatory response, new tools are required to measure NF- $\kappa$ B activity at the cellular level. We have generated an NF- $\kappa$ B transgenic reporter mouse model containing a NF- $\kappa$ B enhancer coupled to the Herpes Simplex Virus thymidine kinase (HSVtk) minimal promoter driving expression of a GFP/Luciferase fusion protein. This model allows for the detection of NF- $\kappa$ B activity *in vivo* in intact, anesthetized animals by bioluminescence and at the level of specific lung cell types by GFP fluorescence microscopy and immunohistochemistry

in lung tissue sections. We have determined the GFP/Luciferase fusion protein half-life to be approximately 2.5 hours in bone marrow derived macrophages, making it ideal as a reporter for transcription factor activity. In three separate methods of LPS administration (IP, IT, and IP osmotic pump) we have identified distinct patterns of NF- $\kappa$ B activation, both temporal and cellular, in the lung. In addition, the role of NF- $\kappa$ B in regulating bacterial infection in the lung was investigated using a *Pseudomonas aeruginosa* pneumonia model. The detection of NF- $\kappa$ B by bioluminescence and GFP immunohistochemistry correlated with the severity of lung inflammation and injury. IP LPS administration resulted in a transient NF- $\kappa$ B activation at 4 hours which returned to baseline by 24 hours. IP Pump LPS administration resulted in a similar increase of NF- $\kappa$ B activation at 4 hours which persisted through 24 and 48 hours. IT LPS administration resulted in a delayed NF- $\kappa$ B activation compared to IT LPS. Moderate NF- $\kappa$ B activity was detected at 4 hours with a substantial increase at 24 hours. Similar to IT LPS, IT *Pseudomonas aeruginosa* administration resulted in substantial NF- $\kappa$ B activation at 24 hours. The ability to detect NF- $\kappa$ B activity by GFP was accomplished by three methods 1) NF- $\kappa$ B activity was identified in specific cell types by GFP immunohistochemistry on lung tissue sections 2) FACS was utilized to identify NF- $\kappa$ B activation by GFP fluorescence in bronchoalveolar lavage cells after IT LPS administration 3) GFP fluorescence imaging was utilized to identify lung NF- $\kappa$ B *ex vivo* after IP and IP Pump LPS administration. These results demonstrate the importance of this model in defining the role of NF- $\kappa$ B in specific cell types with respect to the inflammatory stimulus. Thus, the NGL transgenic reporter mouse model provides a critical tool in the investigation of the role of NF- $\kappa$ B in regulation lung inflammation *in vivo*.

## Results

### NGL Construct Design

In order to develop a new transgenic reporter mouse model to investigate NF- $\kappa$ B regulation *in vivo*, a series of DNA constructs were generated using a combination of NF- $\kappa$ B enhancer elements and promoters driving expression of a GFP/Luciferase fusion protein reporter. The first construct (called 4x Clon) contained a 4x NF- $\kappa$ B enhancer (Clontech)/SV40 minimal promoter driving expression of a GFP/Luciferase fusion protein. Additionally, a series of constructs were generated in which tandem copies of the HIV-LTR 36 base pair enhancer (containing two NF- $\kappa$ B binding sites, GGGACTTTCC) were placed upstream of the Herpes Simplex Virus minimal thymidine kinase promoter driving expression of a GFP/Luciferase fusion protein. These constructs were named NGL (for NF- $\kappa$ B GFP/Luciferase) and are referred to as 4x NGL, 6x NGL, 8x NGL, and 12x NGL based on the number of  $\kappa$ B sites in the enhancer (Figure 8).



- HSVtk minimal promoter (pBLCAT2 vector)
- 8 NF- $\kappa$ B binding sites (GGGACTTTCC)
- GFP/*Photinus* Luciferase fusion protein (Clontech)
- SV40 PolyA

**Figure 8**

### *In vitro* Detection of NF- $\kappa$ B Activity by Luciferase Assay and GFP Fluorescence Microscopy

The NF- $\kappa$ B reporter constructs were tested *in vitro* to determine basal activity and inducibility after treatment with NF- $\kappa$ B dependent stimuli. Transient transfection experiments were performed in multiple cell lines (A549 – human type II alveolar epithelium, RAW 267.4 – murine macrophage, NIH 3T3 – human fibroblast, HeLa – human cervical carcinoma) to ensure reliable expression in a wide range of cell types. In Figure 9, RAW 267.4 cells were transfected with the reporter constructs described above and stimulated with 5  $\mu$ g/ml LPS for 4 hours to activate NF- $\kappa$ B. Luciferase activity was measured as an indicator of NF- $\kappa$ B activation. As a reference, the HIV-LTR luciferase construct used to generate the HLL reporter mouse model was included in the experiment. The HIV-LTR construct produced a 2-3 fold increase in luciferase activity over baseline after LPS treatment. The 4x Clon construct demonstrated increased basal activity, as compared to the HIV-LTR construct, and only a 1 fold increase in luciferase activity over baseline after LPS treatment. Interestingly, the 12x NGL construct demonstrated poor inducibility after LPS treatment similar to the 4x Clon construct. The 4x, 6x, and 8x NGL constructs displayed significant improvements in inducibility compared to the previous constructs (4, 3.5, and 6 fold increases in luciferase activity over baseline after LPS treatment in the 4x, 6x, and 8x NGL constructs respectively).

The NGL constructs were further investigated for the ability to detect NF- $\kappa$ B activity by fluorescence microscopy as well as standard luciferase assays (Figure 10). A549 cells were transiently transfected with the 8x NGL construct and stimulated with 20 ng/ml TNF- $\alpha$  for 6 hours to activate NF- $\kappa$ B. Relatively few GFP positive cells (5%) were observed at baseline (A) corresponding to 2,247 +/- 634 RLU/ $\mu$ g protein. After TNF- $\alpha$  stimulation, 90% of the cells were

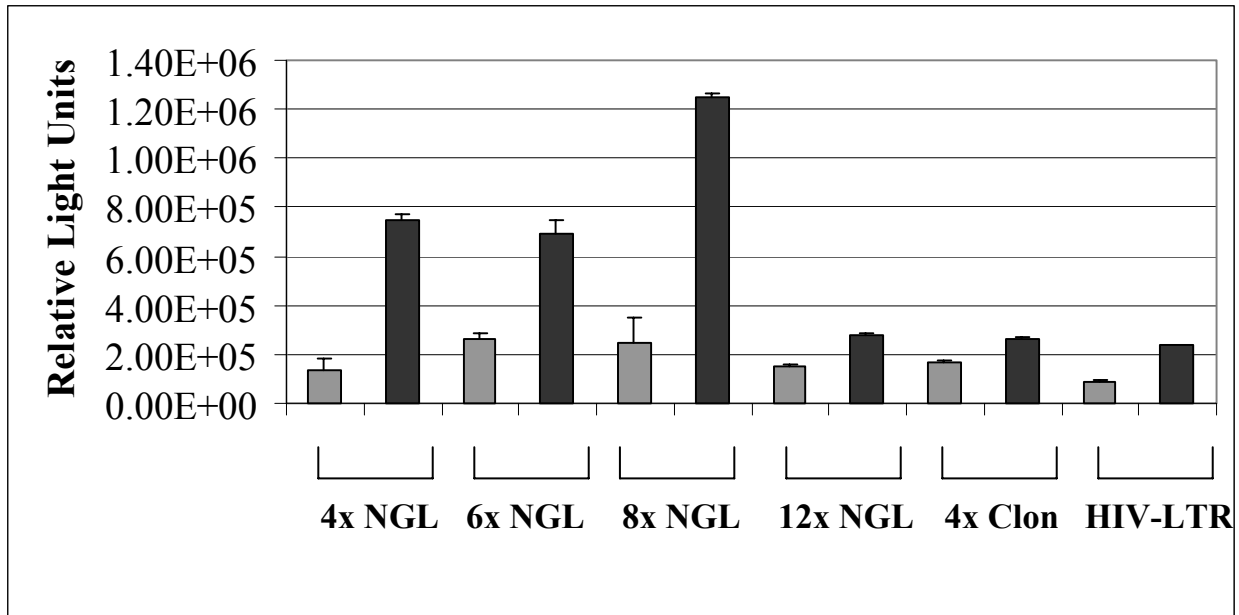


**Figure 9:** Transient transfection of RAW 267.4 cells with reporter constructs to detect NF- $\kappa$ B activity by luciferase assay. After transfection, RAW 267.4 cells were stimulated for 4 hours with 5 mg/ml LPS to activate NF- $\kappa$ B. Baseline (Gray bars) LPS treated (Black bars). Each bar represents mean  $\pm$  SEM of 3 samples per group. Data is representative of three separate experiments.

GFP positive (B) corresponding to 13,258  $\pm$  843 RLU/ $\mu$ g protein (C). These data demonstrate that the detection of NF- $\kappa$ B activity by standard luciferase assay correlates with detection by fluorescence microscopy and thus allows for the detection of NF- $\kappa$ B activity over time in the same cells.

#### NF- $\kappa$ B Transgenic Reporter Mouse Generation

Based on the basal and inducible characteristics observed *in vitro*, the 4x and 8x NGL constructs were chosen for micro-injection at the Vanderbilt Transgenic/ES Cell Shared Resource. In the first round of injections, 3 potential founders (out of 28) containing the 8x NGL

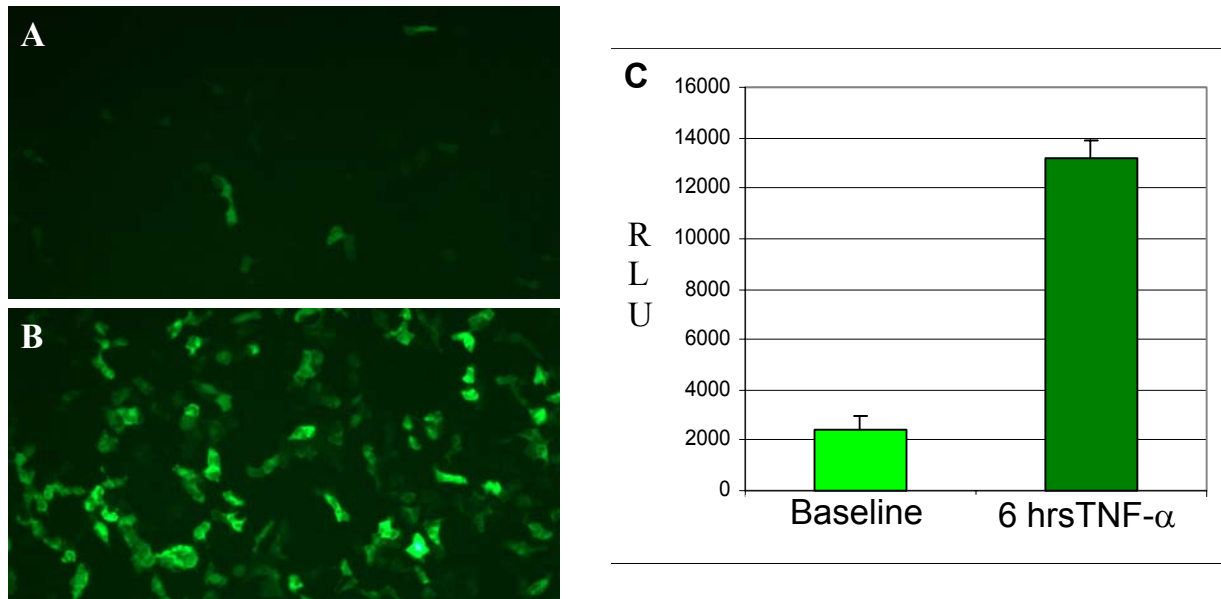


**Figure 10:** *In vitro* detection of NF- $\kappa$ B activation by fluorescence microscopy and luciferase assay in A549 cells transfected with 8x NGL construct. A549 cells were transiently transfected with 8x NGL construct and stimulated with 20 ng/ml TNF- $\alpha$  for 6 hours to activate NF- $\kappa$ B. Relatively few GFP+ cells (5%) were observed at baseline by fluorescence microscopy (A). Six hours after TNF- $\alpha$  treatment, 90% of the cells are GFP+ by fluorescence microscopy (B). TNF- $\alpha$  treatment resulted in a 6 fold increase in NF- $\kappa$ B activity as detected by standard luciferase assay (C). Each bar represents mean  $\pm$  SEM of 3 samples per group. Data is representative of three separate experiments.

construct (1 B6D2, 2 C57/B6 background) and 1 potential founder (out of 20) containing the 4x NGL construct (C57/B6) were identified by southern blot and PCR. No transgene positive offspring were identified in the 4x NGL line. The three 8x NGL lines produced transgene positive offspring and were further characterized. A second round of injections using the 8x NGL construct produced an additional four potential founders (out of 30, B6D2 background). All four lines produced transgene positive offspring and were further characterized. The line designated NGL 8/1 (8x NGL B6D2 from the first round of injections) was used for all subsequent NGL transgenic reporter experiments.

### GFP/Luciferase Protein Half-life

Bone marrow derived macrophages from NGL mice were used to determine the half-life of the GFP/Luciferase fusion protein. BMDM $\Phi$  were stimulated with 5  $\mu\text{g/ml}$  LPS to activate NF- $\kappa\text{B}$ . A luciferase assay time course was performed to determine the peak expression of the GFP/Luciferase reporter protein after stimulation. The highest level of luciferase activity was detected 3 hours after LPS treatment. At this time, cyclohexamide was added to the media to block protein synthesis and luciferase activity was measured after 30 min, 1, 2, and 3 hours (Figure 11). The GFP/Luciferase protein half-life was determined to be 2.5 hours, similar to the half-life of luciferase, making it ideal as a transcription factor reporter.

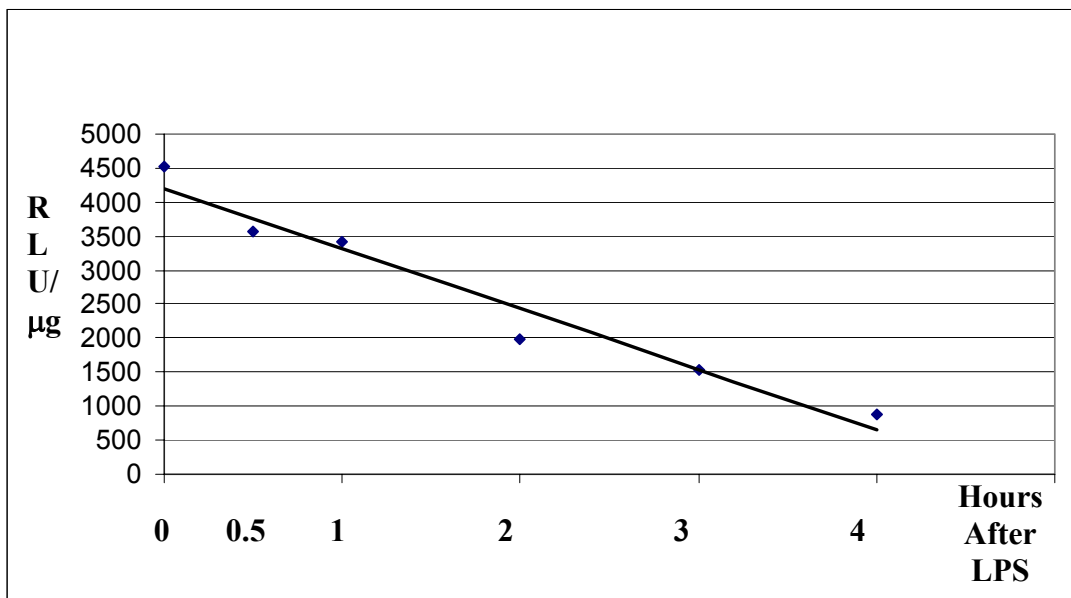


**Figure 11:** The GFP/Luciferase protein half-life was detected in NGL bone marrow derived macrophages. BMDM $\Phi$  were stimulated with 5  $\mu\text{g/ml}$  LPS and a time course performed to identify the peak luciferase activity (peak luciferase detected 3 hours after LPS stimulation). At this time, cyclohexamide was added to block protein synthesis and luciferase activity detected after 30 minutes, 1, 2, 3, and 4 hours. The GFP/Luciferase protein half-life was determined to be 2.5 hours. Data is representative of two separate experiments.

## LPS Model of Lung Inflammation

Despite much effort, the *in vivo* regulation of NF- $\kappa$ B in specific lung cell-types remains unclear. The NGL transgenic reporter mouse model provides a valuable tool to unravel these complex questions by allowing for the quantification of *in vivo* NF- $\kappa$ B lung activity by bioluminescence and subsequent investigation of the cellular contribution to that signal by GFP fluorescence microscopy and immunohistochemistry. To investigate the temporal, cell-specific regulation of NF- $\kappa$ B in the lung, we administered LPS by three separate methods to induce lung inflammation: a single intraperitoneal dose of LPS (3  $\mu$ g/g) to induce an acute systemic inflammatory response, a single intratracheal dose of LPS (75  $\mu$ g) to induce a localized acute inflammatory response, and an intraperitoneal osmotic pump (3  $\mu$ g/g IP priming dose followed by 8  $\mu$ g/hour for 24 hours IP released by pump) to induce a prolonged systemic inflammatory response. Bioluminescence imaging was used to generate a time course (0, 4, 8, 24, 48 hours after LPS delivery) of *in vivo* NF- $\kappa$ B activity for each treatment group. Photon counts were measured over the thorax to quantify NF- $\kappa$ B activity. At each time point, lungs were removed to identify lung inflammation by histology and detect cell-specific NF- $\kappa$ B activity by GFP fluorescence microscopy and immunohistochemistry.

### Intraperitoneal Administration of LPS

NGL mice were administered a single intraperitoneal dose of LPS (3  $\mu$ g/g) to induce an acute, systemic inflammatory response. *In vivo* NF- $\kappa$ B activity was detected by bioluminescence imaging at baseline, 4, 24, and 48 hours after IP LPS administration (Figure 12). The changes

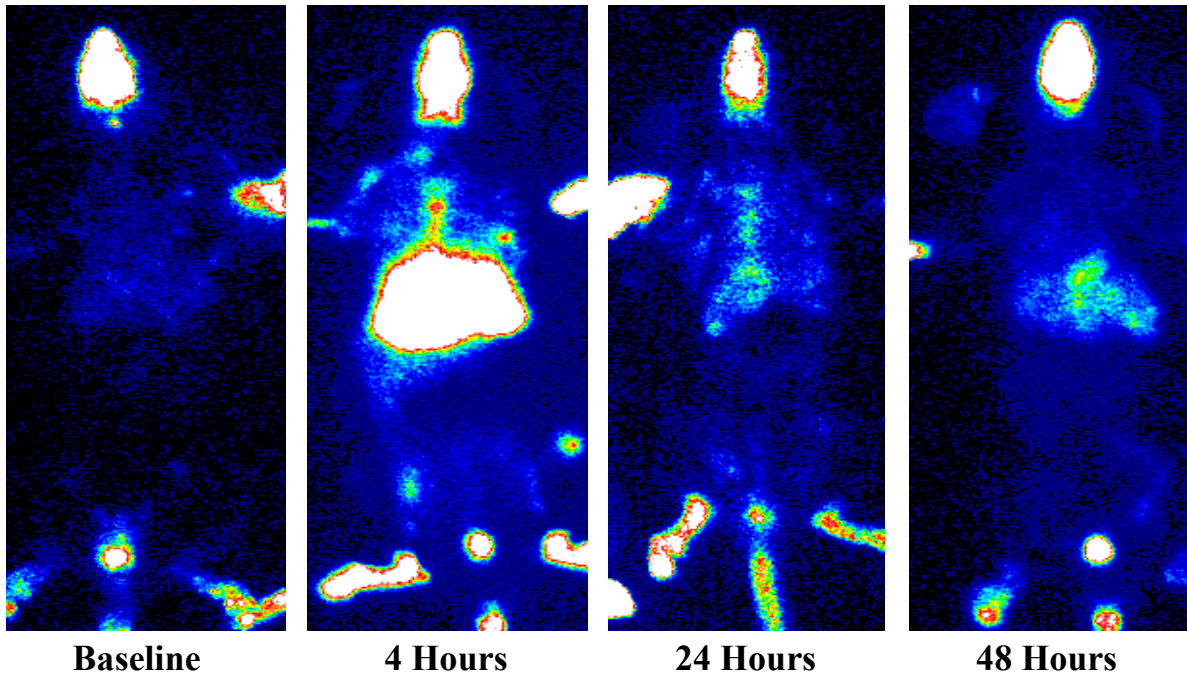


**Figure 12:** Bioluminescence imaging of NGL mice after a single IP injection of LPS (3  $\mu\text{g/g}$ ). Low level NF- $\kappa\text{B}$  activity is detected in the lung at baseline. Four hours after IP LPS administration, a significant increase in NF- $\kappa\text{B}$  activity is observed in the lung followed by a decrease to near baseline levels by 24 hours. NF- $\kappa\text{B}$  activity in the lung at 48 hours after IP LPS administration is comparable to untreated NGL mice. Images are representative of two separate experiments.

observed in the bioluminescence images were quantified by measuring photon counts over the thorax at each time point (Figure 13). NGL mice exhibited low level NF- $\kappa\text{B}$  activity in the lung at baseline. A significant increase in lung NF- $\kappa\text{B}$  activity was observed 4 hours after IP LPS administration followed by a decrease to near baseline levels by 24 hours. NF- $\kappa\text{B}$  activity as detected by bioluminescence imaging correlated with histologic evidence of lung inflammation as seen in Figure 14. Untreated NGL mice displayed normal lung architecture. Four hours after IP LPS, a significant influx of inflammatory cells (mostly neutrophils) was observed in the vessels and interstitium. To better quantify inflammation, neutrophils were counted in the H&E lung tissue sections (Figure 15). A significant increase in neutrophils was detected 4 hours after

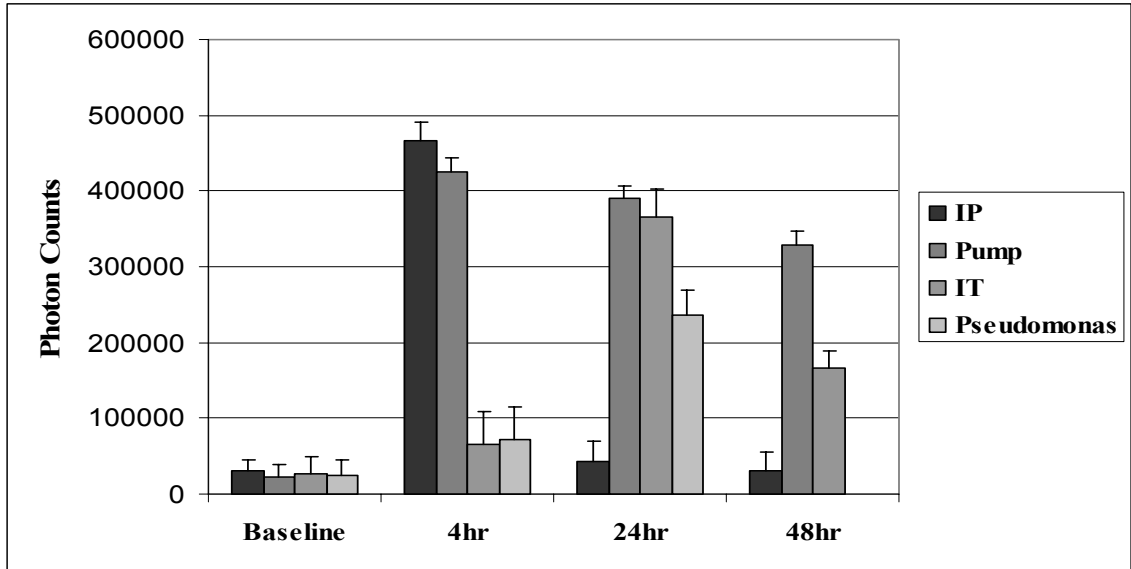


**Figure 13:** Quantification of photon counts measured over the thorax from NGL mice treated with IP, IP osmotic pump, and IT LPS administration. IP LPS administration resulted in an increase in photon counts at 4 hours, followed by a decrease to basal levels by 24 hours. IP pump LPS administration resulted in an increase in photon counts at 4 hours which persisted through 48 hours. IT LPS administration resulted in a modest increase in photon counts at 4 hours followed by a sharp increase at 24 hours. Photon counts decreased at 48 hours. *Pseudomonas aeruginosa* administration resulted in a modest increase at 4 hours followed by a sharp increase at 24 hours. Each bar represents mean +/- SEM 3-5 mice per group. Data is representative of two separate experiments.

LPS compared to baseline, 24, and 48 hours after LPS ( $p < 0.05$ ). To determine the cellular contribution to the NF- $\kappa$ B signal detected by bioluminescence, GFP immunohistochemistry were performed on lung tissue sections from mice at each time point. The detection of increased NF- $\kappa$ B by bioluminescence correlated directly with increased detection of GFP positive cells by immunohistochemistry. GFP was virtually undetectable in the lungs of untreated NGL mice (Figure 14). Four hours after IP LPS, strong GFP immunostaining was seen in airway epithelium, macrophages, neutrophils, and endothelium. As the bioluminescence signal decreased, the intensity of GFP immunostaining decreased, only faint staining in airway

epithelium and macrophages was present at 24 hours after IP LPS. Taken together, these data suggest IP LPS results in an early, transient activation of NF- $\kappa$ B in the lung consisting of NF- $\kappa$ B

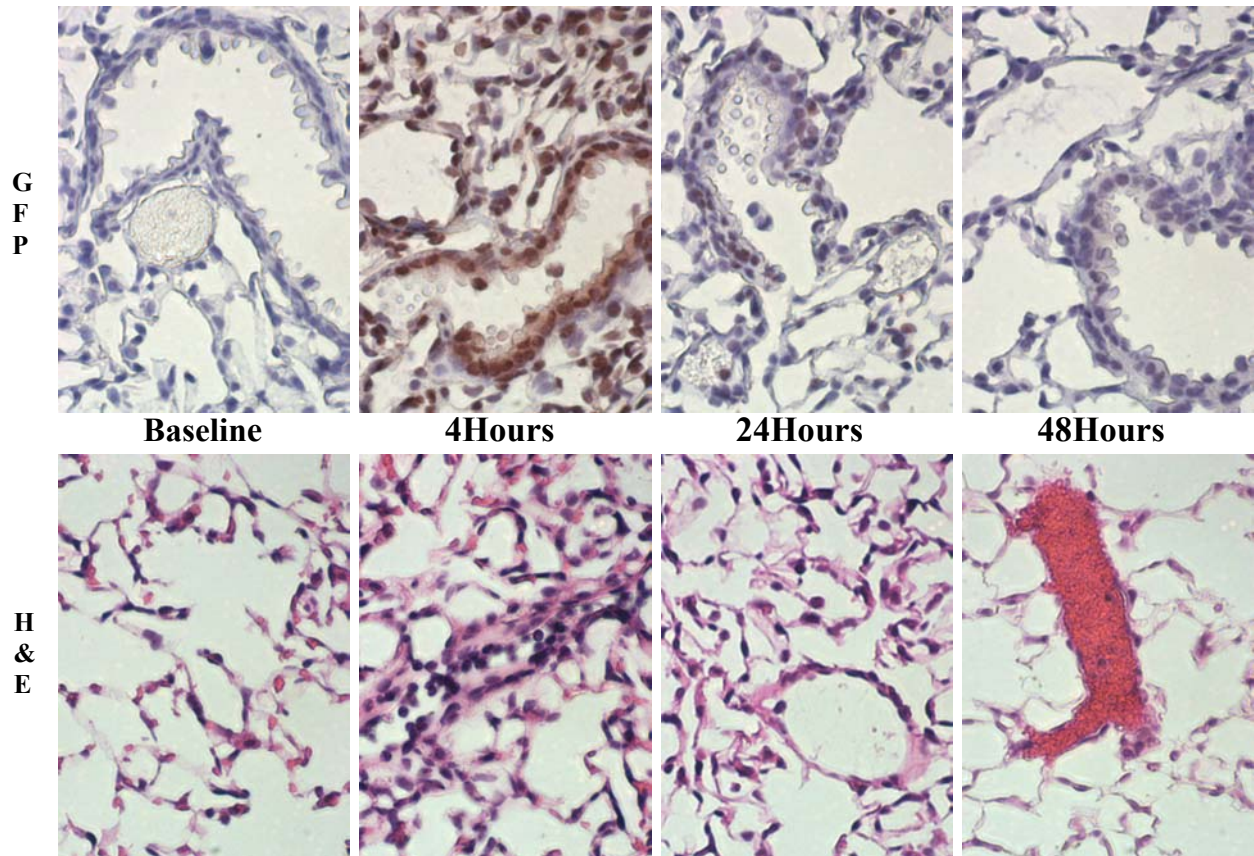


**Figure 14:** GFP immunohistochemistry and H&E histology of lung tissue from NGL mice administered a single IP injection of LPS (3  $\mu$ g/g).

activation in multiple cell types, including airway epithelium, macrophages, neutrophils, and endothelium.

#### Administration of LPS by Intraperitoneal Osmotic Pump

To induce a prolonged systemic inflammatory response, continuous delivery of LPS into the peritoneal space was achieved by surgical implantation of an osmotic pump. The mice were

given a priming dose of LPS by IP injection (3  $\mu\text{g/g}$ ) followed by peritoneal implantation of an osmotic pump which delivered 8  $\mu\text{g/hour}$  for 24 hours. *In vivo* NF- $\kappa\text{B}$  activity was detected by

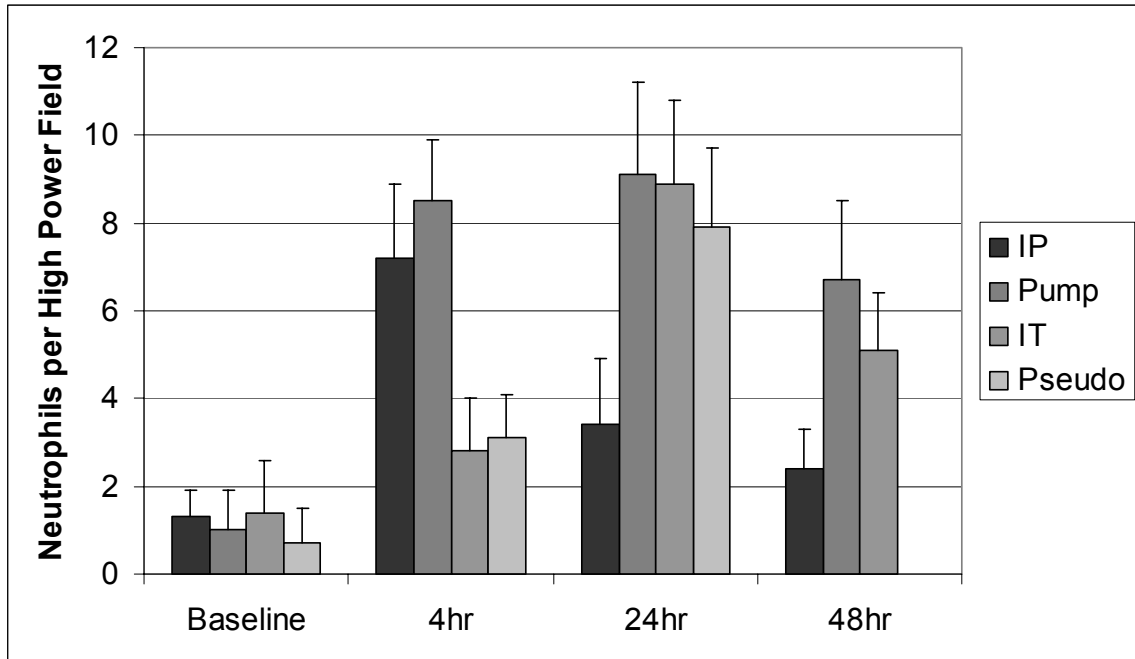


**Figure 15:** Quantification of neutrophils in lung tissue sections of IP, Pump, IT, and Pseudomonas treated mice. Neutrophils were counted in 10 non-overlapping fields per slide. A total of 3 slides per mouse were counted. N = 3 or more for each group. The number of neutrophils detected in the lung correlated with both the histologic evidence of lung inflammation and NF- $\kappa\text{B}$  activity as detected by bioluminescence imaging and photon counts.

bioluminescence imaging at the same time points as the IP LPS group (baseline, 4, 24, and 48 hours after osmotic pump implantation) (Figure 16). Similarly to the IP LPS group, increased NF- $\kappa\text{B}$  activity was detected 4 hours after treatment; however, in contrast to the IP LPS group, persistent NF- $\kappa\text{B}$  activation was present at the 24 hour time point. NF- $\kappa\text{B}$  activity remained increased at 48 hours after treatment. This persistent NF- $\kappa\text{B}$  activation was reflected in the photon counts detected over the thorax (Figure 13). Also, the sustained NF- $\kappa\text{B}$  activity correlated with histologic evidence of lung inflammation and injury. Figure 13 shows a considerable increase in neutrophil influx in the vessels and interstitium at 4 hours, similar to the

IP group. Consistent with NF- $\kappa$ B activity detected by bioluminescence, neutrophil influx was maintained at 24 and 48 hours after treatment. The cellular contribution to the NF- $\kappa$ B

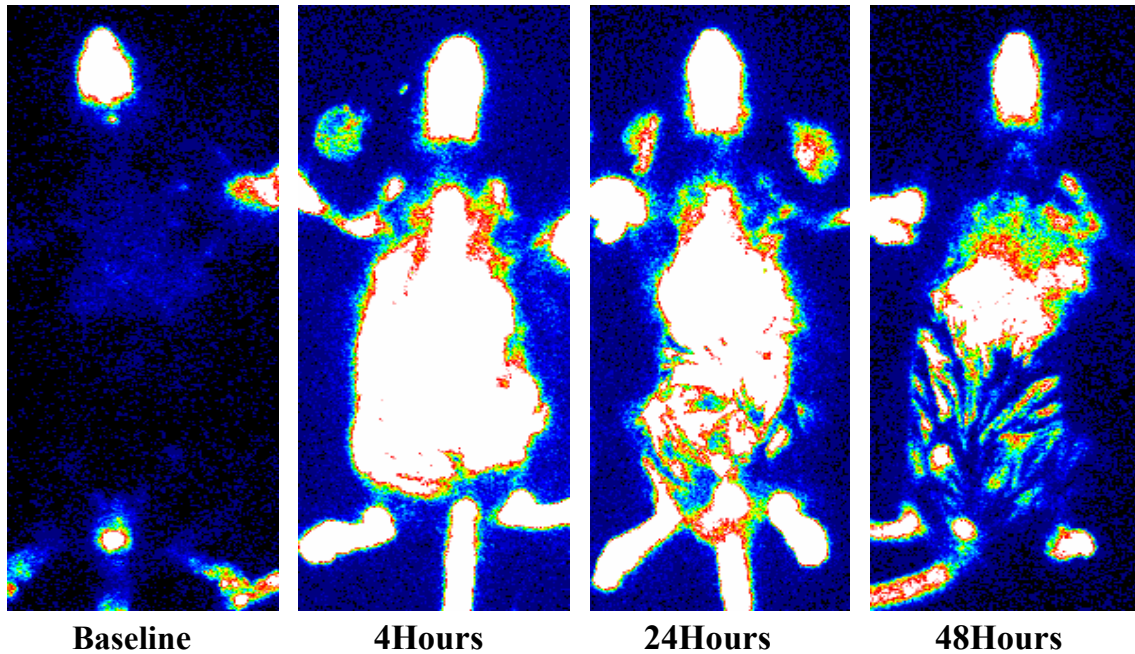


**Figure 16:** Bioluminescence imaging of NGL mice after peritoneal implantation of an osmotic pump delivering LPS (8  $\mu$ g/hour) for 24 hours. Low level NF- $\kappa$ B activity is detected in the lung at baseline. A substantial increase in NF- $\kappa$ B activity is observed in the lung 4 hours after Pump LPS administration. Sustained NF- $\kappa$ B activity is detected in the lung at 24 and 48 hours after Pump LPS administration. Images are representative of two separate experiments.

bioluminescence signal was the same as the IP group. GFP immunostaining revealed positive airway epithelium, macrophages, neutrophils, and endothelium (Figure 17). This pattern was maintained at 24 and 48 hours with persistent, prominent staining particularly in airway epithelium. These data demonstrate prolonged administration of systemic LPS drives NF- $\kappa$ B activation in inflammatory cells and multiple lung cell types. NF- $\kappa$ B activity was observed for the duration of LPS delivery (24 hours) and continued through 48 hours. NF- $\kappa$ B activity as determined by bioluminescence and GFP immunohistochemistry correlated with histologic evidence of lung injury, edema, and neutrophilic alveolitis. As seen in Figure 15, a significant

increase in neutrophils was detected 4, 24, and 48 hours after Pump LPS as compared to baseline ( $p < 0.05$ ) demonstrating a sustained inflammation and neutrophil influx.

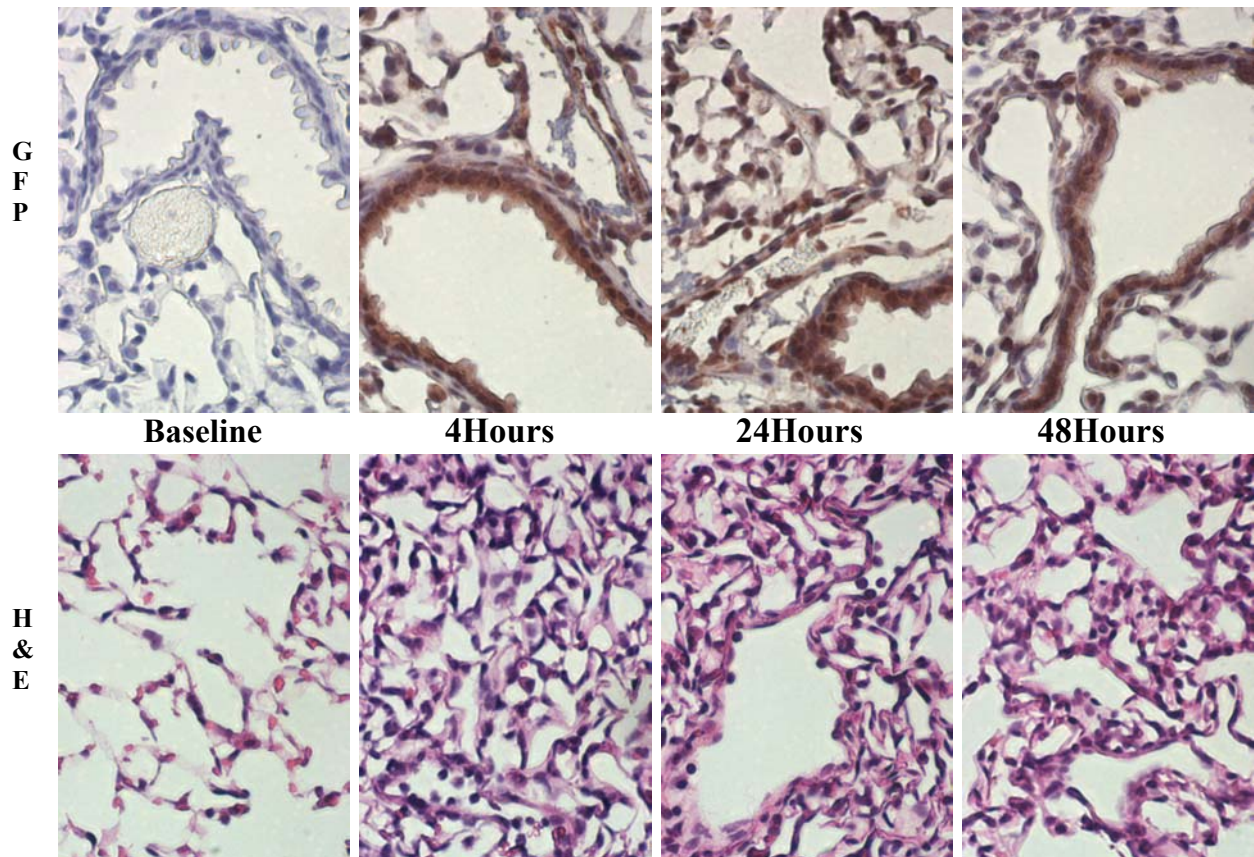


**Figure 17:** GFP immunohistochemistry and H&E histology of lung tissue from NGL mice after intraperitoneal implantation of an osmotic pump delivering 8 µg/hour LPS for 24 hours.

#### Intratracheal Administration of LPS

To induce a localized acute inflammatory response in the lung, a single dose of 75 µg of LPS was administered by intratracheal injection and *in vivo* NF-κB activity detected by bioluminescence imaging (baseline, 4, 24, and 48 hours after IT LPS) (Figure 18). IT LPS challenge resulted in a modest increase in NF-κB activity at 4 hours compared to the IP LPS and LPS Pump groups. The highest NF-κB activity was seen 24 hours after IT LPS followed by a

substantial decrease at 48 hours. These observations reflected the photon counts measured over the thorax (Figure 13). Histology correlated with bioluminescence in that few neutrophils were

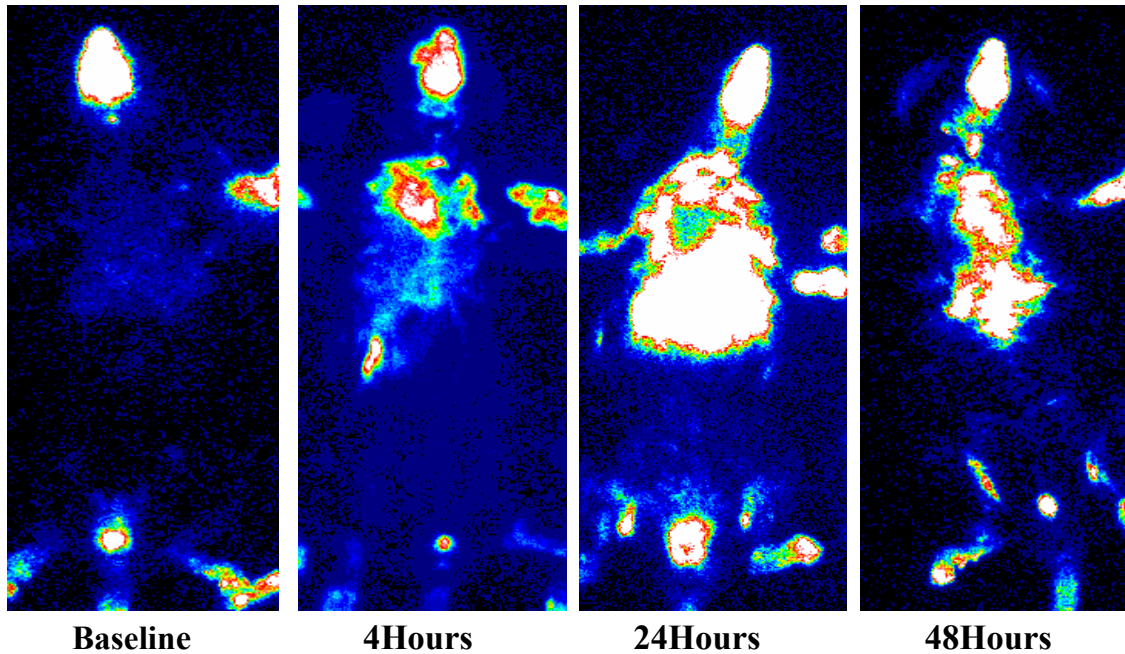


**Figure 18:** Bioluminescence imaging of NGL mice after a single IT injection of LPS (75 µg). Low level NF-κB activity is detected in the lung at baseline. A modest increase in NF-κB activity is detected in the lung 4 hours after IT LPS administration. The highest level of NF-κB activity occurs 24 hours after IT LPS administration followed by a substantial decrease at 48 hours. Images are representative of two separate experiments.

observed in the lung 4 hours after IT LPS (Figure 19). The majority of lung inflammation occurred 24 hours after treatment as demonstrated by a significant increase in neutrophil influx in vessels and interstitium. A significant difference in the number of neutrophils was detected 24 hours after IT LPS (compared to baseline, 4, and 48 hours) and between the 24 and 48 hours time-points ( $p < 0.05$ ) (Figure 15). The cellular contribution to the NF-κB bioluminescence signal once again consisted of airway epithelium, macrophages, neutrophils, and endothelium; however, the timing of NF-κB activation as detected by GFP immunohistochemistry differed

from the IP and Pump groups in that strong NF- $\kappa$ B activity did not occur until 24 hours after IT LPS (Figure 19). The mechanism behind the difference in timing of NF- $\kappa$ B activation between the IP and IT LPS groups is unclear; however, it does not appear to be dose dependent, since

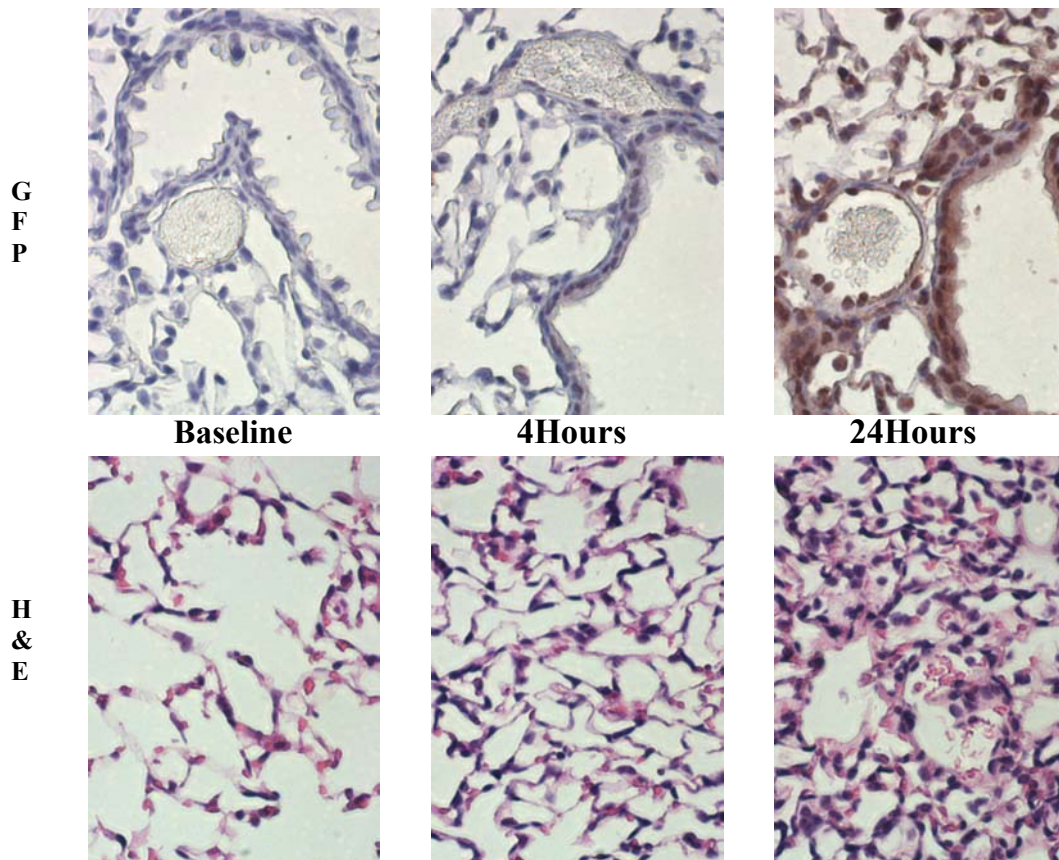


**Figure 19:** GFP immunohistochemistry and H&E histology of lung tissue from NGL mice administered a single intratracheal injection of 3  $\mu$ g/g LPS.

each group receives approximately 75  $\mu$ g LPS per mouse. These data show that IT LPS challenge activates NF- $\kappa$ B in multiple lung cell types similar to IP and Pump LPS, but with a delayed response.

### *Pseudomonas aeruginosa* Model of Lung Inflammation

To study the role of NF- $\kappa$ B in the regulation of bacterial lung inflammation, NGL mice were administered a single intratracheal injection of  $10^6$  cfu *Pseudomonas aeruginosa*. *In vivo* NF- $\kappa$ B activity was detected by bioluminescence imaging (baseline, 4, and 24 hours after IT

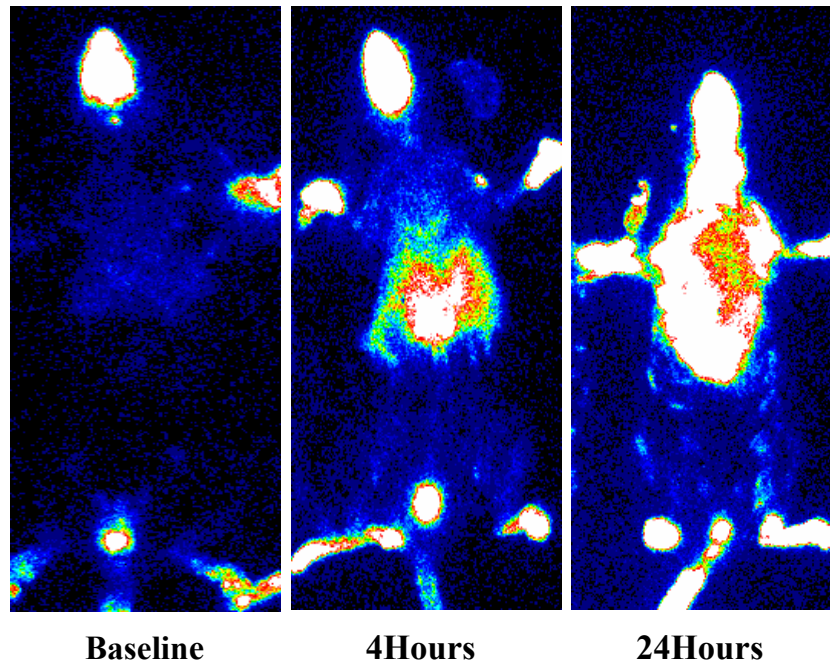


**Figure 20:** Bioluminescence imaging of NGL mice after a single IT injection of  $10^6$  cfu *Pseudomonas aeruginosa*. Low level NF- $\kappa$ B activity is detected in the lung at baseline. A slight increase in NF- $\kappa$ B activity is detected 4 hours after IT *Pseudomonas* followed by a considerable increase at 24 hours. Images are representative of two separate experiments.

*Pseudomonas*) (Figure 20). A modest increase in lung NF- $\kappa$ B activity was detected 4 hours after IT *Pseudomonas* injection followed by a significant increase at 24 hours. These observations reflected the photon counts measured over the thorax (Figure 13). Histology correlated with bioluminescence in that few neutrophils were observed in the lung 4 hours after IT *Pseudomonas*, followed by increased neutrophil influx in vessels and interstitium at 24 hours

(Figure 21). A significant increase in neutrophils was detected 24 hours after IT *Pseudomonas* compared to baseline and 4 hours after IT *Pseudomonas* (Figure 15). The cellular contribution to the bioluminescence signal was different than the three methods of *E. coli* LPS delivery described above (Figure 21). At 4 hours, only airway epithelium and a few scattered macrophages were GFP+. No significant NF-κB activity was detected in endothelium as seen in

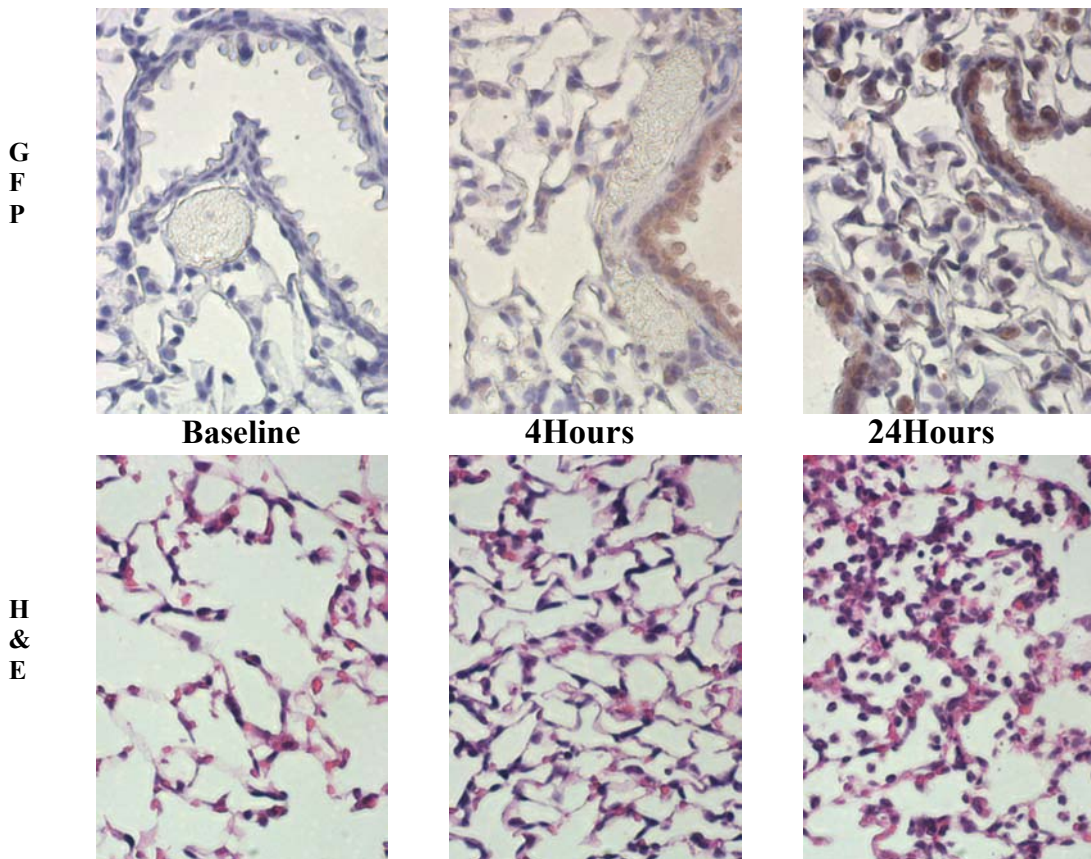


**Figure 21:** GFP immunohistochemistry and H&E histology of lung tissue from NGL mice administered a single IT injection of  $10^6$  cfu *Pseudomonas aeruginosa*.

the LPS groups. Twenty-four hours after *Pseudomonas* injection, airway epithelium displayed an increase in GFP staining intensity and distinct GFP+ macrophages and neutrophils were identified. Taken together, these data demonstrate that the pattern of cellular NF-κB activation

reflects both the type of stimulus (*E. coli* LPS or *Pseudomonas*) and the method of delivery (IP or IT).

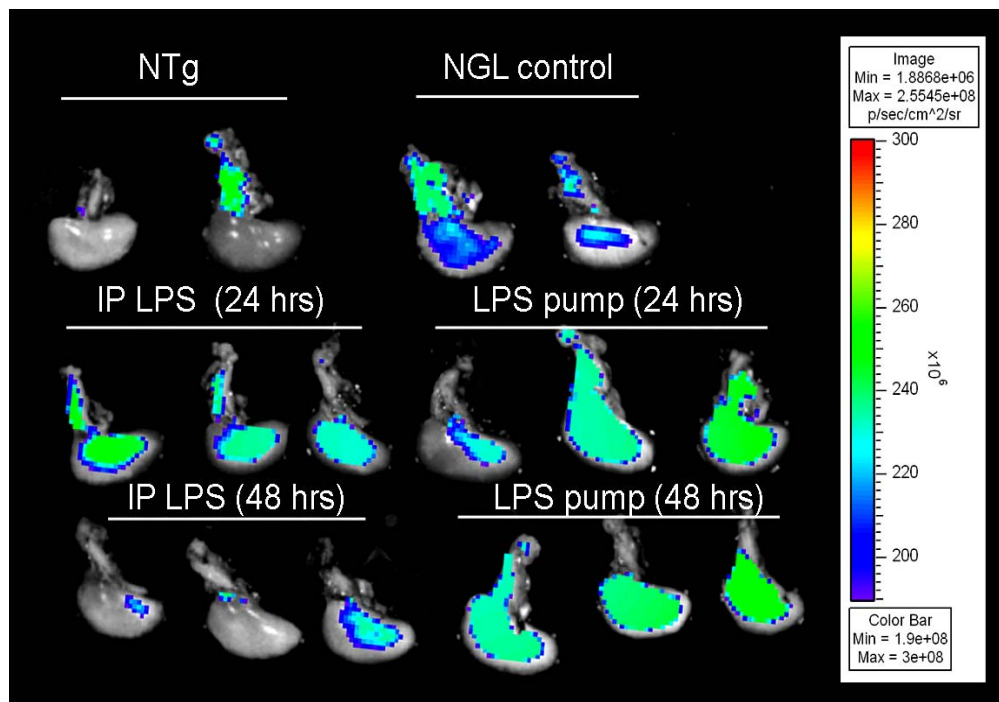


**Figure 22:** *Ex vivo* detection of GFP fluorescence from lungs of NGL mice after IP and IP pump LPS administration. NGL mice were administered LPS by either a single IP injection (3  $\mu\text{g/g}$ ) or IP implantation of an osmotic pump (8  $\mu\text{g}/\text{hour}$  for 24 hours). Lungs were surgically removed after 24 or 48 hours and GFP fluorescence image acquired using the IVIS Imaging System. Images are representative of two separate experiments.

#### Detection of Lung NF- $\kappa$ B Activity by *Ex vivo* GFP Fluorescence Imaging

NGL mice were administered LPS by either a single IP injection or by implantation of an osmotic pump in the intraperitoneal space as previously described. Lungs were removed after 24 or 48 hours and GFP detected by fluorescence imaging using an IVIS System (Xenogen, Alameda, CA) (Figure 22). *Ex vivo* GFP fluorescence correlated with *in vivo* bioluminescence

photon emission. Lung GFP fluorescence increased in both IP LPS and Pump LPS groups at 24 hours (Figure 23). After 48 hours, the IP LPS group returned to baseline, while GFP

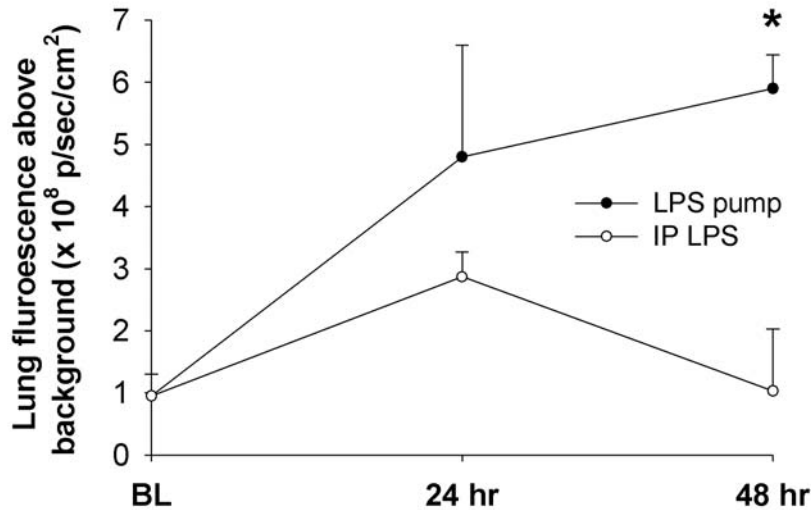


**Figure 23:** *Ex vivo* detection of GFP fluorescence photon counts from lungs of NGL mice after IP and IP pump LPS administration. An increase in GFP fluorescence was detected in both groups 24 hours after LPS administration. At 48 hours after LPS, a significant difference in GFP fluorescence was detected between the IP and IP pump groups ( $p < 0.05$ ). Each bar represents mean  $\pm$  SEM of 2 or 3 samples per group.

fluorescence in the Pump LPS group continued to increase, resulting in a significant difference in lung GFP fluorescence at this time.

#### Detection of NF- $\kappa$ B Activity in Bronchoalveolar Lavage Cells by FACS after IT LPS

In the previous studies, the detection of NF- $\kappa$ B activity by GFP was performed by immunohistochemistry on lung tissue sections. As an alternative method to monitor lung inflammation, we investigated the ability to detect NF- $\kappa$ B activation in bronchoalveolar lavage

cells (macrophages and neutrophils) by FACS. NGL mice were administered 75  $\mu$ g LPS by IT injection. After 24 hours, bronchoalveolar lavage cells were collected and analyzed by FACS to

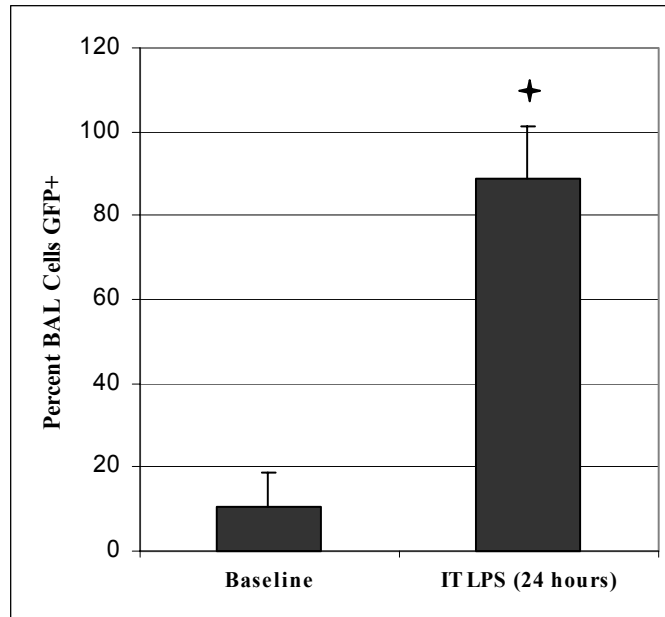


**Figure 20:** Detection of GFP+ bronchoalveolar cells by FACS from NGL mice 24 hours after administration of a single IT injection of LPS (75 mg). At baseline, 10.56 +/- 8.23% of bronchoalveolar cells are GFP+. A significant increase in GFP+ bronchoalveolar cells (88.56 +/- 12.53%) was detected after IT LPS administration ( $p < 0.01$ ). Each bar represents mean +/- SEM of 4 samples per group. Data is representative of two separate experiments.

identify NF- $\kappa$ B activation by GFP detection. In untreated NGL mice, 10.56 +/- 8.23% of lavage cells were GFP+ (Figure 24). After IT LPS, a significant increase in the number of GFP+ lavage cells was detected (88.56 +/- 12.53%). These data correlate with the detection of increased numbers of GFP+ macrophages and neutrophils in the lung 24 hours after IT LPS by GFP immunohistochemistry. The ability to detect NF- $\kappa$ B activation, and thus lung inflammation, *ex vivo* in BAL cells provides an efficient method to monitor the response to a variety of inflammatory stimuli *in vivo*.

## Summary

Developing effective and practical therapeutic interventions that modulate the NF- $\kappa$ B signal transduction pathway demands a thorough understanding of the initiation, duration, and intensity of NF- $\kappa$ B activation in all relevant cell types. We have demonstrated that the timing and cell-specific pattern of NF- $\kappa$ B activity in the lung changes depending on the stimulating agent (*E. coli* LPS vs. *Pseudomonas*) and the method of delivery (IP, IT, and IP Pump LPS). These data highlight the importance of studying biological processes in a natural, intact environment in order to correctly elucidate the pathways and mechanisms involved.

Several important findings are derived from this new model. In the context of LPS induced lung inflammation, NF- $\kappa$ B activation occurs in multiple cell types (macrophage, neutrophil, epithelium, endothelium). Since the receptor for LPS (Toll-like receptor 4, TLR4) is not believed to be expressed in all of these cell types, the NF- $\kappa$ B activation observed in cells which do not express TLR4 must result from indirect activation by TLR4 expressing cells, most likely through cytokine and chemokine signaling networks. Also, the timing of NF- $\kappa$ B activation in different cell types changes depending on the method of LPS delivery. Compared to IP LPS administration, we observed prolonged NF- $\kappa$ B activation after IP Pump LPS and delayed activation after IT LPS in airway epithelium, macrophages, neutrophils, and endothelium. Since NF- $\kappa$ B may perform different functions in different cell types, global inhibition of NF- $\kappa$ B in the lung may not be beneficial to the host. Therefore, targeting NF- $\kappa$ B therapeutically not only requires an understanding of the cell types involved, but also knowledge about the timing and duration of NF- $\kappa$ B activation in those specific cells.

While bioluminescence imaging is a powerful methodology for *in vivo* detection of NF- $\kappa$ B dependent gene expression, some limitations remain. Photon emission can be detected at the

organ level; however, more specific or three dimensional localization of the signal is currently not possible. The GFP/Luciferase reporter protein in the NGL model provides the ability to detect NF- $\kappa$ B activity at the organ level, but provides a tool to detect NF- $\kappa$ B activity at the cellular level. Therefore, the NGL transgenic reporter mouse model provides several advantages over conventional methods for studying NF- $\kappa$ B *in vivo*. Bioluminescence imaging allows multiple images in the same mouse over time, reducing the number of mice needed for each experiment and enabling each mouse to serve as its own control. When NF- $\kappa$ B activity is detected in a target organ by bioluminescence, the organ can be analyzed to determine the cell-specific contribution to that signal by GFP fluorescence microscopy and immunohistochemistry. The ability to study signal transduction pathways in complex biological systems will provide a more meaningful and realistic interpretation of results.

In conclusion, the NGL transgenic reporter model provides a powerful tool for the study of the NF- $\kappa$ B signal transduction pathway *in vivo* and will hopefully lead to important discoveries in the role of NF- $\kappa$ B in development, tumorigenesis, inflammation, and other biological processes.

### **Future Directions**

The ability to study the role of activators and inhibitors of the NF- $\kappa$ B pathway will be investigated in future experiments. For example, we have recently obtained a selective IKK2 inhibitor which can be given by i.v. or oral administration. We plan to investigate the ability of this compound to inhibit LPS induced lung inflammation in the NGL model, identifying inhibition in specific cell-types and the result on neutrophil influx and lung injury.

We have begun initial experiments to investigate the role of NF- $\kappa$ B in specific tissues and cell types during embryonic development using the NGL model. Because of the relatively short half-life of the GFP/Luciferase reporter protein, these studies should provide a better timeline for NF- $\kappa$ B activation compared to studies which utilize proteins with a longer half-life such as  $\beta$ -galactosidase (half-life 24 hours).

## KINETICS OF ALVEOLAR MACROPHAGE REPOPULATION FOLLOWING FETAL LIVER TRANSPLANTATION

### **Introduction**

Investigating unique signaling pathways in pulmonary macrophages in the context of complex animal models is a challenging but attractive approach to unraveling the complexities of the biological processes that lead to inflammation and lung disease. The ability to utilize cell-specific transgenic and knockout mouse technology is limited by the lack of reliable, highly functional macrophage restricted promoters or other techniques that specifically isolate the functional contribution of macrophages. In order to study the role of specific genes in lung macrophages, we have developed a method to maximally repopulate alveolar macrophages with cells that have altered genotypes. We have utilized lethal irradiation followed by fetal liver transplantation in order to reconstitute bone marrow by hematopoietic stem cells from fetal livers. FLT, in contrast to bone marrow transplantation from adult animals, results in immune tolerance for donor cells, absence of graft-versus-host responses, and the ability to use genetically modified donors that do not survive beyond embryonic day 15 (E15) (Horwitz, 1997; Mizgerd, 1999; Royo, 1987). The counterpart of the adult bone marrow common lymphoid progenitor in E14 fetal liver was recently identified and was shown to give rise to all lymphoid

lineages, including the macrophage (Mebius, 2001). While this approach has been applied to specifically reconstitute perivascular macrophages with cells of altered genotype/phenotype for study in atherosclerosis (Fazio, 1997; Linton, 1995), data applying this methodology to the study of lung macrophages are few. A major obstacle to this experimental approach is that resident lung macrophages are long-lived, and incomplete reconstitution by donor cells can lead to ambiguous phenotypes that confound interpretation of results.

In the lungs, the extent and timing of alveolar macrophage reconstitution is not well defined; therefore, we undertook studies to determine the kinetics of alveolar macrophage reconstitution following FLT. Fetal liver transplant experiments were performed using transgenic donors (Nagy GFP) that constitutively express GFP under the control of the cytomegalovirus immediate early enhancer coupled to a  $\beta$ -actin promoter. After determining the percentage reconstitution of peripheral blood monocytes by fluorescence activated cell sorting (FACS), repopulation of alveolar macrophages with donor-derived macrophages in bone marrow chimeric mice was determined by identifying recipient and donor macrophages by immunohistochemistry on tissue sections and FACS analysis of macrophages obtained by bronchoalveolar lavage. We reasoned that elimination of residual recipient macrophages following FLT would accelerate repopulation with donor-derived cells. To eliminate alveolar macrophages, we administered liposomal clodronate by intratracheal (IT) injection. This treatment has been shown to result in selective apoptosis of macrophages (Berg, 1993; van Rooijen, 1994b). We administered clodronate at 6 weeks after FLT, a time point at which peripheral blood monocytes were reconstituted but alveolar macrophages were still predominantly of recipient genotype. In these studies, we demonstrate that clodronate treatment

accentuated repopulation of macrophages and resulted in a greater proportion of alveolar macrophages that displayed the donor genotype.

## **Results**

### Kinetics of Peripheral Blood Monocyte Reconstitution

To determine the kinetics of alveolar macrophage repopulation after fetal liver transplantation, bone marrow chimeric mice were generated using transgenic Nagy GFP mice as donors and WT mice as recipients. GFP was used as a marker to track cellular repopulation following lethal irradiation and FLT. Initial experiments were performed 4 weeks after FLT to determine the extent of reconstitution of peripheral blood monocytes (PBM). To evaluate PBM reconstitution, the percentage of donor derived monocytes in the peripheral blood of bone marrow chimeras was determined by FACS analysis. The monocyte population was identified by forward and side scatter characteristics and by positive labeling with anti-CD11b conjugated phycoerythrin (PE) and anti-Gr-1 conjugated allophycocyanin (APC) antibodies (Lagasse, 1996) (Figure 25). The donor monocyte population was identified by detection of endogenous GFP fluorescence in addition to CD-11b and Gr-1 positivity. Figure 25, A and B, demonstrate the selection of the monocyte population from peripheral blood of an untreated Nagy GFP transgenic control animal. Figure 25, C demonstrates the number of CD11b<sup>+</sup>/Gr-1<sup>+</sup> monocytes that were

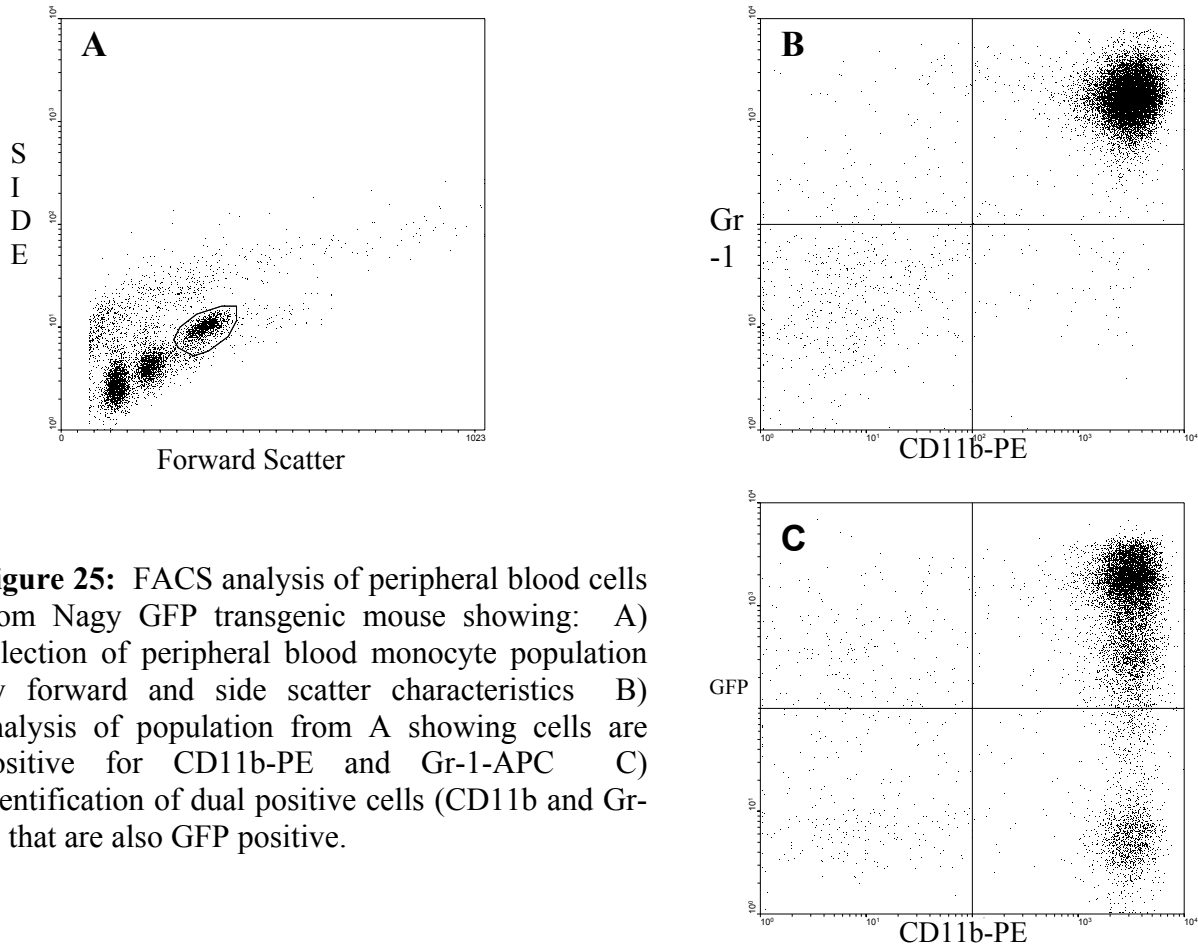


**Figure 25:** FACS analysis of peripheral blood cells from Nagy GFP transgenic mouse showing: A) selection of peripheral blood monocyte population by forward and side scatter characteristics B) analysis of population from A showing cells are positive for CD11b-PE and Gr-1-APC C) identification of dual positive cells (CD11b and Gr-1) that are also GFP positive.

also GFP+. Compared with untreated Nagy GFP controls, 85.7 +/- 1.6% of CD11b+/Gr-1+ monocytes were GFP+ four weeks after FLT in Nagy GFP/WT chimeras, demonstrating near complete reconstitution of peripheral blood monocytes at this time (Figure 26).

In initial experiments, we observed that few alveolar macrophages were of donor origin 4 weeks after FLT. Therefore, subsequent experiments were performed in which mice were harvested 10 weeks after FLT. We hypothesized that elimination of resident recipient macrophages (after peripheral blood monocytes were reconstituted) would enhance repopulation of alveolar macrophages by cells of donor origin. To achieve this goal, mice were treated with IT administration of liposomal clodronate 6 weeks following FLT, a time point at which

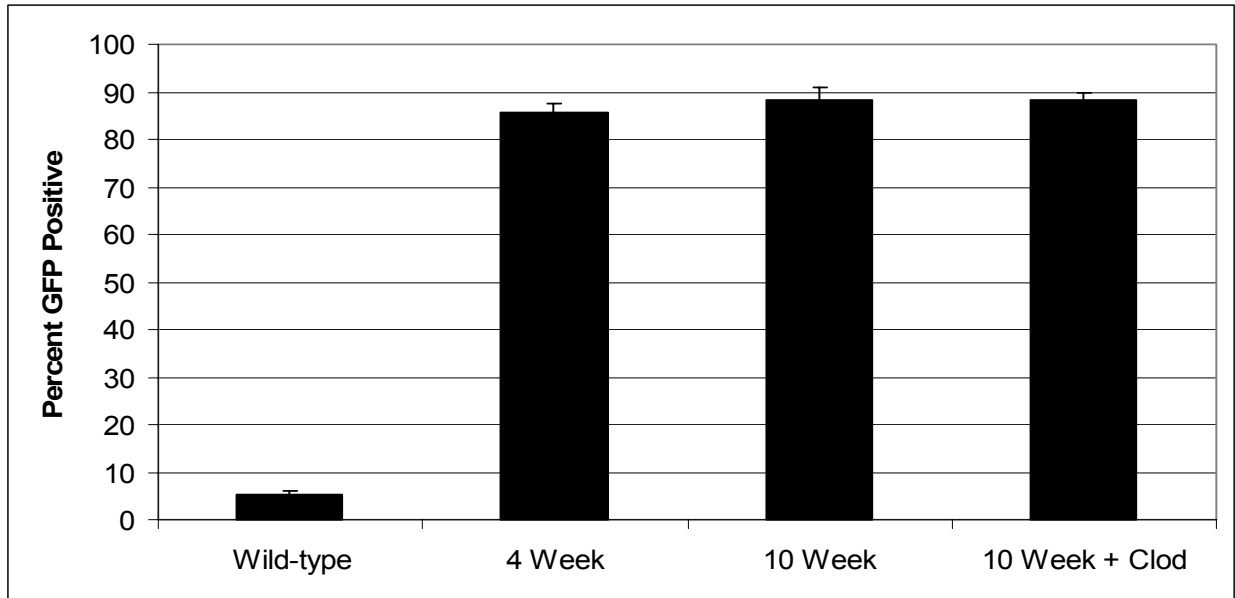


**Figure 26:** Kinetics of peripheral blood monocyte reconstitution following fetal liver transplantation (FLT) with GFP<sup>+</sup> donor cells. CD11b/Gr-1 dual positive monocytes were analyzed by FACS to determine the percentage that were GFP<sup>+</sup> (donor genotype) in the following groups: wild-type mice, chimeric mice 4 weeks after FLT with GFP<sup>+</sup> donor cells (4 week), chimeric mice 10 weeks after FLT with GFP<sup>+</sup> donor cells (10 week), and chimeric mice 10 weeks after FLT + treatment with liposomal clodronate (10 week + Clod). Each bar represents the mean  $\pm$  SEM of 7 mice per group.

peripheral blood leukocytes were predominantly of donor origin. Mice were then analyzed at 10 weeks following FLT to determine the degree of peripheral blood monocyte and alveolar macrophage reconstitution. All experiments were performed using untreated Nagy GFP and WT mice as controls. Compared to the 4 week time point, there was no significant increase in the number of donor-derived PBMCs at 10 weeks post-FLT (88.1%  $\pm$  2.9 and 88.3%  $\pm$  1.6 GFP positive monocytes in the 10 week and 10 week + clodronate groups, respectively) (Figure 26).

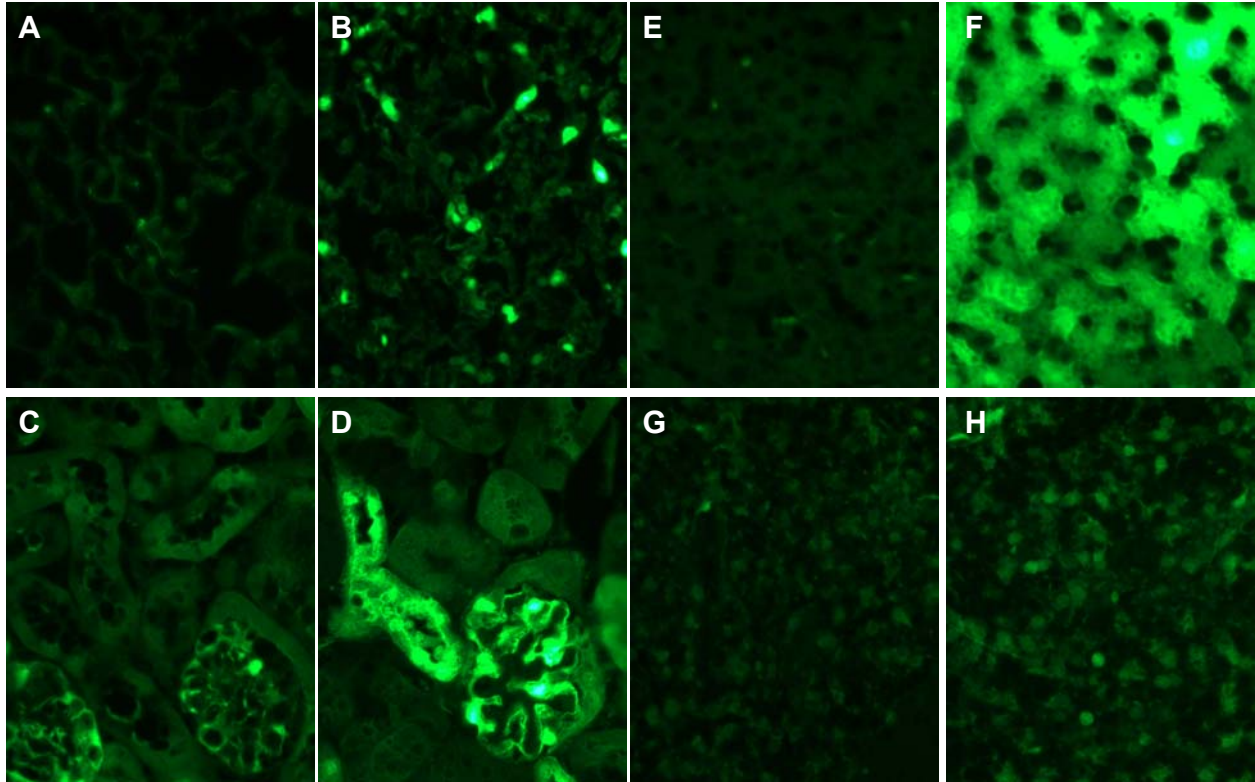


**Figure 27:** Fluorescence microscopy of lung, liver, spleen, and kidney tissue sections from Nagy GFP mice. Tissues were fixed for 24 hours at 4<sup>0</sup>C in either 4% Paraformaldehyde [lung (A), kidney (C), liver (E), spleen (G)] or 10% Neutral Buffered Formalin [lung (B), kidney (D), liver (F), spleen (H)].

---

### Fixation Affects the Detection of GFP by Fluorescence Microscopy and Immunohistochemistry

In initial experiments, the detection of GFP+ macrophages by fluorescence microscopy and immunohistochemistry in untreated Nagy GFP lung tissue sections was variable and unreliable. The consensus within the literature for the analysis of GFP in paraffin embedded tissue was to use 4% paraformaldehyde (PFA) as the fixative. We investigated the effects of fixation on the ability to detect GFP in various organs of Nagy GFP mice by fluorescence microscopy and immunohistochemistry. Figure 27, shows the detection of GFP in lung, liver,

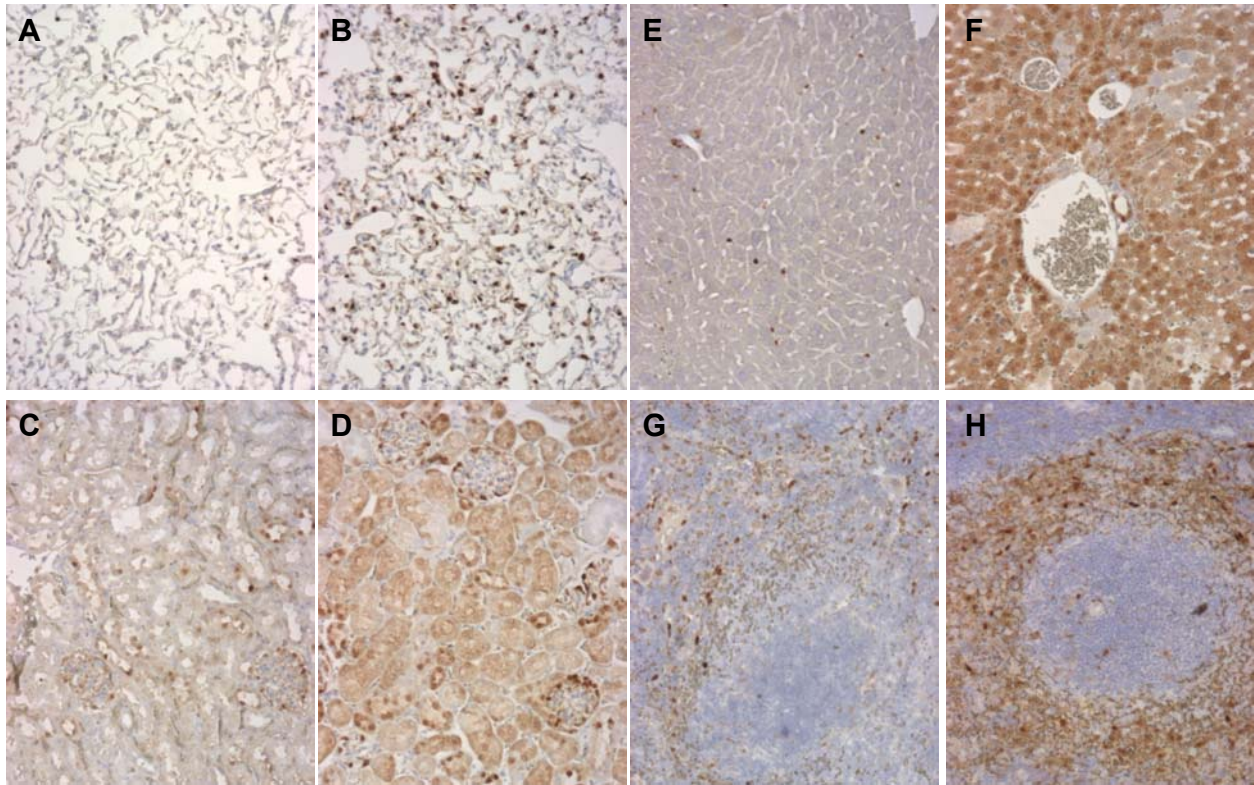


**Figure 28:** GFP immunohistochemistry of lung, liver, spleen, kidney tissue sections from Nagy GFP mice. Tissues were fixed for 24 hours at 4<sup>0</sup>C in either 4% Paraformaldehyde [lung (A), kidney (C), liver (E), spleen (G)] or 10% Neutral Buffered Formalin [lung (B), kidney (D), liver (F), spleen (H)].

spleen, and kidney by fluorescence microscopy after either 4% PFA or 10% Neutral Buffered Formalin (NBF) fixation at 4<sup>0</sup>C for 24 hours. The ability to detect GFP+ specific cell populations is greatly enhanced by 10% NBF fixation in all organs examined, especially the identification of alveolar macrophages (Figure 27, A and B). In addition to increased fluorescence detection using NBF, compared to PFA, the intensity and specificity of GFP immunohistochemistry is enhanced as demonstrated in Figure 28. While the specific mechanism for improved detection of GFP using NBF remains unclear, optimal detection is critical for using GFP as a cellular marker to study the kinetics of alveolar macrophage repopulation after FLT. All subsequent experiments were performed using NBF fixation at 4<sup>0</sup>C for 24 hours.

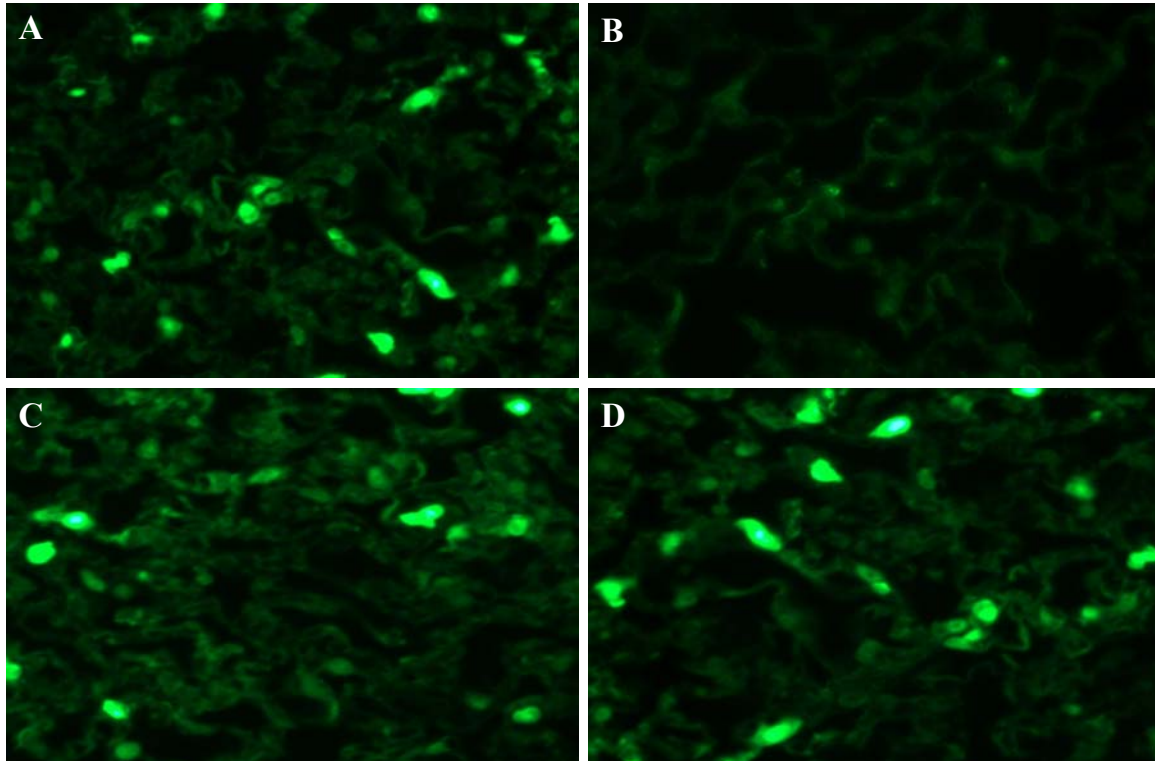


**Figure 29:** Fluorescence microscopy of lung tissue sections showing GFP+ cells in the following groups: A) Nagy GFP transgenic mouse, B) wild-type mouse, C) chimeric mouse 10 weeks after FLT with Nagy GFP+ donor cells, D) chimeric mouse 10 weeks after FLT + treatment with liposomal clodronate.

---

#### Identification of Donor Macrophages in the Lung by Fluorescence Microscopy

We evaluated lung tissue sections to determine the extent of repopulation of resident alveolar macrophages with GFP+ donor macrophages after FLT. Distinct GFP+ cells, primarily macrophages as identified by morphology and location, were visible in Nagy GFP untransplanted controls (Figure 29, A). No brightly green fluorescent cells were observed in untransplanted WT controls (Figure 29, B). At 10 weeks after FLT, green fluorescent cells with the characteristic appearance of macrophages were observed in the lungs (Figure 29, C). Increased numbers of GFP+ cells were observed in lung tissue sections of clodronate treated

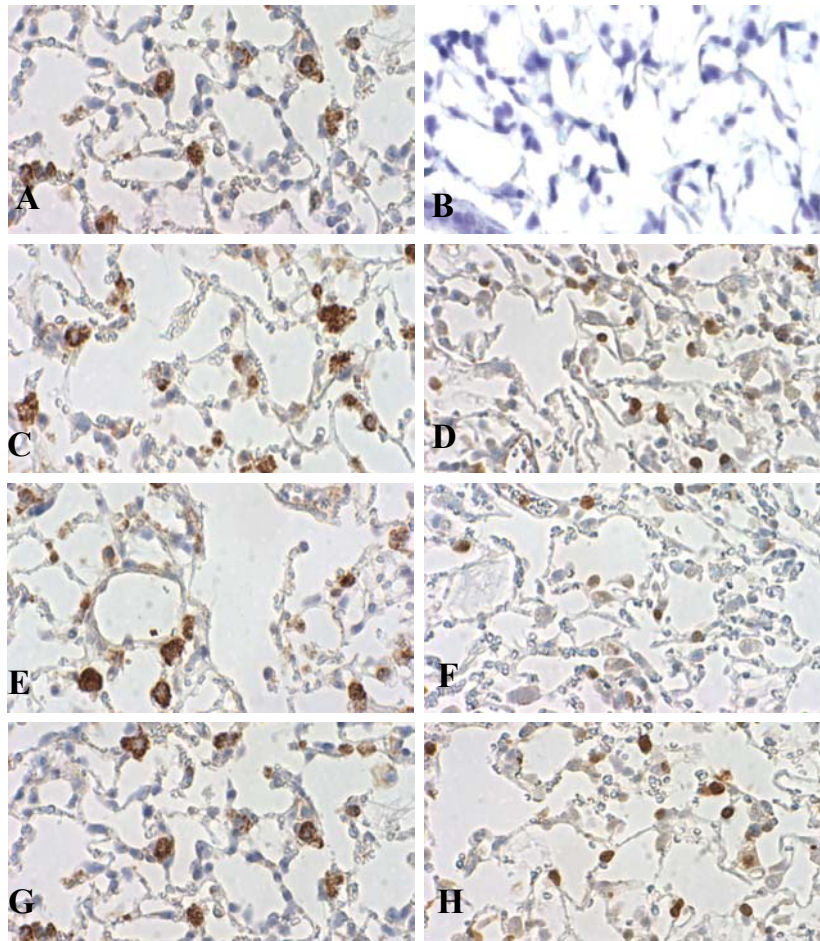


**Figure 30:** Immunohistochemistry of lung tissue sections using anti-CD68 and anti-GFP antibodies to identify all macrophages (CD68) and donor-derived (GFP+) cells following FLT. Wild-type controls stained for CD68 (A) and GFP (B) demonstrate CD68+ cells but no GFP+ cells, whereas Nagy GFP transgenic mice showed equal numbers of CD68+ (C) and GFP+ (D) cells. In chimeric mice 10 weeks after FLT with GFP+ donor cells, immunostaining for CD68 (E) and GFP (F) shows similar numbers of CD68+ cells compared to untreated controls, but fewer GFP+ than CD68+ macrophages. In chimeric mice treated with liposomal clodronate 6 weeks after FLT, the number of CD68+ cells (G) was unchanged but GFP+ macrophages (H) were increased compared to mice undergoing FLT without subsequent clodronate treatment.

mice 10 weeks following FLT (Figure 29, D); however, the inability to identify all macrophages with confidence warranted the use of an additional method to quantify alveolar macrophage repopulation.

#### Quantification of Donor Alveolar Macrophage Repopulation in the Lung by Immunohistochemistry and Tissue Cell Counts

To better quantify the extent of lung macrophage repopulation after FLT, immunohistochemistry was used to identify alveolar macrophages using an anti-CD68 antibody (Lang, 2002) and cells of donor origin using an anti-GFP antibody. Serial sections were stained

and alveolar macrophage repopulation was quantified by counting CD68<sup>+</sup> and GFP<sup>+</sup> macrophages in 10 high power fields of lung parenchyma per slide (Figure 30). Figure 31 illustrates the number of CD68<sup>+</sup> and GFP<sup>+</sup> macrophages observed in each treatment group. CD68 immunostaining revealed no significant differences in the number of macrophages in untreated Nagy GFP and untreated WT controls. Comparatively, CD68<sup>+</sup> macrophage numbers were similar at 4 and 10 weeks after FLT (with or without clodronate treatment). No GFP<sup>+</sup> macrophages were identified in untransplanted WT controls, and 4 weeks after FLT, only 1.4 +/- 0.4 cells per field were identified as immunoreactive for GFP, representing 9.5 percent of total macrophages (Figure 31). By 10 weeks after FLT, however, there were 6.8 +/- 0.4 GFP<sup>+</sup> macrophages per field, representing 48 percent of total macrophages. Mice treated with clodronate displayed a significant increase in GFP<sup>+</sup> macrophages (14.4 +/- 0.5, representing 90 percent of total macrophages) as compared to untreated 10 week FLT chimeras (p<0.001). No epithelial or endothelial cells in the lung were observed to be GFP<sup>+</sup> at any time point after FLT.

#### Quantification of Donor Alveolar Macrophage Repopulation in the Lung by Bronchoalveolar Lavage Macrophage FACS Analysis

In addition to immunostaining of lung sections, alveolar macrophage repopulation was evaluated by FACS. Lung lavage cells were purified and stained with an anti-CD11b-PE antibody to identify macrophages. Repopulation was evaluated by determining the number of

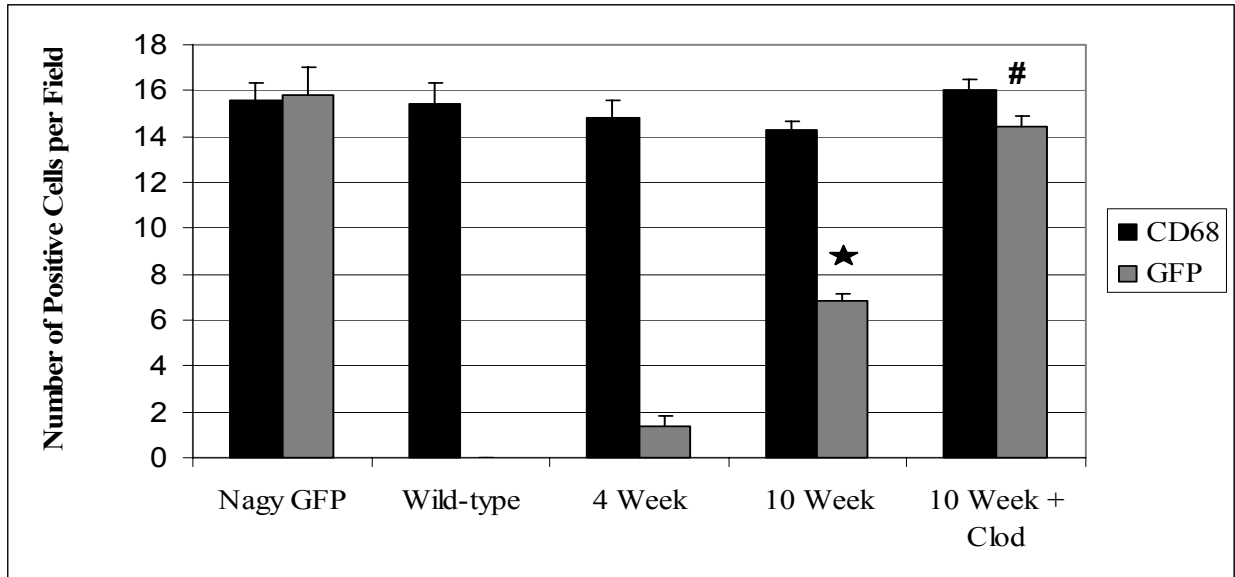


**Figure 31:** Quantification of total lung and GFP+ macrophages. Serial lung sections were immunostained to identify the macrophage population (anti-CD68) and donor-derived cells (anti-GFP) in the following groups: Nagy GFP transgenic mice, wild-type mice, chimeric mice 4 weeks after FLT with GFP+ donor cells (4 week), chimeric mice 10 weeks after FLT with GFP+ donor cells (10 week), and chimeric mice 10 weeks after FLT + treatment with liposomal clodronate (10 week + Clod). Positive cells per field from ten sequential non-overlapping fields per slide were counted. Each bar represents the mean number of positive cells per field +/- SEM. N=8 mice per group. \* =  $p < 0.001$  between 4 week GFP+ cells and 10 week GFP+ cells, and # =  $p < 0.001$  between GFP+ cells in the 10 week group and GFP+ cells in 10 week + Clod group.

CD11b+ macrophages that were also GFP+. In untreated Nagy GFP and wild-type controls, 93.0% +/- 1.2 and 2.3% +/- 0.5 of macrophages were identified as GFP+, respectively (Figure 32). Ten weeks after FLT, 55.1% +/- 1.6 of alveolar macrophages were GFP+, similar to the number of donor macrophages identified in lung tissue sections. In mice treated with clodronate, 81.4% +/- 4.1 of alveolar macrophages were GFP+ (87.5% of Nagy positive control), demonstrating a significant increase over non-clodronate treated bone marrow chimeric mice at 10 weeks. These data show that elimination of resident alveolar macrophages by liposomal clodronate treatment improves alveolar macrophage repopulation in bone marrow chimeric mice.

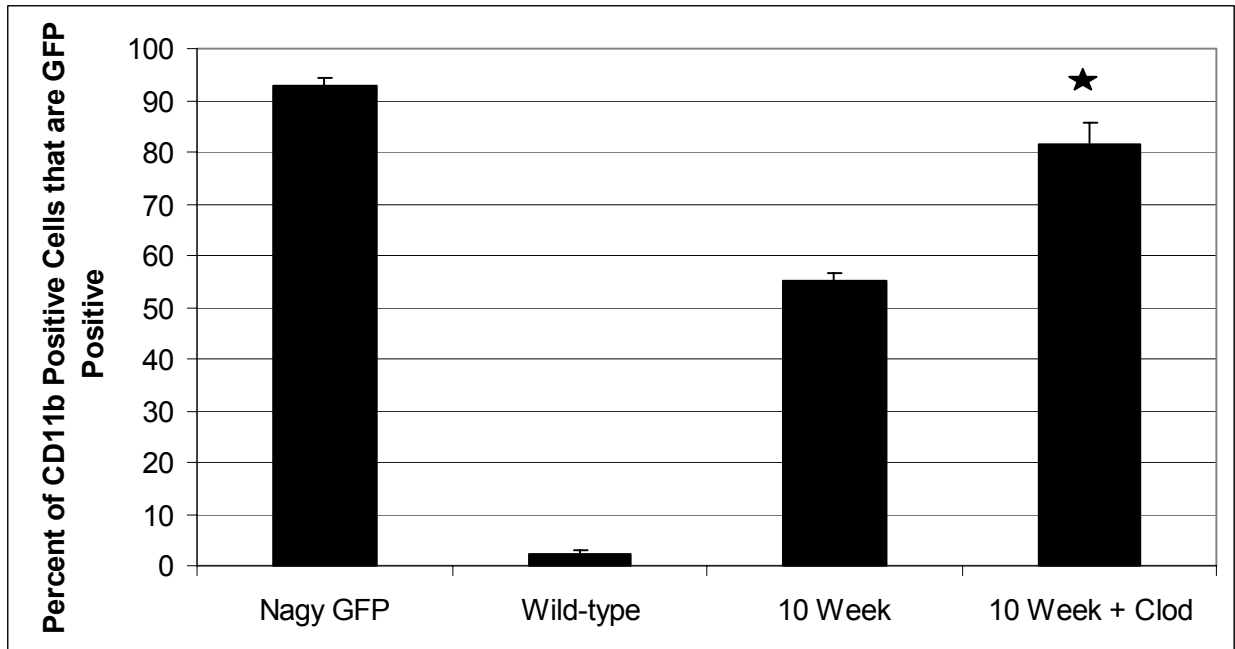


**Figure 32:** Quantification of GFP+ alveolar macrophages in lung lavage from Nagy GFP transgenic mice, wild-type mice, chimeric mice 10 weeks after FLT with GFP+ donor cells (10 week), and chimeric mice 10 weeks after FLT + treatment with liposomal clodronate (10 week + Clod). Cells were collected, labeled with anti-CD11b-PE antibody and analyzed by FACS to determine the percent of CD11b+ cells that were of GFP+. Each bar represents the mean +/- SEM. N=6 mice per group. \* = p<0.001 between 10 week GFP+ cells and 10 week + clodronate GFP+ cells.

By 10 weeks, high level repopulation of alveolar macrophages by cells of donor genotype can be achieved.

#### Investigation of Alveolar Macrophage Function in FLT Chimeras

To ensure that newly recruited donor macrophages in FLT chimera mice maintained normal functions, *Pseudomonas aeruginosa* clearance was investigated in WT and Nagy GFP FLT chimeras. Alveolar macrophages and neutrophils have been shown to be critical in regulating *Pseudomonas aeruginosa* clearance (Kooguchi, 1998). *Pseudomonas* ( $10^6$  cfu) was

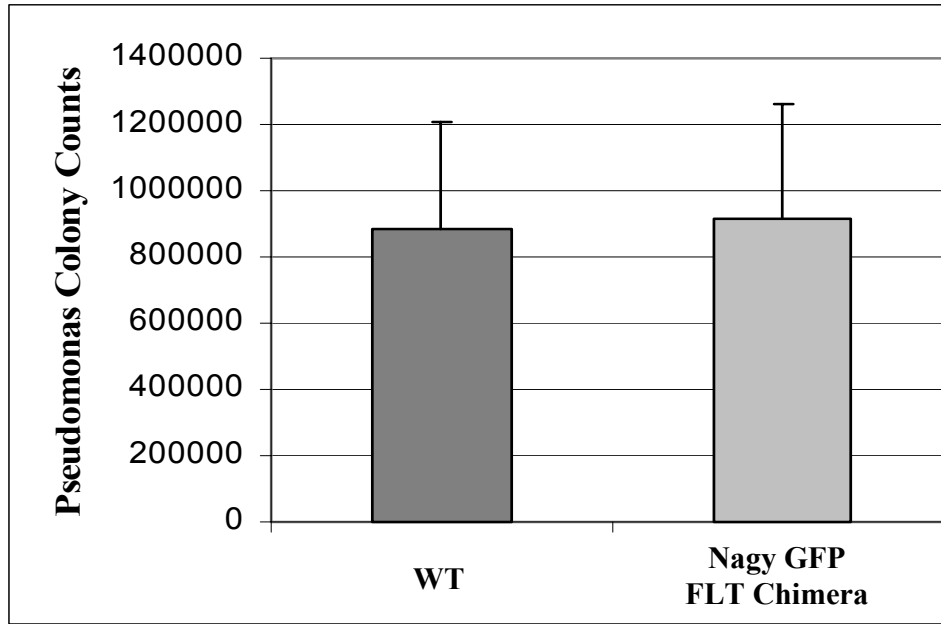


**Figure 33:** *Pseudomonas aeruginosa* clearance in WT and Nagy GFP FLT chimeras 24 hours after  $10^6$  cfu administration. No difference in *Pseudomonas aeruginosa* colony counts from the lung was observed between the two groups.

administered by IT injection. After 24 hours, lungs were harvested and *Pseudomonas* colony counts determined (Figure 33). No difference was detected between WT and Nagy GFP FLT chimeras, suggesting that macrophage and neutrophil function in regulating the clearance of *Pseudomonas aeruginosa* was intact in FLT chimeras.

### Summary

We have demonstrated that alveolar macrophage repopulation after lethal irradiation and FLT is a process that can be enhanced by selective depletion of resident alveolar macrophages in the recipient. In peripheral blood, near complete reconstitution of monocytes occurs by 4 weeks after FLT. Lung macrophage repopulation, however, is a slower process and few donor macrophages are observed in the lung at this time. Approximately 50% of alveolar macrophages

are repopulated by macrophages of donor origin 10 weeks after FLT. To maximize repopulation, we eliminated resident alveolar macrophages by IT administration of liposomal clodronate, an agent that causes selective macrophages apoptosis. Through a mechanism of enhanced monocyte recruitment, we were able to increase repopulation of alveolar macrophages 10 weeks after FLT. At this time point, we determined that approximately 90% of alveolar macrophages were derived from the donor by calculating the percentage of CD68+ macrophages that were also GFP+ by immunohistochemistry and lung tissue cell counts. These findings were confirmed by FACS analysis of alveolar macrophages obtained by bronchoalveolar lavage. In addition, FLT chimeras were analyzed 10 months after transplantation. No significant difference in the number of donor alveolar macrophages was detected by immunohistochemistry and lung tissue cell counts or BAL macrophage FACS, suggesting maximal alveolar macrophage repopulation can be achieved 10 weeks after FLT when recipient macrophages are selectively eliminated, stimulating repopulation with donor derived monocytes.

Prior studies have not adequately clarified the kinetics of lung macrophage repopulation following bone marrow transplantation or FLT. In the literature, the reported rate of repopulation varies greatly. For example, one study investigated the migration of donor cells from GFP positive transgenic mice into several tissues in bone marrow chimeras (Ono, 1999). GFP+ cells were detected in lung sections by fluorescence microscopy and verified as macrophages by immunohistochemistry with CD-11b antibodies. Analysis of lung tissue demonstrated donor cells were present at seven days, suggesting rapid repopulation. In a separate study, bone marrow chimeras were generated using ROSA 26 mice to track  $\beta$ -galactosidase positive cells into various organs (Kennedy, 1997). In these experiments, donor cells were not observed in the lung until after one month. Only 61% of lung macrophages were

of donor origin one year after transplant. These data suggest significantly slower kinetics for repopulation of macrophages and imply that achieving complete repopulation is impossible. The efficiency of bone marrow engraftment and subsequent lung macrophage repopulation is likely to depend on several factors, including the method of recipient marrow depletion, the number of donor cells delivered, and the effects of the conditioning treatment on turnover of resident lung macrophages. For example, methods used to deplete recipient marrow ranges from intraperitoneal administration of 5-fluorouracil to lethal irradiation by administering a single dose of radiation (1050 cGy) from a dual cesium source. We utilized a protocol designed to achieve complete marrow depletion while minimizing damage to structural cell components. In our experiments, no histological evidence of radiation induced pneumonitis in the lung was identified 4 or 10 weeks after FLT.

In addition to alveolar macrophages, other bone marrow derived immune cells, such as neutrophils and eosinophils, are reconstituted with cells of donor genotype following FLT; however, these cells are not present in the lungs in substantial numbers in the absence of an inflammatory stimulus. Since lung macrophages serve a sentinel function to initiate innate immune responses in the lungs, it is possible to study their function using a bone marrow chimera strategy. We have demonstrated that alveolar macrophage repopulation can be enhanced by elimination of resident macrophages by treatment with liposomal clodronate, and have defined the extent of alveolar macrophage repopulation using this methodology. This method will allow efficient replacement of alveolar macrophages with macrophages of altered genotype in order to study the role of specific molecules and signal transduction components in macrophages *in vivo*.

# ROLE OF ALVEOLAR MACROPHAGE I $\kappa$ B- $\alpha$ AND p50 IN THE REGULATION OF LUNG INFLAMMATION

## Introduction

While it is known that the NF- $\kappa$ B signal transduction pathway is important in the regulation of lung inflammation, the specific role of NF- $\kappa$ B in individual cell types in the lung remain unclear. In order to obtain meaningful results from *in vivo* experiments designed to investigate the NF- $\kappa$ B pathway, it is necessary to ensure that all of the cellular and signaling pathways are intact. For example, Alcamo et al. (Alcamo, 2001) investigated the role of RelA in neutrophil emigration using an *E. coli* LPS intranasal insufflation model. RelA-deficient mice exhibit embryonic lethality secondary to liver apoptosis (Beg, 1995b). Therefore, RelA/TNF type I receptor double knockout mice, which rescues the TNF mediated liver apoptosis phenotype, were used to investigate RelA-deficiency *in vivo* (Alcamo, 2001). WT, TNFRI, and TNFRI/RelA deficient mice (P3-5) were administered LPS and neutrophil emigration determined by morphometric analysis. WT and TNFRI mice displayed neutrophil emigration 6 hours after LPS treatment; however, significantly less neutrophils were observed in TNFRI/RelA deficient mice, suggesting RelA is essential for initiating maximal neutrophil emigration in the lung in response to LPS. To determine if the above observation resulted from the inability of TNFRI/RelA deficient neutrophils to be recruited to inflammatory loci, FLT was performed using TNFRI, RelA, and TNFRI/RelA deficient mice as donors and WT mice as recipients. Six weeks after FLT, mice were administered IT LPS and neutrophil emigration was determined by morphometric analysis. Neutrophil emigration was comparable in all three groups, suggesting the emigration defect in the TNFRI/RelA deficient mice was not a cell intrinsic defect of RelA-deficient neutrophils. They suggest that the reduction in neutrophil recruitment in TNFRI/RelA

mice is due to the requirement for RelA in structural cells in addition to macrophages to produce neutrophil chemoattractants. While this may be partially true, they did not adequately monitor alveolar macrophage repopulation in the TNFR1/RelA FLT chimeras. Our alveolar macrophage repopulation kinetics data suggest that at 6 weeks post FLT, repopulation of macrophages is incomplete. The presence of a substantial percentage of WT alveolar macrophages may be sufficient to recruit neutrophils in the TNFR1/RelA FLT chimeras, whereas the reduction in neutrophil recruitment observed in TNFR1/RelA deficient mice may result from the loss of RelA dependent activation in alveolar macrophages. An alternative interpretation of their results is that RelA in alveolar macrophages is not absolutely essential for optimal neutrophil emigration in response to LPS.

To study the role of NF- $\kappa$ B components in hematopoietic cells in the regulation of lung inflammation *in vivo*, we developed a method to replace resident hematopoietic cells with donor cells of an altered genotype (see Chapter IV). Modulation of the NF- $\kappa$ B pathway in hematopoietic cells (macrophages, neutrophils, lymphocytes, etc.) was achieved by using donor fetal liver cells from I $\kappa$ B- $\alpha$ <sup>-/+</sup>, I $\kappa$ B- $\alpha$ <sup>-/-</sup>, or p50<sup>-/-</sup> mice. HLL mice were used as recipients to measure *in vivo* NF- $\kappa$ B activity in structural cells (epithelium, endothelium, etc.) by bioluminescence imaging. Clodronate was administered to all FLT chimeras as described in Chapter IV to ensure maximal repopulation of alveolar macrophages after FLT.

WT, I $\kappa$ B- $\alpha$ <sup>-/+</sup>, I $\kappa$ B- $\alpha$ <sup>-/-</sup>, and p50<sup>-/-</sup> bone marrow chimeras were analyzed for signs of lung inflammation by histology and bioluminescence imaging at baseline and after a single IP injection of LPS (3  $\mu$ g/g). WT chimeras and HLL untransplanted controls exhibited the same response after IP LPS, early (4 hours) NF- $\kappa$ B activation and neutrophil influx which resolved by 24 hours. I $\kappa$ B- $\alpha$ <sup>-/+</sup> chimeras displayed a distinct phenotype characterized by enhanced,

prolonged NF- $\kappa$ B activity and neutrophil influx which resolved 6 days after IP LPS administration. Although the mice appeared ill during the duration of inflammation, no mortality was observed. After IP LPS administration, I $\kappa$ B- $\alpha^{-/-}$  chimeras exhibited a rapid increase in NF- $\kappa$ B activity and neutrophil influx up to 24 hours. Similarly, p50 $^{-/-}$  chimeras displayed a rapid increase in NF- $\kappa$ B activity and neutrophil influx; however, significant mortality (72%) was observed at 48 hours after IP LPS.

Since alveolar macrophages have been shown to be critical in initiating lung inflammation, we investigated NF- $\kappa$ B activation in I $\kappa$ B- $\alpha^{-/+}$  and p50 $^{-/-}$  BMDM $\Phi$  by Western blot for cytoplasmic I $\kappa$ B- $\alpha$  and nuclear RelA. Compared to WT BMDM $\Phi$ , I $\kappa$ B- $\alpha^{-/+}$  and p50 $^{-/-}$  BMDM $\Phi$  demonstrated altered cytoplasmic I $\kappa$ B- $\alpha$  levels at baseline and after LPS treatment. The return to basal levels of I $\kappa$ B- $\alpha$  protein was delayed in I $\kappa$ B- $\alpha^{-/+}$  BMDM $\Phi$ , while p50 $^{-/-}$  BMDM $\Phi$  failed to generate basal levels of I $\kappa$ B- $\alpha$  protein after 24 hours. To determine the affect of modulation of NF- $\kappa$ B on other cell types, a co-culture apparatus was utilized to culture WT, I $\kappa$ B- $\alpha^{-/+}$ , and p50 $^{-/-}$  BMDM $\Phi$  with A549 epithelial cells transfected with the 8x NGL construct. A549 cells exhibited prolonged NF- $\kappa$ B activity in the I $\kappa$ B- $\alpha^{-/+}$ , and p50 $^{-/-}$  BMDM $\Phi$  co-culture in comparison to the WT BMDM $\Phi$  co-culture, suggesting continued NF- $\kappa$ B activation in macrophages drives sustained NF- $\kappa$ B activity in epithelium.

These data suggest that I $\kappa$ B- $\alpha$  and p50 in hematopoietic cells, predominantly macrophages, are critical in coordinating the inflammatory response through regulation of NF- $\kappa$ B activation in other lung cell types (epithelium and endothelium) and subsequent regulation of neutrophilic lung emigration.

## Results

### Generation of Fetal Liver Transplant Chimeras

Fetal liver transplant chimeras were generated as described in Chapter IV: The Kinetics of Alveolar Macrophage Repopulation following Fetal Liver Transplantation. Since I $\kappa$ B- $\alpha$  deficient mice survive only 7-10 days after birth, I $\kappa$ B- $\alpha$ <sup>-/+</sup>/ I $\kappa$ B- $\alpha$ <sup>-/+</sup> matings were set up to generate I $\kappa$ B- $\alpha$ <sup>-/-</sup>, I $\kappa$ B- $\alpha$ <sup>-/+</sup>, and WT donors for transplant. p50 deficient donors were generated by setting up p50<sup>-/-</sup>/p50<sup>-/-</sup> matings. HLL mice were used as recipients for all FLT experiments in order to detect *in vivo* NF- $\kappa$ B activation in structural cells by bioluminescence imaging. To maximize alveolar macrophage repopulation in our chimeras, the clodronate protocol as described in Chapter IV was used for all FLT experiments.

### Wild-type FLT Chimeras

WT FLT chimeras were studied in conjunction with HLL untransplanted control mice to ensure that FLT did not result in abnormal basal NF- $\kappa$ B activation or altered response to LPS. WT FLT chimeras and HLL untransplanted control mice were given a single IP dose of LPS (3  $\mu$ g/g) and NF- $\kappa$ B activity detected by bioluminescence imaging (Figure 34). WT chimeras exhibited the same response as untransplanted HLL controls. A significant increase in NF- $\kappa$ B activity was detected 4 hours after IP LPS and decreased to near baseline levels by 24 hours. The NF- $\kappa$ B activity observed by bioluminescence imaging correlated with quantification of photon counts measured over the thorax (Figure 35). In addition, bioluminescence directly

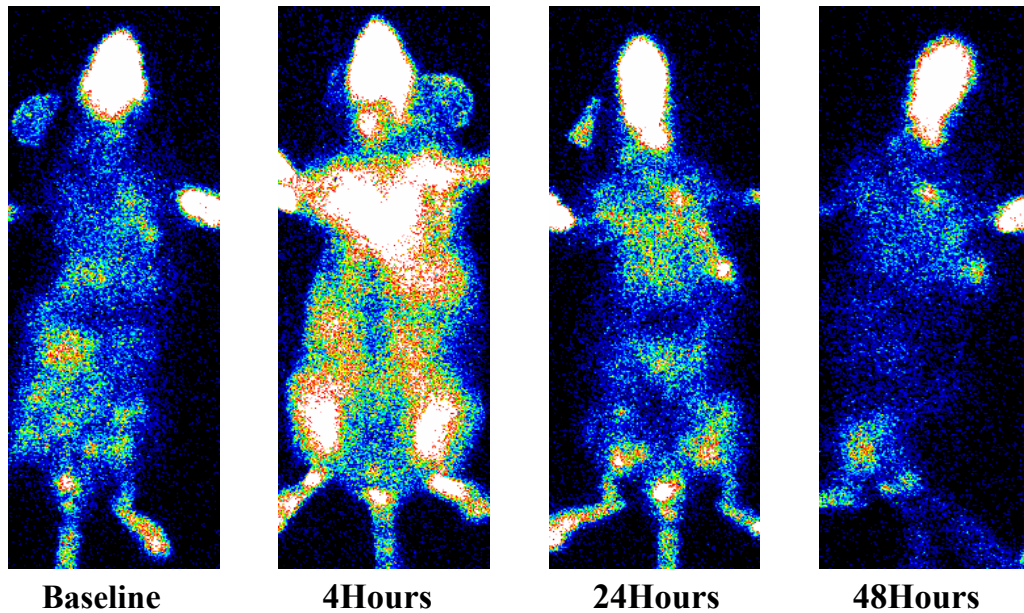


**Figure 34:** Bioluminescence detection of NF- $\kappa$ B activity in WT FLT chimeras. WT FLT chimeras were administered a single IP dose of LPS (3  $\mu$ g/g). An increase in NF- $\kappa$ B activity was detected 4 hours after IP LPS administration followed by a decrease to near baseline levels by 24 hours. Images are representative of two separate experiments.

correlated with histologic evidence of lung inflammation (Figure 36), as demonstrated by neutrophilic influx in the interstitium 4 hours after IP LPS. A significant increase in neutrophils in the lung was detected 8 hours after IP LPS compared to baseline and 4 hours ( $p < 0.05$ ) followed by a decrease toward baseline through 48 hours (Figure 37). Since the donor hematopoietic cells did not contain the luciferase reporter, the observation that the WT FLT chimeras and HLL untransplanted controls exhibited similar levels of bioluminescence suggested that the majority of the detected NF- $\kappa$ B activity was derived from the parenchyma cells.

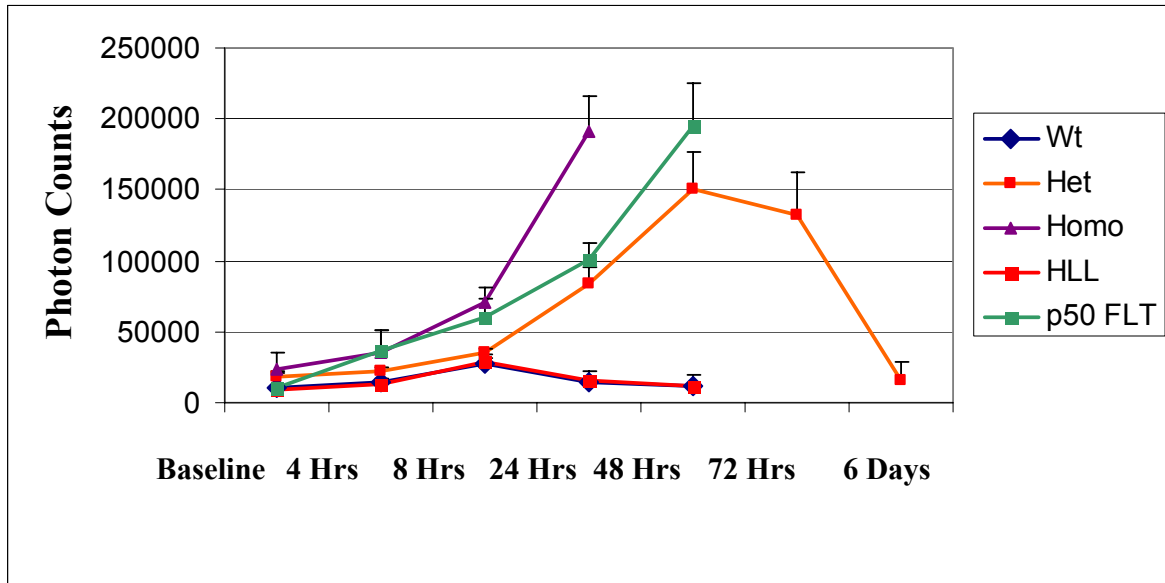


**Figure 35:** Quantification of photon counts measured over the thorax in FLT chimeras. Untransplanted HLL controls and WT FLT chimeras displayed similar kinetics of lung NF- $\kappa$ B activity.  $\text{I}\kappa\text{B-}\alpha^{-/+}$  FLT chimeras demonstrated enhanced and prolonged lung NF- $\kappa$ B activity for 72 hours followed by a return to baseline by 6 days.  $\text{I}\kappa\text{B-}\alpha^{-/-}$  FLT chimeras generated a rapid activation of NF- $\kappa$ B in the lung which steadily increased over 24 hours.  $\text{p50}^{-/-}$  FLT chimeras displayed similar kinetics of lung NF- $\kappa$ B activity compared to  $\text{I}\kappa\text{B-}\alpha^{-/-}$  FLT chimeras. NF- $\kappa$ B activity in the lung rapidly increased over 48 hours after IP LPS administration.

### $\text{I}\kappa\text{B-}\alpha^{-/+}$ FLT Chimeras

$\text{I}\kappa\text{B-}\alpha^{-/+}$  FLT chimeras displayed a distinct phenotype compared to WT FLT chimeras and untransplanted HLL controls.  $\text{I}\kappa\text{B-}\alpha^{-/+}$  FLT chimeras were given a single IP dose of LPS (3  $\mu\text{g/g}$ ) and NF- $\kappa$ B activity detected by bioluminescence (Figure 38). Similar to WT FLT chimeras, NF- $\kappa$ B activity increased 4 hours after IP LPS; however, NF- $\kappa$ B activity continued to increase at 24 hours and persisted until 72 hours. After 6 days, NF- $\kappa$ B activity returned to baseline. These observations were supported by quantification of photon counts measured over

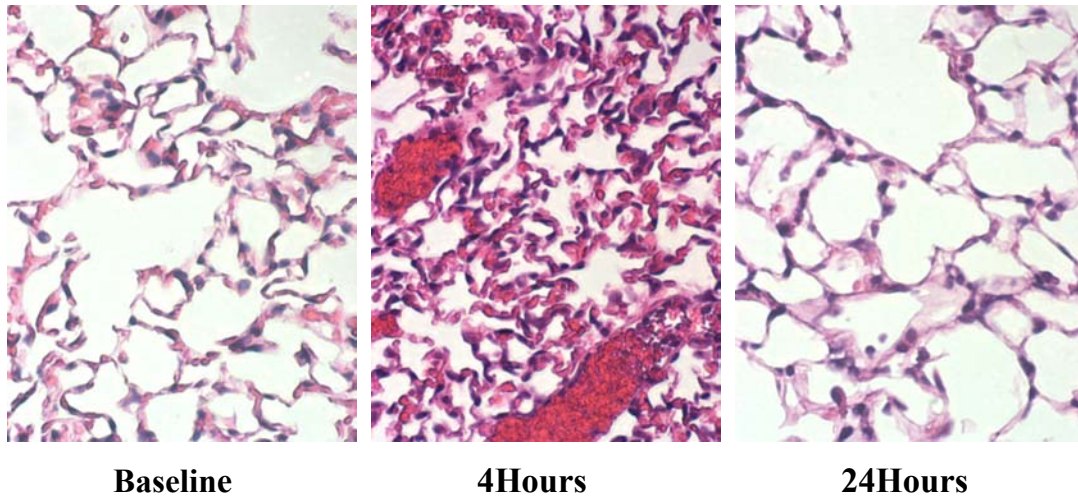


**Figure 36:** Detection of lung inflammation by histology in WT FLT chimeras after administration of a single IP dose of 3 LPS ( $\mu\text{g/g}$ ).

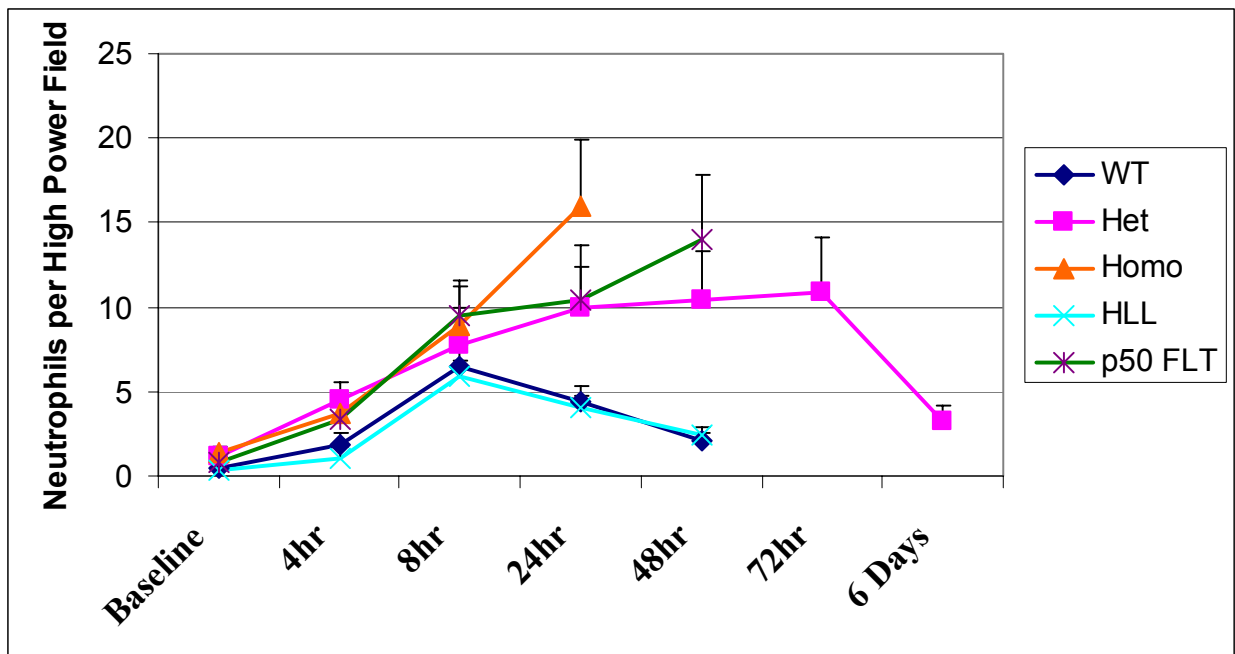


**Figure 37:** Quantification of neutrophils in lung tissue sections of WT, HLL,  $\text{IkB-}\alpha^{-/+}$ ,  $\text{IkB-}\alpha^{-/-}$ , and  $\text{p50}^{-/-}$  mice. Neutrophils were counted in 10 non-overlapping fields per slide. A total of 3 slides per mouse were counted.  $N = 3$  or more for each group. The number of neutrophils detected in the lung correlated with both the histologic evidence of lung inflammation and  $\text{NF-}\kappa\text{B}$  activity as detected by bioluminescence imaging and photon counts.

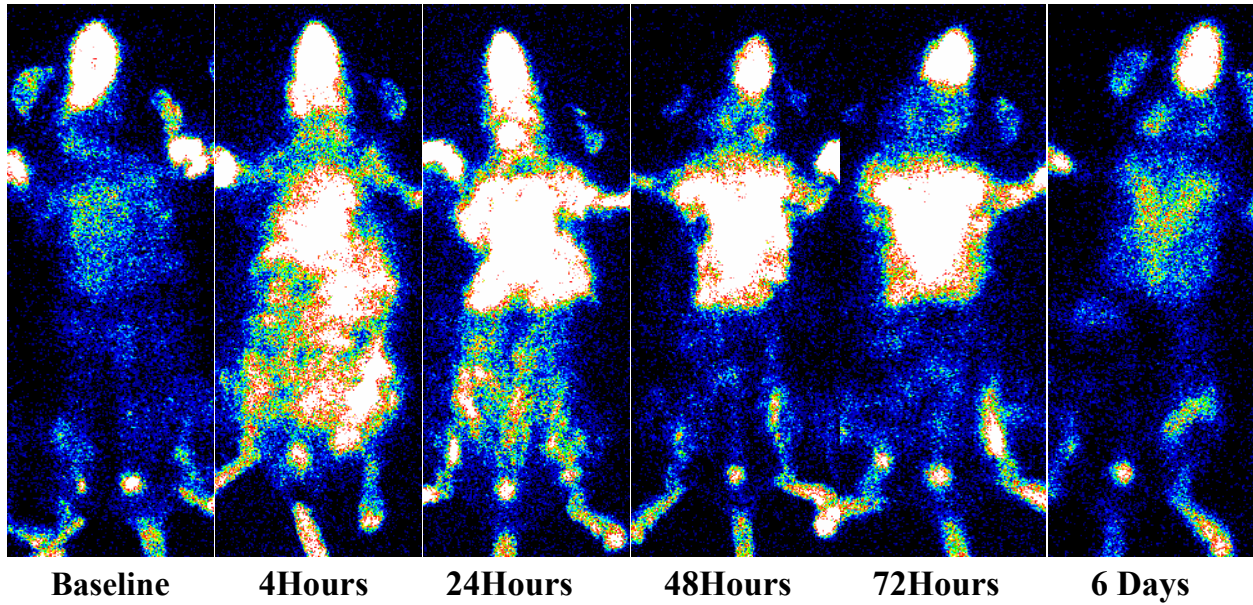


**Figure 38:** Bioluminescence detection of NF- $\kappa$ B activity in I $\kappa$ B- $\alpha$ <sup>-/+</sup> FLT chimeras. I $\kappa$ B- $\alpha$ <sup>-/+</sup> FLT chimeras were administered a single IP dose of 3  $\mu$ g/g LPS. Increased NF- $\kappa$ B activity was detected 4 hours after IP LPS administration and persisted for 72 hours. Baseline NF- $\kappa$ B activity was not achieved until 6 days after IP LPS administration. Images are representative of two separate experiments.

the thorax (Figure 35). Histologic evidence of lung inflammation correlated with bioluminescence imaging (Figure 39), as demonstrated by interstitial neutrophilic influx detected at 4 hours after IP LPS which continued through 72 hours. A significant increase in lung neutrophils over baseline was detected at all time points after IP LPS ( $p < 0.05$ ), demonstrating a sustained lung inflammation (Figure 37). While I $\kappa$ B- $\alpha$ <sup>-/+</sup> FLT chimeras displayed physical signs of illness (inactivity, ruffled fur) after IP LPS, no mortality was observed and all mice resolved the inflammatory insult. These data show that the loss of a single I $\kappa$ B- $\alpha$  allele in hematopoietic derived cells resulted in enhanced and prolonged NF- $\kappa$ B activity in epithelium of the lung and sustained neutrophilic inflammation after a single dose of IP LPS.

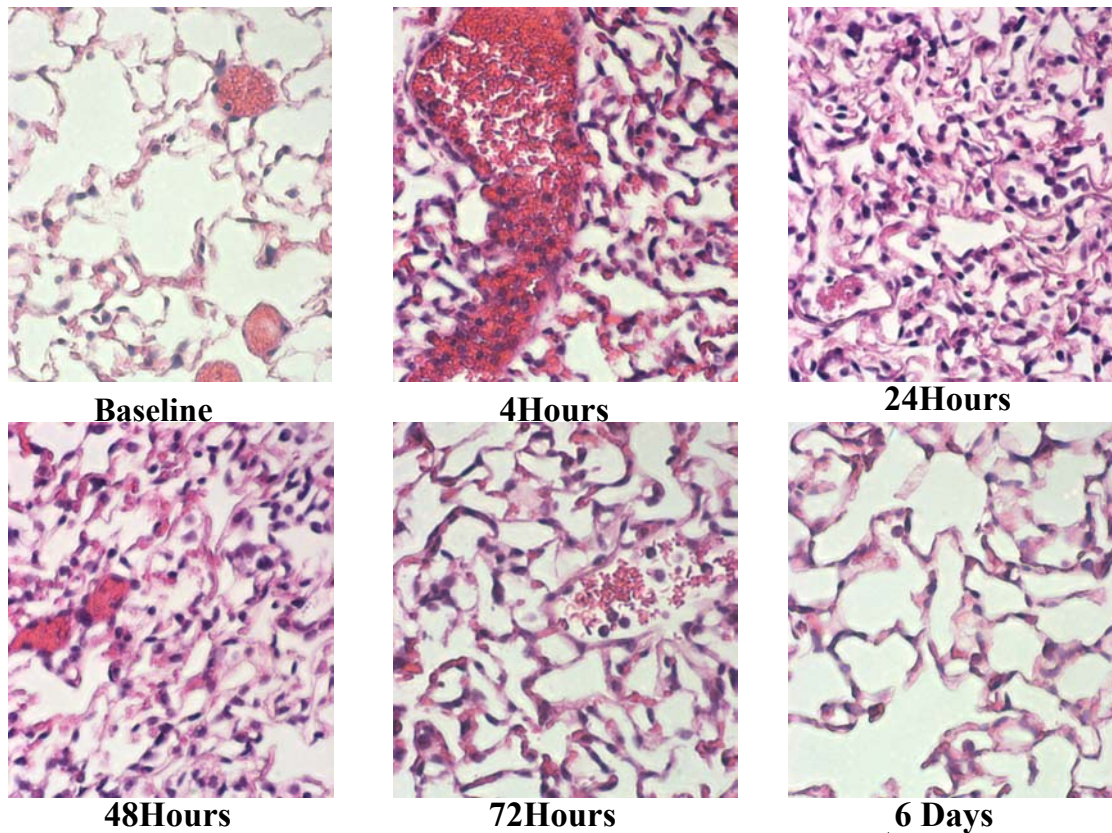


**Figure 39:** Detection of lung inflammation by histology in  $\text{IkB-}\alpha^{+/+}$  FLT chimeras after administration of a single IP dose of LPS (3  $\mu\text{g/g}$ ).

### $\text{IkB-}\alpha^{-/-}$ FLT Chimeras

$\text{IkB-}\alpha^{-/-}$  FLT chimeras displayed a more severe phenotype compared to  $\text{IkB-}\alpha^{+/+}$  FLT chimeras.  $\text{IkB-}\alpha^{-/-}$  FLT chimeras were given a single IP dose of LPS (3  $\mu\text{g/g}$ ) and NF- $\kappa\text{B}$  activity detected by bioluminescence imaging (Figure 40). Interestingly, no increase in NF- $\kappa\text{B}$  activity was detected at baseline. NF- $\kappa\text{B}$  activity increased 4 hours after IP LPS similarly to  $\text{IkB-}\alpha^{+/+}$  FLT chimeras; however, after 24 hours, NF- $\kappa\text{B}$  activity was greater in the  $\text{IkB-}\alpha^{-/-}$  FLT chimeras as determined by photon count emission (Figure 35). Histology demonstrated interstitial neutrophil influx which increased through 24 hours after IP LPS (Figure 41). A

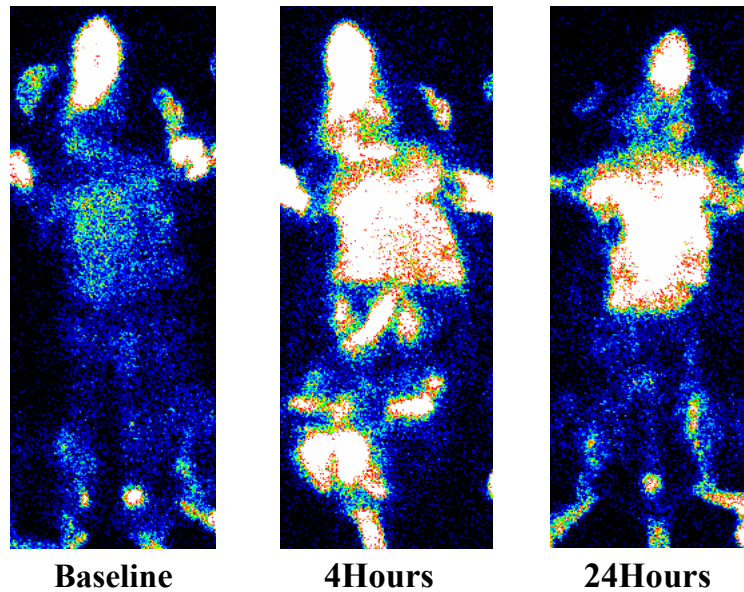


**Figure 40:** Bioluminescence detection of NF- $\kappa$ B activity in I $\kappa$ B- $\alpha^{-/-}$  FLT chimeras. I $\kappa$ B- $\alpha^{-/-}$  FLT chimeras were administered a single IP dose of 3  $\mu$ g/g LPS. Increased NF- $\kappa$ B activity was detected 4 hours after IP LPS administration which continued to increase through 24 hours. Images are representative of two separate experiments.

significant increase in neutrophils was detected at each time point after IP LPS compared to baseline ( $p < 0.05$ ) (Figure 37). Few I $\kappa$ B- $\alpha^{-/-}$  FLT chimeras were available for study because of a limited number of donors and mortality after LPS administration. In contrast to I $\kappa$ B- $\alpha^{-/+}$  FLT chimeras, I $\kappa$ B- $\alpha^{-/-}$  FLT chimeras displayed signs of severe illness including inactivity, secretions around the eye, and diarrhea. Therefore, animals were euthanized after 24 hours, prohibiting study beyond this time. These data demonstrate a continuous increase in NF- $\kappa$ B activation and neutrophilic lung inflammation through 24 hours after a single dose IP LPS in I $\kappa$ B- $\alpha^{-/-}$  FLT chimeras.

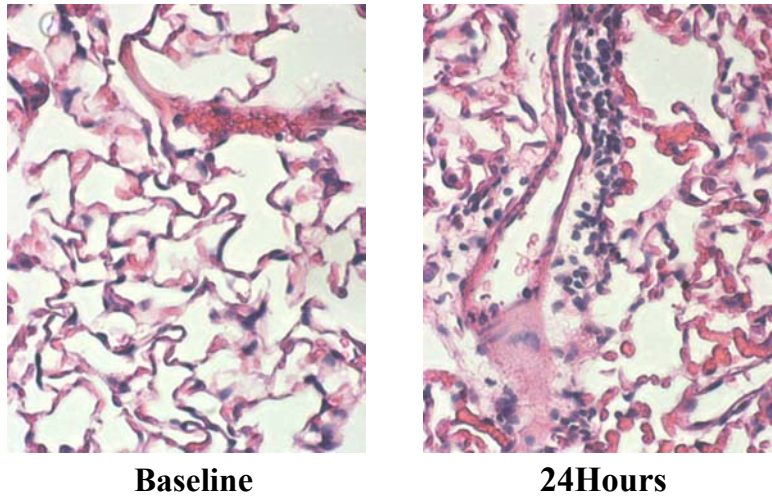


**Figure 41:** Detection of lung inflammation by histology in  $I\kappa B-\alpha^{-/-}$  FLT chimeras after administration of a single IP dose of LPS (3  $\mu\text{g/g}$ ).

---

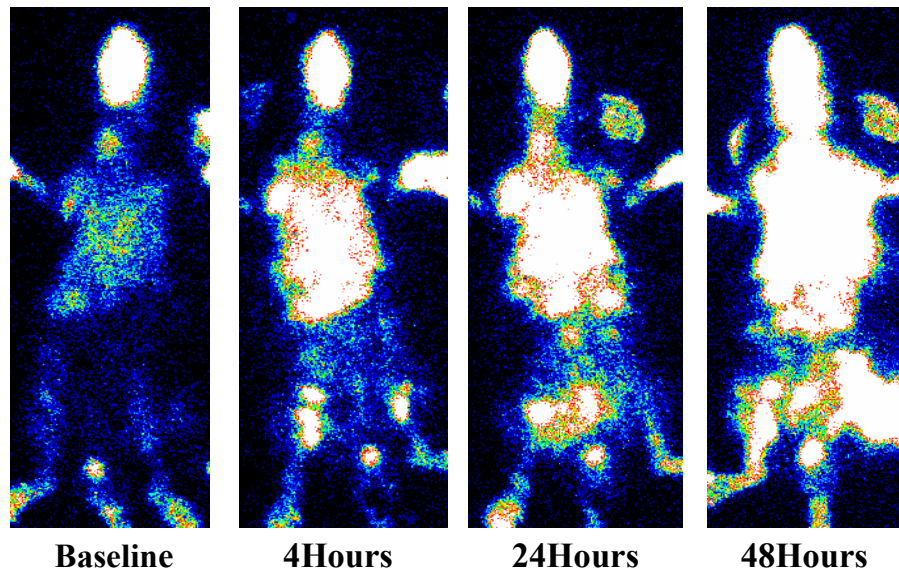


**Figure 42:** Bioluminescence detection of NF- $\kappa$ B activity in  $p50^{-/-}$  FLT chimeras.  $p50^{-/-}$  chimeras were administered a single IP dose of 3  $\mu\text{g/g}$  LPS. An increase in NF- $\kappa$ B activity was detected 4 hours after IP LPS administration, which continued to increase through 24 and 48 hours. Images are representative of two separate experiments.

---

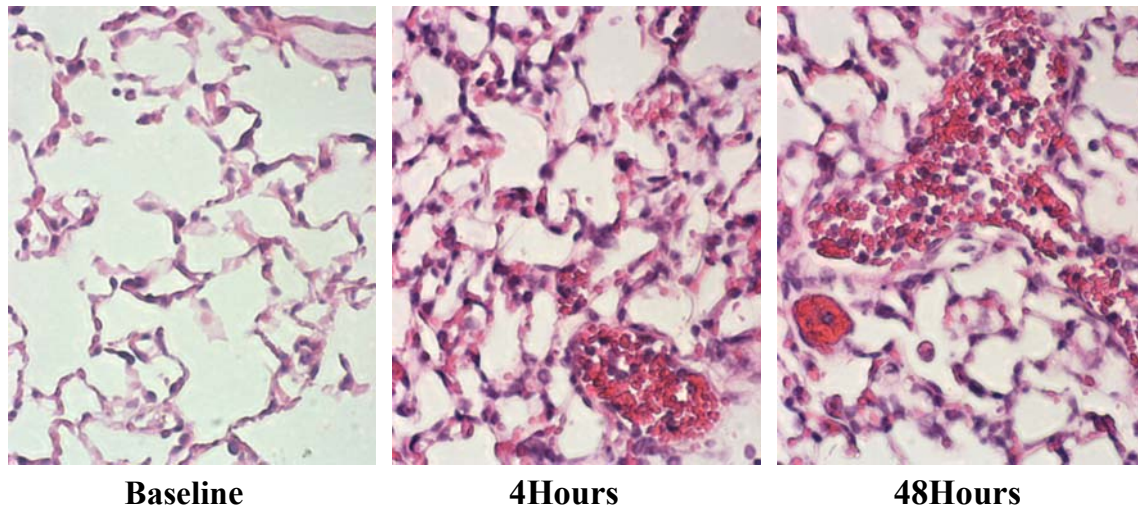


**Figure 43:** Detection of lung inflammation by histology in  $I\kappa B-\alpha^{-/-}$  FLT chimeras after administration of a single IP dose of LPS (3  $\mu\text{g/g}$ ).

---

#### $p50^{-/-}$ FLT Chimeras

$p50^{-/-}$  FLT chimeras displayed a phenotype similar to  $I\kappa B-\alpha^{-/-}$  FLT chimeras.  $p50^{-/-}$  FLT chimeras were given a single IP dose of LPS (3  $\mu\text{g/g}$ ) and NF- $\kappa$ B activity detected by bioluminescence imaging (Figure 42). NF- $\kappa$ B activity was minimal at baseline and rapidly increased over 48 hours after IP LPS. These observations were supported by quantification of photon counts measured over the thorax (Figure 35). Histology revealed neutrophil influx in the vessels, interstitium, and alveolar space at 4, 24, and 48 hours after IP LPS (Figure 43). A significant increase in neutrophils was detected over baseline at 4, 24, and 48 hours after IP LPS ( $p < 0.05$ ) (Figure 37). In addition to increased lung NF- $\kappa$ B activity and neutrophilic inflammation, significant mortality (72% survival at 24 hours and 28% survival at 48 hours) was observed after IP LPS administration (Figure 44). These data suggest  $p50$  deficient

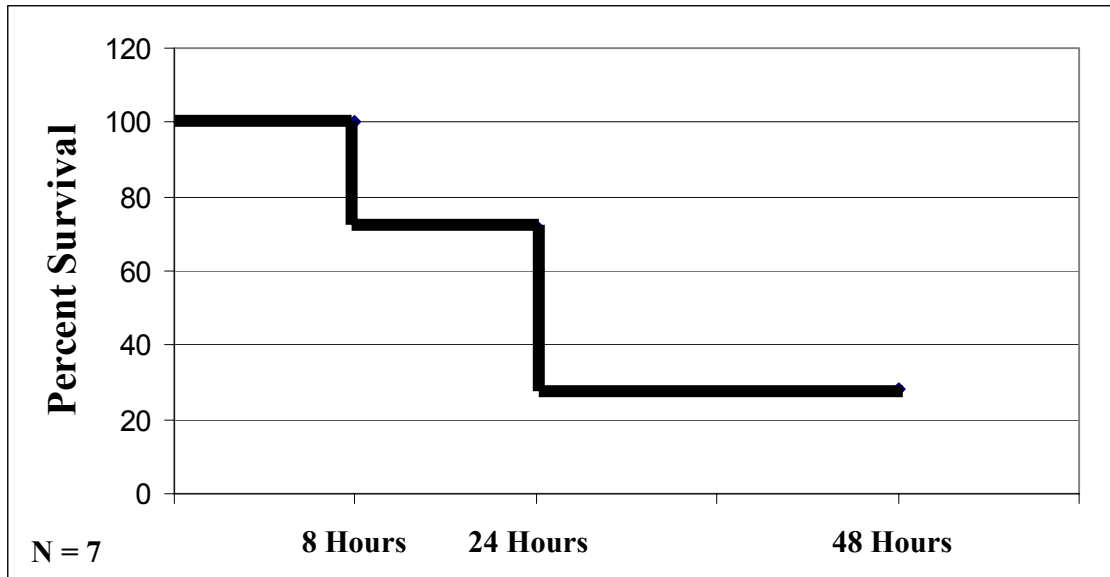


**Figure 44:**  $p50^{-/-}$  FLT chimeras exhibit mortality after intratracheal administration of a single dose of 3  $\mu\text{g/g}$  LPS resulting in 72% survival at 24 hours and 28% survival at 48 hours.  $N=7$   $p50^{-/-}$  FLT chimeras.

hematopoietic cells exhibit persistent NF- $\kappa$ B activation which in turn drives NF- $\kappa$ B activity in other cell types, thus prolonging the inflammatory response.

#### Bioluminescence Correlates with Tissue Luciferase Activity

To ensure that bioluminescence measurements reflected tissue luciferase expression, luciferase assay was performed on lung tissue collected from WT and  $\text{I}\kappa\text{B-}\alpha^{-/+}$  FLT chimeras 48 hours after IT LPS administration. At this time, NF- $\kappa$ B activity, as detected by bioluminescence imaging, was higher in  $\text{I}\kappa\text{B-}\alpha^{-/+}$  FLT chimeras than WT FLT chimeras. Figure 45 shows that lung luciferase activity in  $\text{I}\kappa\text{B-}\alpha^{-/+}$  FLT chimeras was 2 times greater (6725 +/- 725 vs. 3052 +/-

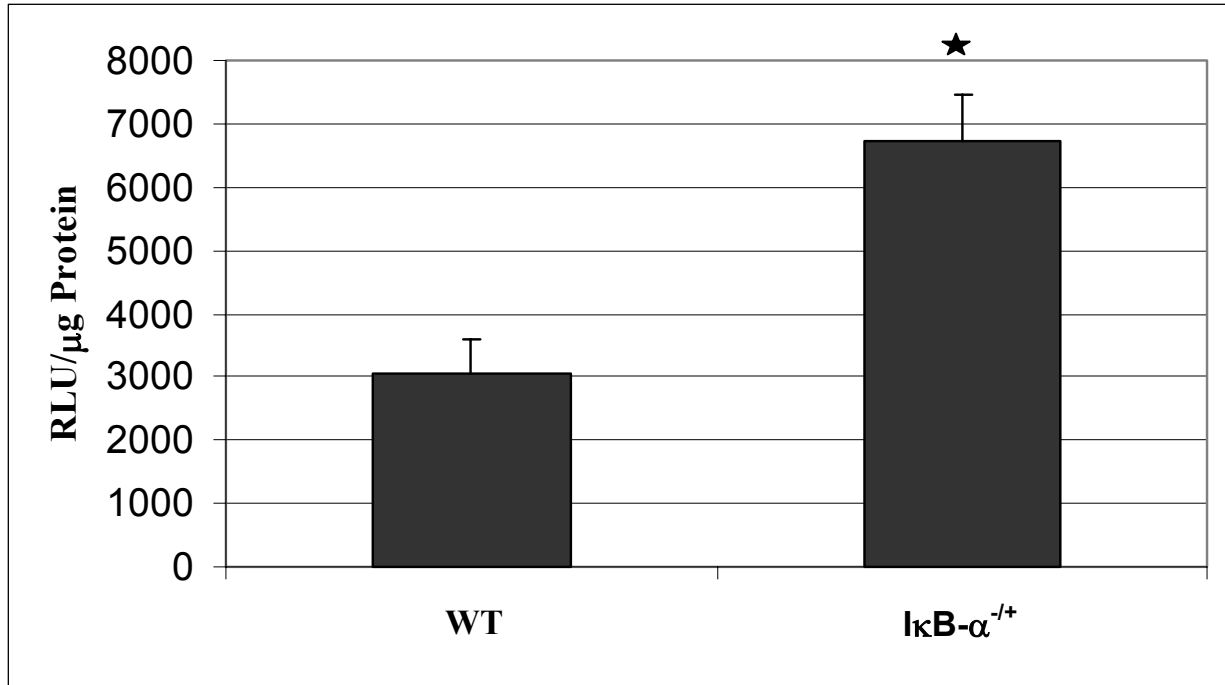


**Figure 45:** Detection of tissue luciferase activity from WT and IκB-α<sup>-/+</sup> FLT lungs 48 hours after administration of a single intraperitoneal dose of 3 μg/g LPS. IκB-α<sup>-/+</sup> FLT chimeras exhibit a significant increase (6725 +/- 725 vs. 3052 +/- 532 RLU/mg protein) in NF-κB activity compared to WT FLT chimeras 48 hours after IP LPS (p < 0.05).

532 RLU/μg protein) than in WT FLT chimeras, further supporting the use of bioluminescence as a measure of *in vivo* NF-κB activity.

#### NF-κB Regulation in IκB-α<sup>-/+</sup> and p50<sup>-/-</sup> Bone Marrow Derived Macrophages

NF-κB activation was determined in BMDMΦ by Western blots for cytoplasmic IκB-α and nuclear RelA. IκB-α<sup>-/+</sup> BMDMΦ cells were treated with 5 μg/ml LPS and nuclear and cytoplasmic protein collected at baseline, 4 and 24 hours after LPS treatment. Western blots were performed to identify cytoplasmic IκB-α and nuclear RelA proteins (Figure 46). A decrease in IκB-α protein was detected at baseline in IκB-α<sup>-/+</sup> macrophages compared to WT

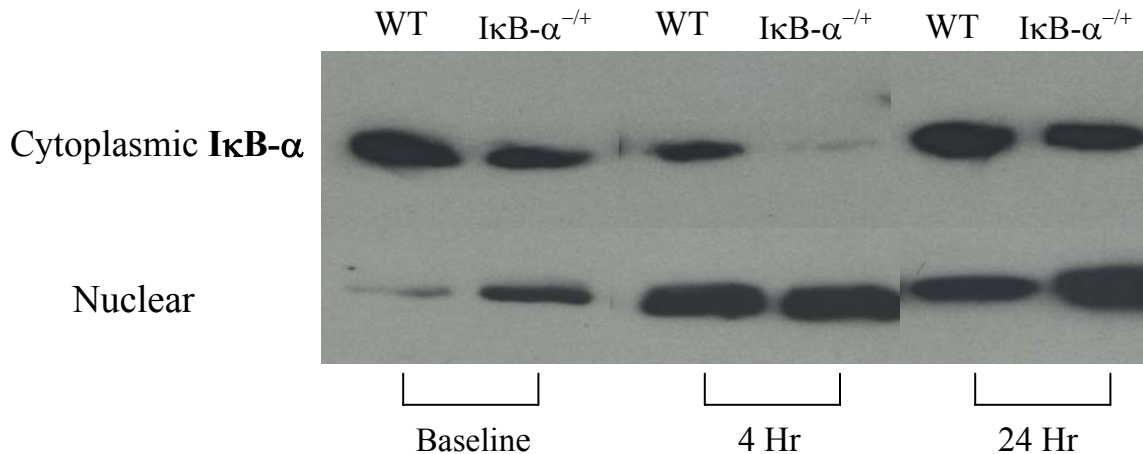


**Figure 46:** Detection of cytoplasmic IκB-α and nuclear RelA protein by western blot in WT and IκB-α<sup>-/+</sup> BMDMΦ cells after stimulation with 5 μg/ml LPS. IκB-α<sup>-/+</sup> BMDMΦ contained decreased IκB-α and increased RelA protein at baseline compared to WT BMDMΦ. Four hours after LPS stimulation, increased RelA was detected in both WT and IκB-α<sup>-/+</sup> BMDMΦ; however, IκB-α protein was virtually undetectable in IκB-α<sup>-/+</sup> BMDMΦ. While IκB-α protein had returned to basal levels by 24 hours after LPS stimulation, nuclear RelA protein was significantly higher in IκB-α<sup>-/+</sup> BMDMΦ compared to WT BMDMΦ. Data is representative of two separate experiments.

macrophages. Four hours after LPS treatment, IκB-α protein was evident in WT macrophages; however, IκB-α<sup>-/+</sup> macrophages exhibited lower levels of IκB-α protein. By 24 hours after LPS treatment, basal levels of IκB-α protein were observed in both WT and IκB-α<sup>-/+</sup> macrophages.

Differences in nuclear RelA protein levels were detected between the two groups. At baseline, RelA was virtually undetectable in WT macrophages; however, IκB-α<sup>-/+</sup> macrophages possessed increased RelA corresponding to the decrease in IκB-α. After 4 hours, both groups displayed a significant increase in nuclear RelA. By 24 hours, IκB-α<sup>-/+</sup> macrophages contained more RelA compared to WT macrophages. Taken together, these data suggest that the loss of one allele of *IκB-α* in BMDMΦ resulted in the delayed cytoplasmic IκB-α and prolonged RelA nuclear localization after LPS treatment.

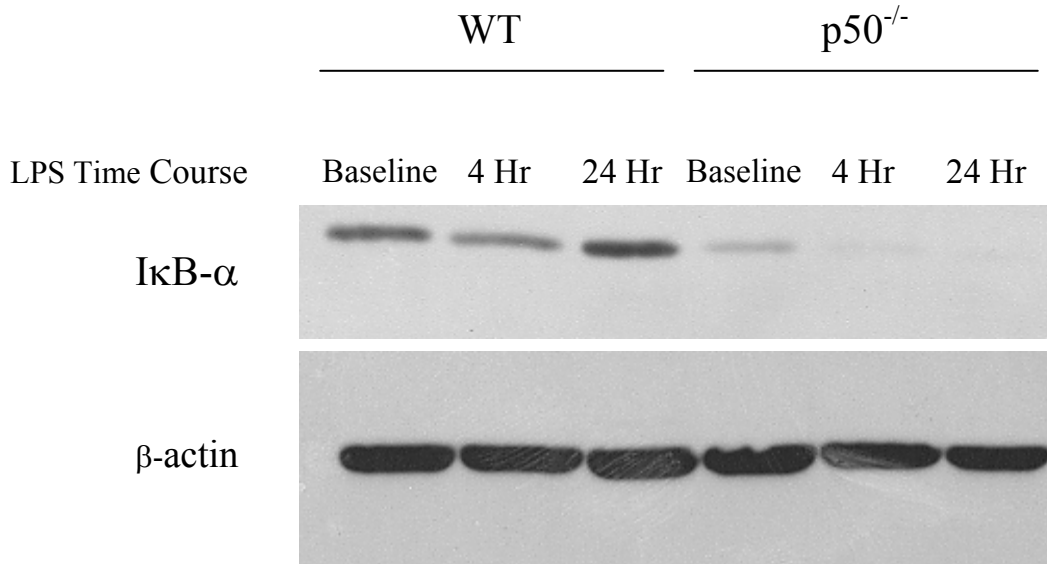


**Figure 47:** Detection of cytoplasmic IκB-α protein by western blot in WT and p50<sup>-/-</sup> BMDMΦ after stimulation with 5 μg/ml LPS. Decreased IκB-α protein was detected in p50<sup>-/-</sup> BMDMΦ at baseline compared to WT BMDMΦ. In WT BMDMΦ, IκB-α protein decreased 4 hours after LPS and returned to basal levels by 24 hours after LPS stimulation. In contrast, IκB-α protein was undetectable in p50<sup>-/-</sup> BMDMΦ 4 and 24 hours after LPS stimulation. Data is representative of two separate experiments.

p50<sup>-/-</sup> BMDMΦs were treated with 5 μg/ml LPS and Western blot performed to detect cytoplasmic IκB-α protein (Figure 47). Interestingly, p50<sup>-/-</sup> macrophages possessed less IκB-α protein at baseline compared to WT macrophages, suggesting p50 plays a role in IκB-α homeostasis. Four hours after LPS treatment, IκB-α protein was present in WT macrophages; however, IκB-α protein was undetectable in p50<sup>-/-</sup> macrophages. As previously demonstrated, WT macrophages reached basal levels of IκB-α protein 24 hours after LPS treatment; however, p50<sup>-/-</sup> macrophages exhibited undetectable levels of IκB-α protein even after 24 hours. These data implicate p50 as a critical player in regulating NF-κB activity through IκB-α homeostasis.

The IκB-α Western blot data suggests that p50 plays a role in IκB-α homeostasis. We have performed pilot experiments to detect IκB-α mRNA by Northern blot. Our initial data

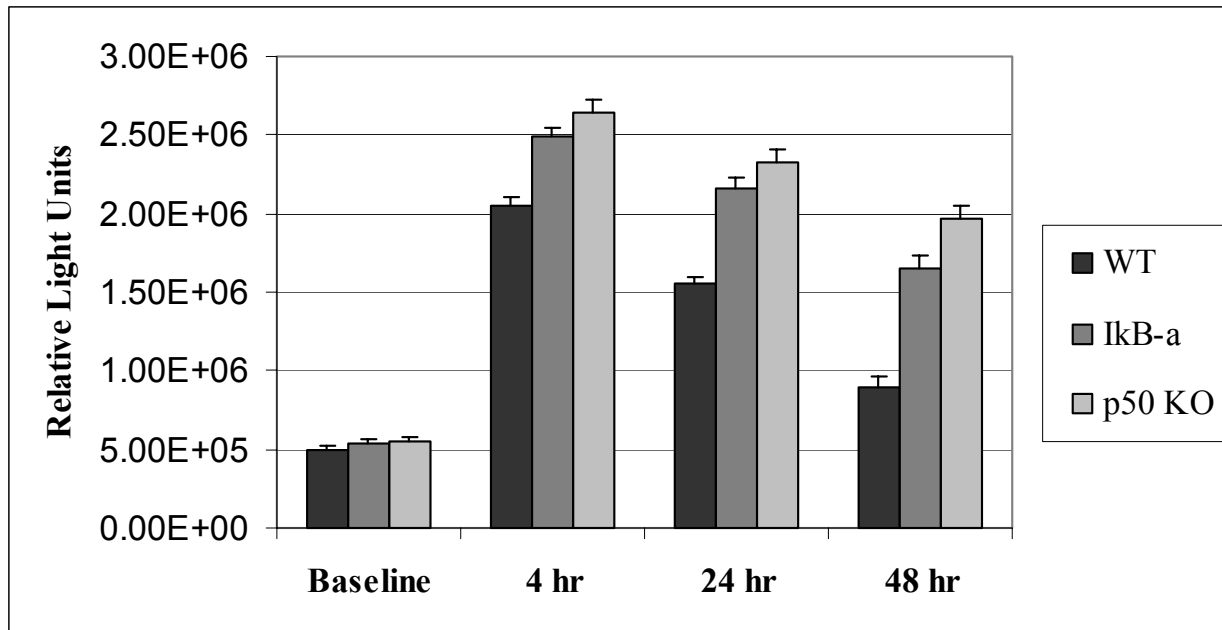


**Figure 48:** The role of NF- $\kappa$ B in macrophage/epithelium communication was investigated using a co-culture system. WT, I $\kappa$ B- $\alpha$ <sup>-/+</sup>, and p50<sup>-/-</sup> BMDM $\Phi$  were placed in the top chamber and 8x NGL transfected A549 cells were placed in the bottom chamber of a co-culture apparatus. The cells were stimulated with 5  $\mu$ g/ml LPS and NF- $\kappa$ B activity in A549 cells detected by luciferase assay at baseline, 4, 24, and 48 hours after LPS. No significant differences in A549 NF- $\kappa$ B activity were detected at baseline between the three groups; however, the I $\kappa$ B- $\alpha$ <sup>-/+</sup> and p50<sup>-/-</sup> groups displayed significantly higher NF- $\kappa$ B activity in A549 cells at 4, 24, and 48 hours compared to the WT group ( $p < 0.05$ ). Each bar represents mean  $\pm$  SEM of 3 samples per group. Data is representative of three separate experiments.

shows no difference in I $\kappa$ B- $\alpha$  message between WT and p50<sup>-/-</sup> BMDM $\Phi$  4, 24, and 48 hours after LPS treatment, suggesting the differences observed in I $\kappa$ B- $\alpha$  protein are possibly regulated through protein stability, and/or degradation via IKK phosphorylation/ubiquitination.

### The Role of NF- $\kappa$ B in Macrophage/Epithelium Communication

The FLT chimera studies suggest that modulation of NF- $\kappa$ B in macrophages can impact NF- $\kappa$ B activity in other cell types, specifically epithelium. To study the role of NF- $\kappa$ B in macrophage/epithelium communication, BMDM $\Phi$ s from WT, I $\kappa$ B- $\alpha$ <sup>-/+</sup> and p50<sup>-/-</sup> mice were

cultured in a co-culture apparatus with A549 cells transfected with the 8x NGL construct. The co-culture apparatus allows for cell-cell communication through shared cell culture media. The cells were treated with 5  $\mu\text{g/ml}$  LPS (which only activates NF- $\kappa\text{B}$  in BMDM $\Phi$ , not A549 cells) and NF- $\kappa\text{B}$  activity from A549 cells was detected by luciferase assay (Figure 48). No significant difference in NF- $\kappa\text{B}$  activity in A549 cells was detected at baseline in WT, I $\kappa\text{B-}\alpha^{-/+}$  or p50 $^{-/-}$  BMDM $\Phi$  co-culture. Four hours after LPS treatment, increased A549 NF- $\kappa\text{B}$  activity was detected in I $\kappa\text{B-}\alpha^{-/+}$  and p50 $^{-/-}$  co-culture (8.5% and 11.5% increase over WT in I $\kappa\text{B-}\alpha^{-/+}$  and p50 $^{-/-}$  respectively compared to WT co-culture). At 24 hours after LPS, the difference between the WT co-culture group and I $\kappa\text{B-}\alpha^{-/+}$  and p50 $^{-/-}$  co-culture groups increased to 21% and 28% respectively ( $p < 0.05$ ). At 48 hours, A549 luciferase activity decreased towards baseline in the WT co-culture group but I $\kappa\text{B-}\alpha^{-/+}$  and p50 $^{-/-}$  co-culture groups remained high (85% and 120% increase over WT in I $\kappa\text{B-}\alpha^{-/+}$  and p50 $^{-/-}$  respectively,  $p < 0.05$ ) demonstrating sustained NF- $\kappa\text{B}$  activity. These data demonstrate that changes in the NF- $\kappa\text{B}$  pathway in BMDM $\Phi$  alter NF- $\kappa\text{B}$  activity in A549 cells after LPS stimulation. Since LPS does not activate NF- $\kappa\text{B}$  in A549 cells, the differences observed in NF- $\kappa\text{B}$  activity in the A549 cells in the co-culture experiments result from changes in cell-cell communication mediated by the macrophage. These data directly support the phenotype observed in the I $\kappa\text{B-}\alpha$  and p50 FLT chimera studies.

### Summary

The role of the NF- $\kappa\text{B}$  signal transduction pathway in specific cell types in the regulation of lung inflammation remains unclear. Previous studies have primarily utilized *in vitro* cell culture models to investigate or manipulate the NF- $\kappa\text{B}$  pathway in specific cell types. There are

two primary limitations inherent to these methods: 1) the nature of immortalized cell lines introduces factors that may not reflect normal functions 2) the experimental environment does not include the cellular interactions and signaling networks that exist in the *in vivo* environment. In order to elucidate meaningful information about cellular functions and molecular pathways in specific cell types, it is necessary to perform the experiments within the complex, integrated system in which the cells normally reside.

I $\kappa$ B- $\alpha$  deficient mice are apparently normal at birth, but die within 7-10 days (Beg, 1995a; 2000; Klement, 1996). Enhanced granulopoiesis, severe dermatitis, and increased TNF- $\alpha$  in the skin are present at the time of death. I $\kappa$ B- $\alpha$ -deficient B-cells were shown to exhibit enhanced proliferative responses, while T-cells displayed reduced proliferative responses. I $\kappa$ B- $\alpha$ -deficiency in macrophages has not been described. The observation that WT, I $\kappa$ B- $\alpha$ <sup>-/+</sup>, and I $\kappa$ B- $\alpha$ <sup>-/-</sup> FLT chimeras showed similar NF- $\kappa$ B activity in the lung at baseline suggests that the loss of I $\kappa$ B- $\alpha$  alone does not lead to increased NF- $\kappa$ B activation. However, after stimulation with a single dose of IP LPS, I $\kappa$ B- $\alpha$ <sup>-/+</sup> and I $\kappa$ B- $\alpha$ <sup>-/-</sup> FLT chimeras demonstrated enhanced NF- $\kappa$ B lung activity and neutrophilic inflammation. The partial loss of I $\kappa$ B- $\alpha$  protein in the I $\kappa$ B- $\alpha$ <sup>-/+</sup> FLT chimeras resulted in an intermediate phenotype between WT and I $\kappa$ B- $\alpha$ <sup>-/-</sup> FLT chimeras, characterized by prolonged and enhanced NF- $\kappa$ B activity which resolved by 6 days after stimulation. I $\kappa$ B- $\alpha$ <sup>-/-</sup> FLT chimeras further support the role of I $\kappa$ B- $\alpha$  in de-activation, as characterized by an inability to resolve NF- $\kappa$ B activity and lung inflammation.

Previous studies have demonstrated that LPS administration in the lungs induces nuclear translocation of RelA and p50 (Blackwell, 1999c; Mizgerd, 2002). RelA increases gene expression through the interaction of the transactivation domain and coactivator complexes (Ghosh, 1998). In RelA/TNFR1-deficient mice, intranasal LPS administration resulted in a

considerable reduction in neutrophil emigration and pulmonary expression of the chemokines KC and MIP-2 and the adhesion molecule ICAM-1, compared to WT and TNFRI-deficient mice (Alcorno, 2001). These data suggest RelA is essential for regulating TNFRI-independent mechanisms of innate immunity for protection against pathogens.

In contrast to RelA, p50 has been shown to both increase and decrease gene expression *in vitro* (Baek, 2002; Dechend, 1999; Franzoso, 1992; Zhong, 2002). In p50-deficient mice, increased expression of multiple NF- $\kappa$ B-regulated genes occur during *E. coli* pneumonia, resulting in increased neutrophil recruitment and excessive inflammatory injury (Mizgerd, 2003). In addition, 100% mortality was observed in p50-deficient mice 72 hours after IT administration of  $10^6$  cfu *Pseudomonas*. Our studies support previous reports and provide additional information about the role of p50 in regulating lung inflammation. In p50<sup>-/-</sup> FLT chimeras, a single IP dose of LPS resulted in a dramatic neutrophil influx accompanied by significant NF- $\kappa$ B activity in structural cells in the lung. Additionally, the high mortality (28% survival at 48 hours after IP LPS) in p50<sup>-/-</sup> FLT chimeras implicates inflammatory cells as the mediators of lethality. We have also performed IP LPS studies in untransplanted p50-deficient mice. These mice also demonstrate dramatic neutrophil influx and significant mortality after 48 hours. The exaggerated response to LPS may result from the loss of p50/p50 inhibitory function in regulating a variety of pro-inflammatory genes.

The data from the FLT chimera studies and the BMDM $\Phi$  studies show that I $\kappa$ B- $\alpha$  and p50 are critical in a “turn-off” mechanism in the regulation of LPS induced neutrophilic lung inflammation. While the macrophage is thought to be important in the initiation of lung inflammation, these data support the possible role of the macrophage in the resolution phase of lung inflammation as well. Prolonged NF- $\kappa$ B activation in macrophages drives NF- $\kappa$ B

activation in support cell types (predominantly epithelia) resulting in a sustained neutrophilic lung inflammatory response. The role of active turn-off of lung inflammation by NF- $\kappa$ B components is novel and may lead to a better understanding of the role of the NF- $\kappa$ B pathway in contributing to lung inflammation and injury. Perhaps these and future studies will continue to unravel the complex regulatory mechanisms that coordinate the lung inflammatory response, leading to therapeutic interventions that enhance the innate immune response while limiting host derived lung injury.

### **Future Directions**

The role of I $\kappa$ B- $\alpha$  and p50 in the regulation of NF- $\kappa$ B turn-off in macrophages needs additional investigation. Initial Northern blot experiments suggest the changes in I $\kappa$ B- $\alpha$  protein levels in I $\kappa$ B- $\alpha$ <sup>-/+</sup> and p50<sup>-/-</sup> BMDM $\Phi$  do not result from altered I $\kappa$ B- $\alpha$  transcription. If these results are confirmed, other mechanisms for decreased I $\kappa$ B- $\alpha$  protein levels will be studied. For example, the possibility of continued I $\kappa$ B- $\alpha$  protein phosphorylation and degradation could be analyzed by determining IKK kinase activity by kinase assay. In the BMDM $\Phi$  experiments, increased levels of KC and MIP-2 were detected at 24 and 48 hours after LPS in the I $\kappa$ B- $\alpha$ <sup>-/+</sup> and p50<sup>-/-</sup> co-culture groups compared to the WT co-culture group. These observations need to be confirmed with additional experiments. These data demonstrate a functional consequence of sustained NF- $\kappa$ B activity in macrophages and epithelium and help to explain the sustained neutrophil influx observed in the FLT chimeras. Additionally, these data would further support an active role for NF- $\kappa$ B in the turn-off as well as the turn-on mechanism of lung inflammation.

## CHAPTER IV

### DISCUSSION

Evidence demonstrates the macrophage plays a critical role in the initiation of lung inflammation. Our data compliments these findings and suggests that NF- $\kappa$ B activation in the macrophage is a key component in this process. Several studies have demonstrated the role of the macrophage in the initiation of lung inflammation. The most convincing of these studies involve selective elimination of the macrophage population by administration of liposomal clodronate. For example, in an immune complex model of lung inflammation, NF- $\kappa$ B activation in lung tissue, cytokine gene expression, and neutrophilic influx are blocked after liposomal clodronate treatment (Lentsch, 1999). Also, we have performed macrophage depletion studies by administering clodronate via intratracheal (IT) and/or intravenous (IV) routes, demonstrating 90% alveolar macrophage depletion 48 hours after treatment by IT + IV route (Koay, 2002). In these studies, aerosolized LPS challenge and neutrophilic alveolitis was attenuated by 80% in clodronate treated mice compared to empty liposome treated controls. Reduced neutrophil influx was associated with impaired activation of NF- $\kappa$ B in lung tissue, lower concentrations of TNF- $\alpha$  in lung lavage fluid, and decreased MIP-2 in lung homogenate. Additionally, lung NF- $\kappa$ B activation and neutrophilic alveolitis were markedly reduced in clodronate treated mice in a systemic inflammatory model (IP injection of *E. coli* LPS). These studies support the model that early NF- $\kappa$ B activation in alveolar macrophages induces the production of pro-inflammatory mediators that promotes the activation of NF- $\kappa$ B in other lung cell types and subsequent neutrophilic immigration.

To more specifically address the importance of NF- $\kappa$ B signaling in the macrophage in the regulation of lung inflammation, we replaced resident alveolar macrophages with macrophages with an alteration in the NF- $\kappa$ B signaling pathway. Bone marrow chimeras were generated through fetal liver transplantation using transgenic NF- $\kappa$ B reporter mice as recipients (HLL mice) and WT, I $\kappa$ B- $\alpha$  heterozygous and homozygous, and p50 knockout fetal liver cells as donors. The goal of these studies was to determine if altering the NF- $\kappa$ B pathway in macrophages would alter the inflammatory response in the lung following a single dose of IP LPS.

We hypothesized that I $\kappa$ B- $\alpha$  deficient macrophages would result in NF- $\kappa$ B activation at baseline, since the inhibitory effect of I $\kappa$ B- $\alpha$  would be absent. Surprisingly, I $\kappa$ B- $\alpha$  deficient FLT chimeras do not demonstrate increased NF- $\kappa$ B activity (as detected by bioluminescence imaging) or lung inflammation (as detected by histology) at baseline, suggesting that elimination of I $\kappa$ B- $\alpha$  function is not sufficient to activate the NF- $\kappa$ B pathway. It is only after a stimulus (single dose of IP LPS), that the effects of I $\kappa$ B- $\alpha$  deficiency are observed. I $\kappa$ B- $\alpha$  heterozygous FLT chimeras develop an increased and sustained NF- $\kappa$ B activation (as detected by bioluminescence imaging) after IP LPS which correlated with increased and prolonged lung inflammation as detected by neutrophil quantification. The finding that the loss of one allele of I $\kappa$ B- $\alpha$  resulted in altered NF- $\kappa$ B activity was unexpected. The data suggests that I $\kappa$ B- $\alpha$  heterozygous macrophages are unable to “turn-off” NF- $\kappa$ B activation in the same time frame compared to WT macrophages, resulting in prolonged production of pro-inflammatory cytokines, continual activation of other cell types, and prolonged neutrophilic lung inflammation. Similar to I $\kappa$ B- $\alpha$  heterozygous FLT chimeras, I $\kappa$ B- $\alpha$  homozygous knockout FLT chimeras demonstrate an increased and sustained NF- $\kappa$ B activation after IP LPS challenge. However, while the I $\kappa$ B- $\alpha$

heterozygous FLT chimeras appear to resolve the inflammatory insult with time (returning to baseline 6 days after IP LPS), I $\kappa$ B- $\alpha$  homozygous knockout FLT chimeras are unable to control/resolve the inflammatory insult and die after 24-30 hours. These results more powerfully illustrate the role of I $\kappa$ B- $\alpha$  in the active “turn-off” of NF- $\kappa$ B activation in macrophages. In addition to the evidence supporting NF- $\kappa$ B in macrophages, the detection of NF- $\kappa$ B activity by bioluminescence imaging highlights the importance of NF- $\kappa$ B activity in other cell types such as epithelium and endothelium, since the inflammatory cells do not carry the NF- $\kappa$ B reporter in these chimeras. In addition to I $\kappa$ B- $\alpha$  FLT chimeras, the role of p50 in the regulation of macrophage NF- $\kappa$ B activation was investigated by generating bone marrow chimeras using HLL mice as recipients and p50 knockout donor fetal liver cells. These mice displayed a similar phenotype as I $\kappa$ B- $\alpha$  homozygous knockout FLT chimeras, increasing NF- $\kappa$ B activity and inflammation accompanied by high mortality.

While these studies provide strong support that macrophage NF- $\kappa$ B activation is central to lung inflammation, the role/contribution of NF- $\kappa$ B in other cell types cannot be underestimated. FLT not only results in repopulation of donor macrophages, but also other inflammatory cell types, including neutrophils and lymphocytes. It is possible that alteration of NF- $\kappa$ B in donor neutrophils, once recruited to the site of inflammation, could contribute to the prolonged phenotype observed. One possible experimental approach to address this question would be to perform neutrophil depletion studies in these FLT chimeras. In the absence of circulating neutrophils, is prolonged NF- $\kappa$ B activity still observed?

We tested our hypothesis that manipulation of the NF- $\kappa$ B pathway in macrophages would alter NF- $\kappa$ B activity in other cell types by performing co-culture studies using bone marrow derived macrophages from WT, I $\kappa$ B- $\alpha$  heterozygous and homozygous knockout, and p50

knockout mice and alveolar epithelial cell line containing our NGL NF- $\kappa$ B reporter. These studies corroborated our *in vivo* studies. After LPS stimulation, NF- $\kappa$ B epithelial reporter cells in co-culture with macrophages derived from I $\kappa$ B- $\alpha$  heterozygous and p50 homozygous knockout mice exhibited prolonged NF- $\kappa$ B activity compared WT macrophage co-cultures. To understand how NF- $\kappa$ B signaling was altered in these macrophages, Western blots were performed to monitor the classic I $\kappa$ B- $\alpha$  degradation process. I $\kappa$ B- $\alpha$  resynthesis appeared to be delayed in I $\kappa$ B- $\alpha$  heterozygous macrophages. Surprisingly, p50 knockout macrophages appeared to be unable to generate sufficient amounts of I $\kappa$ B- $\alpha$  even after 24 hours. These data suggest p50 is critical for I $\kappa$ B- $\alpha$  transcription after LPS treatment. We have begun to investigate the mechanism behind these observations. Initial Northern blot experiments for I $\kappa$ B- $\alpha$  show no differences in the rate of resynthesis after LPS in WT, I $\kappa$ B- $\alpha$  heterozygous, and p50 knockout macrophages. We are currently performing RT-PCR for I $\kappa$ B- $\alpha$  as confirmation. Another possibility for the observed decrease in I $\kappa$ B- $\alpha$  protein levels could be through continuous degradation. We plan to test for changes in NF- $\kappa$ B signaling by performing IKK2 kinase assays.

Other questions remain concerning the mechanism for prolonged NF- $\kappa$ B activity in I $\kappa$ B- $\alpha$  and p50 deficient macrophages. The most plausible explanation for prolonged NF- $\kappa$ B activity in I $\kappa$ B- $\alpha$  deficient macrophages is the inability to “turn-off” NF- $\kappa$ B transcriptional activity through the I $\kappa$ B- $\alpha$  negative-feedback loop. This prolonged NF- $\kappa$ B activation could result in continuous production of pro-inflammatory genes leading to enhanced and prolonged inflammation. The mechanism for prolonged NF- $\kappa$ B activity in p50 deficient macrophages is more complicated. As stated above, preliminary experiments suggest p50 is critical for I $\kappa$ B- $\alpha$  resynthesis, thus offering a similar explanation as in I $\kappa$ B- $\alpha$  deficient macrophages. However,

p50 has been shown to effect gene transcription in numerous ways. For example, p50 homodimers have been shown to repress gene transcription. Another explanation for the prolonged NF- $\kappa$ B activity could involve the loss of this inhibitory effect on the transcription of inflammatory genes. Also, in the absence of p50, p65 could form dimers with other Rel family members such as p52, resulting in altered binding kinetics of the promoters of inflammatory genes normally activated in response to LPS or activation of a different set of inflammatory genes. All of these possible mechanisms must be investigated further to understand p50's role in regulating the response of macrophages to LPS.

In conclusion, the following paradigm for the role of NF- $\kappa$ B in regulating lung inflammation is proposed (Figure 49). In the normal host, the alveolar macrophage initiates the inflammatory cascade in response to LPS stimulus through activation of NF- $\kappa$ B and production of pro-inflammatory cytokines (such as TNF- $\alpha$  and IL-1). These cytokines activate the NF- $\kappa$ B pathway in other lung cell types (predominantly epithelium) resulting in production of pro-inflammatory cytokines and chemokines (such as KC and MIP-2) and neutrophil immigration. Resolution of inflammation is achieved through the active turn-off of NF- $\kappa$ B in the macrophage, resulting in NF- $\kappa$ B turn-off in other cell types and a return to normal neutrophil numbers. In a host with altered NF- $\kappa$ B signaling in the macrophage through manipulation of I $\kappa$ B- $\alpha$  or p50, initiation of the inflammatory cascade proceeds as described above. However, after removal of the inflammatory stimulus, macrophages are unable to turn-off NF- $\kappa$ B, resulting in continued production of pro-inflammatory cytokines. Persistent macrophage activation drives the activation of NF- $\kappa$ B in other cell types (epithelium), thus perpetuating the inflammatory cascade. Ultimately, prolonged NF- $\kappa$ B activation in multiple lung cell types leads to an enhanced neutrophilic lung inflammation.

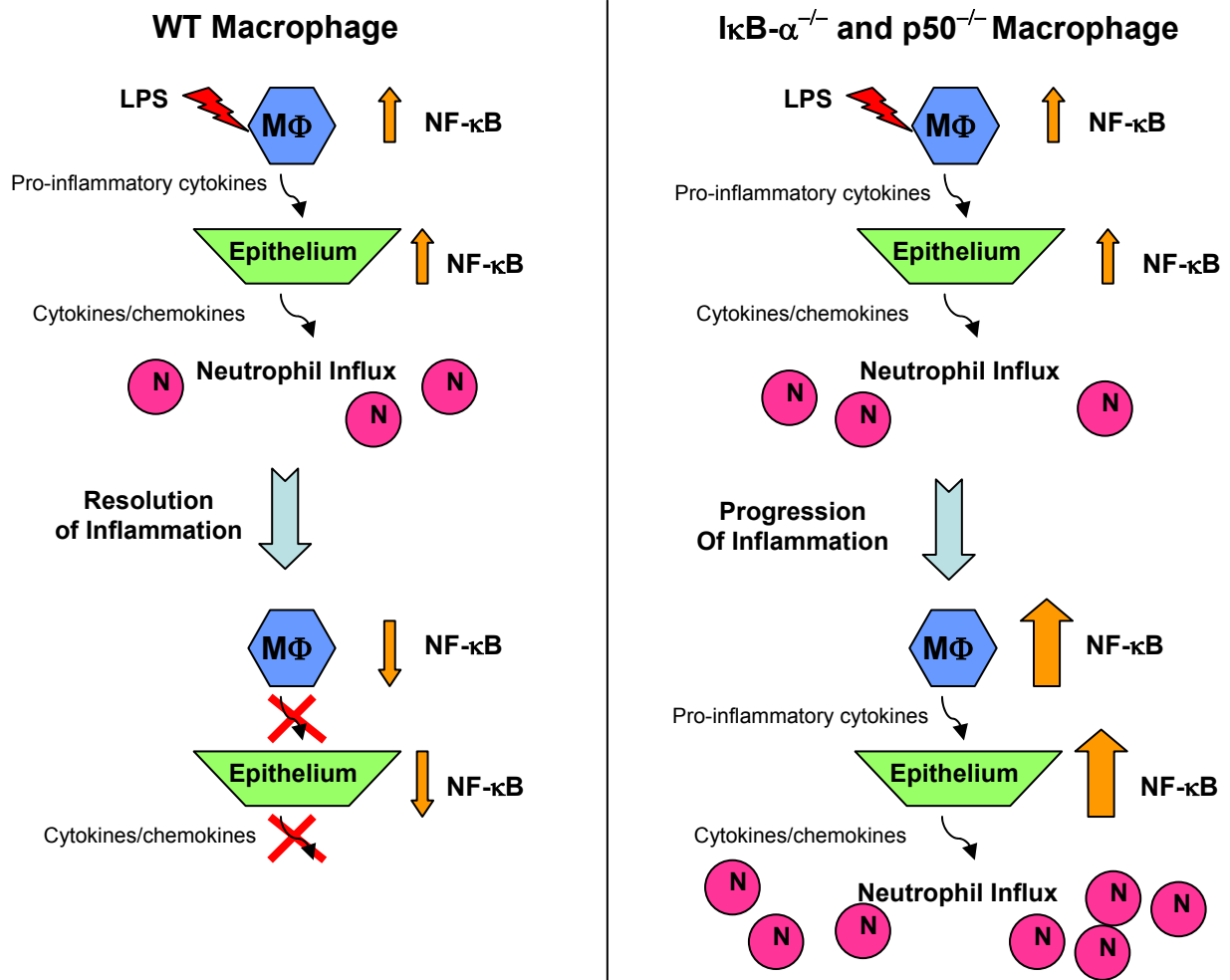


Figure 49

In conclusion, the data presented in this dissertation provide an important contribution to the understanding of the NF- $\kappa$ B signaling pathway in the regulation of inflammation. Elucidating role of NF- $\kappa$ B in specific cell types in the lung is critical for the development of appropriate therapeutic interventions that enhance the innate immune response but limit host derived lung injury. These studies add a new piece to the NF- $\kappa$ B story and will

hopefully lead to further discovery of the role of this important transcription factor family in the regulation of inflammation.

## APPENDIX

### Publications

**Everhart MB**, Han WH, Polosukhin VV, Li B, Yull FE, Sadikot RT, Christman JW, Blackwell TS. Generation of an NF- $\kappa$ B inducible transgenic reporter mouse model utilizing a green fluorescent protein/luciferase dual reporter. In Progress

**Everhart MB**, Han WH, Polosukhin VV, Li B, Yull FE, Christman JW, Blackwell TS. The role of macrophage I $\kappa$ B- $\alpha$  and p50 in the active turn-off of lipopolysaccharide induced lung inflammation. In Progress

**Everhart MB**, Han WH, Parman KS, Polosukhin VV, Li B, Yull FE, Christman JW, Blackwell TS. Intratracheal administration of liposomal clodronate accelerates lung macrophage reconstitution following fetal liver transplantation. Journal of Leukocyte Biology *Accepted February 2005*

Musiek, ES, **Everhart MB**, Milne GL, Wang D, Backlund MG, McLaughlin B, DuBois RN, Blackwell TS, Porta A, Vidari G, Zanoni G, Morrow JD. Cyclopentenone isoprostanes suppress LPS-induced iNOS and COX-2 expression in macrophages via inhibition of NF-kappaB. In Progress

Stathopoulos GT, Zhu Z, **Everhart MB**, Kalomenidis I, Lawson, WE, Bilaceroglu S, Peterson TE, Mitchell D, Yull FE, Light RW, Blackwell TS. Nuclear Factor- $\kappa$ B activation is an indicator of tumor progression in a mouse model of malignant pleural effusion. *Submitted Cancer Research*

Maus UA, Srivastava M, Paton JC, Mack M, **Everhart MB**, Blackwell TS, Christman JW, Schlondorff D, Seeger W, Lohmeyer J. CCR2 positive monocytes recruited to inflamed lungs downregulate local CCL2 chemokine levels. American Journal of Physiology – Lung Cellular and Molecular Physiology *Accepted*

Maus UA, Srivastava M, Paton JC, Mack M, **Everhart MB**, Blackwell TS, Christman JW, Schlondorff D, Seeger W, Lohmeyer J. Pneumolysin-induced lung injury is independent of leukocyte trafficking into the alveolar space. Journal of Immunology 2004 Jul 15;173(2):1307-12

Yull FE, Han W, Jansen ED, **Everhart MB**, Sadikot RT, Christman JW, Blackwell TS. Bioluminescent detection of endotoxin effects on HIV-1 LTR-driven transcription in vivo. Journal of Histochemistry and Cytochemistry 2003 Jun;51(6):741-9

Sadikot RT, Han W, **Everhart MB**, Zoia O, Peebles RS, Jansen ED, Yull FE, Christman JW, Blackwell TS. Selective I kappa B kinase expression in airway epithelium generates neutrophilic lung inflammation. Journal of Immunology 2003 Jan 15;170(2):1091-8.

## REFERENCES

- Alcami, J., Lain de Lera, T., Forgueira, L., Pedraza, M. A., Jacque, J. M., Bachelierie, F., Noriega, A. R., Hay, R. T., Harrich, D., Gaynor, R. B., Virelizier, J. L., Arenzana-Seisdedos, F. (1995). Absolute dependence on kappa-B responsive elements for initiation and Tat-mediated amplification of HIV transcription in blood CD4 T lymphocytes. *EMBO J*, **14**, 1552-1560.
- Alcamo, E., Mizgerd, J. P., Horwitz, B. H., Bronson, R., Beg, A. A., Scott, M., Doerschuck, C. M., Hynes, R. O., Baltimore, D. (2001). Targeted mutation of TNF receptor I rescues the RelA-deficient mouse and reveals a critical role of NF-kB in leukocyte recruitment. *J Immunol*, **167**, 1592-1600.
- Ashburner, B.P., Westerheide, S. D., Baldwin, A. S. (2001). The p65 (RelA) subunit of NF-kB interacts with the histone deacetylase (HDAC) corepressors HDAC1 and HDAC2 to negatively regulate gene expression. *Mol Cell Biol*, **21**, 7065-7077.
- Baek, S.H., Ohgi, K. A., Rose, D. W., Koo, E. H., Glass, C. K., Rosenfeld, M. G. (2002). Exchange of N-CoR corepressor and Tip60 coactivator complexes links gene expression by NF-kappaB and beta-amyloid precursor protein. *Cell*, **110**, 55-67.
- Baeuerle, P.A., Baltimore, D. (1996). NF-kB: ten years later. *Cell*, **87**, 13-20.
- Baldwin, A.S. (2001). The transcription factor NF-kB and human disease. *J Clin Invest*, **107**, 3-6.
- Baltathakis, I., Alcantara, O., Boldt, D. H. (2001). Expression of different NF-kB pathway genes in dendritic cells (DCs) or macrophages assessed by gene expression profiling. *J Cell Biochem*, **83**, 281-290.
- Beg, A.A., Sha, W. C., Bronson, R. T., Baltimore, D. (1995a). Constitutive NF-kB activation, enhanced granulopoiesis, and neonatal lethality in Ikb-alpha deficient mice. *Genes & Develop*, **9**, 2736-2746.
- Beg, A.A., Sha, W. C., Bronson, R. T., Ghosh, S., Baltimore, D. (1995b). Embryonic lethality and liver degeneration in mice lacking the RelA component of NF-kB. *Nature*, **376**, 167-170.
- Benaron, D.A., Contag, P. R., Contag, C. H. (1997). Imaging brain structure and function, infection and gene expression in the body using light. *Philos Trans Royal Soc London Series B-Bio Sciences*, **352**, 755-761.
- Berg, J.T., Lee, S. T., Thepen, T., Lee, C. Y., Tsan, M. F. (1993). Depletion of alveolar macrophages by liposomal-encapsulated dichloromethylene diphosphonate. *J. Appl. Physiol.*, **74**, 2812-2819.

- Berger, S.L. (1999). Gene activation by histone and factor acetyltransferases. *Current Opinion Cell Biol*, **11**, 336-341.
- Blackwell, T.S., Debelak, J. P., Venkatakrishnan, A., Schot, D. J., Harley, D. H., Pinson, C. W., Williams, P., Washington, K., Christman, J. W., Chapman, W. C. (1999a). Acute lung injury after hepatic cryoablation: correlation with NF-kB activation and cytokine production. *Surgery*, **126**, 518-526.
- Blackwell, T.S., Holden, E. P., Blackwell, T. R., Christman, B. W., Christman, J. W. (1996). Activation of NF-kB in rat lungs by treatment with endotoxin: modulation by treatment with N-acetylcysteine. *J Immunol*, **157**, 1630-1637.
- Blackwell, T.S., Lancaster, L. H., Blackwell, T. R., Venkatakrishnan, A., Christman, J. W., (1999b). Chemotactic gradients predict neutrophilic alveolitis in endotoxin treated rats. *Am J Respir Crit Care Med*, **159**, 1644-1652.
- Blackwell, T.S., Lancaster, L. H., Blackwell, T. R., Venkatakrishnan, A., Christman, J. W., (1999c). Differential NF-kB activation after intratracheal endotoxin: correlation with cytokine gene expression and neutrophilic alveolitis. *Am J Physiol Lung Cell Mol Physiol*, **277**, L823-L830.
- Blackwell, T.S., Yull, F. E., Chen, C. L., Venkatakrishnan, A., Blackwell, T. S., Hicks, D. J., Lancaster, L. H., Christman, J. W., Kerr, L. D. (1999d). Use of genetically altered mice to investigate the role of nuclear factor-kappa B activation and cytokine gene expression in sepsis-induced ARDS. *Chest*, **116**, 73S-74S.
- Blackwell, T.S., Yull, F. E., Chen, C. L., Venkatakrishnan, A., Blackwell, T. S., Hicks, D. J., Lancaster, L. H., Christman, J. W., Kerr, L. D. (2000). Multi-organ NF-kB activation in a transgenic mouse model of systemic inflammation. *Am J Respir Crit Care Med*, **162**, 1095-1101.
- Blair, W.S., Bogerd, H. P., Madore, S. J., Cullen, B. R. (1994). Mutational analysis of the transcription activator domain of RelA: identification of a highly synergistic minimal acidic activation module. *Mol Cell Biol*, **14**, 7226-7234.
- Bohrer, H., Qui, F., Zimmerman, T., Zhang, Y., Jilmer, T., Mannel, D., Bottiger, B. W., Stern, D. M., Walder, R., Saeger, H. D., Zeigler, R., Bierhaus, A., Martin, E., Nawroth, P. P. (1997). Role of NF-kB in the mortality of sepsis. *J Clin Invest*, **100**, 972-985.
- Bradford, M.M. (1976). A rapid and sensitive method for the quantification of microgram quantities of protein utilizing the principle of protein-dye binding. *Anal Biochem*, **72**, 248-254.
- Broug-Holub, E., Toews, G., Strieter, R., Kunkel, S., Paine, R., Standiford, T. (1997). Alveolar macrophages are required for protective pulmonary defenses in murine *Klebsiella*

- pneumonia*: elimination of alveolar macrophages increases neutrophil recruitment but decreases bacterial clearance and survival. *Infect Immun*, **65**, 1139-1146.
- Browder, W., Ha, T., Li, C., Kalbfleisch, J. H., Ferguson, D. A., Williams, D. L. (1999). Early detection of pulmonary nuclear factor kB and nuclear factor interleukin-6 in polymicrobial sepsis. *J Trauma: Injury, Infection, and Crit Care*, **46**, 590-596.
- Chan, H.M., La Thangue, N. B. (2001). p300/CBP proteins: HATs for transcriptional bridges and scaffolds. *J Cell Sci*, **114**, 2363-2373.
- Chen, C.L., Singh, N., Yull, F. E., Strayhorn, D., Van Kaer, L., Kerr, L. D. (2000). Lymphocytes lacking I $\kappa$ B- $\alpha$  develop normally, but have elective defects in proliferation and function. *J Immunol*, **165**, 5418-5427.
- Chen, L., Fischle, W., Verdin, E., Greene, W. C. (2001). Duration of nuclear NF- $\kappa$ B action regulated by reversible acetylation. *Science*, **293**, 1653-1657.
- Contag, C.H., Contag, P. R., Mullins, J. L., Spilman, S. D., Stevenson, D. K., Benarson, D. A. (1995). Photonic detection of bacterial pathogens in living hosts. *Molecular Microbiology*, **18**, 593-603.
- Contag, C.H., Contag, P. R., Spilman, S. D., Stevenson, D. K., Benarson, D. A. (1996). Photonic monitoring of infectious diseases and gene regulation. *Biomed Optical Spectros and Diag*, **3**, 220-224.
- Contag, C.H., Jenkins, D., Contag, F. R., Negrin, R. S. (2000). Use of reporter genes for optical measurements of neoplastic disease in vivo. *Neoplasia*, **2**, 41-52.
- Contag, C.H., Spilman, S. D., Contag, P. R., Oshiro, M., Eames, B., Dennery, P. (1997). Visualizing gene expression in living mammals using a bioluminescent reporter. *Photochem and Photobio*, **66**, 523-531.
- Dechend, R., Hirano, F., Lehmann, K., Heissmeyer, V., Ansieau, S., Wulczyn, F. G., Scheidereit, C., Leutz, A. (1999). The Bcl-3 oncoprotein acts as a bridging factor between NF- $\kappa$ B/Rel and nuclear co-regulators. *Oncogene*, **18**, 3316-3323.
- Deryckere, F., Gannon, F. (1994). A one-hour miniprep technique for extraction of DNA binding proteins from animal tissues. *BioTechniques*, **16**, 405.
- Didonato, J.A., Hayakawa, M., Rothwarf, D. M., Zandi, E., Karin, M. (1997). A cytokine-responsive I $\kappa$ B kinase that activates the transcription factor NF- $\kappa$ B. *Nature*, **388**, 548-554.
- Edinger, M., Cao, Y. A., Hornig, Y. S., Jenkins, D. E., Verneris, M. R., Bachmann, M. H. (2002). Advancing animal models of neoplasia through in vivo bioluminescence imaging. *Eur J Cancer*, **38**, 2128-2136.

- Fan, J., Ye, R. D., Malik, A. B. (2001). Transcriptional mechanisms of acute lung injury. *Am J Physiol Lung Cell Mol Physiol*, **281**, L1037-1050.
- Fazio, S., Hasty, A. H., Carter K. J., Murray A. B., Price J. O., Linton, M. F. (1997). Leukocyte low density lipoprotein receptor (LDL-R) does not contribute to LDL clearance in vivo; bone marrow transplantation studies in the mouse. *J. Lipid. Res.*, **38**, 391-400.
- Foo, S.Y., Nolan, G. P. (1999). NF- $\kappa$ B to the rescue - RELs, apoptosis, and cellular transformation. *Trends Genet*, **15**, 229-235.
- Francis, K.P., Joh, D., Bellinger-Kawahara, C., Hawkinson, M. J., Purchio, T. F., Contag, P. R. (2000). Monitoring bioluminescent *Staphylococcus aureus* infections in living mice using a novel luxABCDE construct. *Infect Immun*, **68**, 3594-3600.
- Francis, K.P., Yu, J., Bellinger-Kawahara, C. Joh, D., Hawkinson, M. J., Xiao, G. (2001). Visualizing pneumococcal infections in the lungs of live mice using bioluminescent *Streptococcus pneumoniae* transformed with a novel gram-positive lux transposon. *Infect Immun*, **69**, 3350-3358.
- Franzoso, G., Bours, V., Park, S., Tomita-Yamaguchi, M., Kelly, K., Siebenlist, U. (1992). The candidate oncoprotein Bcl-3 is an antagonist of p50/NF- $\kappa$ B-mediated inhibition. *Nature*, **359**, 339-342.
- Franzoso, G., et al. (1997). Requirement for NF- $\kappa$ B in osteoclast and B-cell development. *Genes & Develop*, **11**, 3482-3496.
- Gerondakis, S., Grumont, R., Rourke, I., Grossmann, M. (1998). The regulation and roles of Rel/NF- $\kappa$ B transcription factors during lymphocyte activation. *Curr Opin Immunol*, **10**, 353-359.
- Gerritsen, M.E., Williams, A. J., Neish, A. S., Moore, S., Shi, Y., Collins, T. (1997). CREB-binding protein/p300 are transcriptional co-activators of p65. *Proc Natl Acad Sci USA*, **94**, 2927-2932.
- Ghosh, S., May, M. J., Kopp, E. B. (1998). NF- $\kappa$ B and Rel proteins: Evolutionarily conserved mediators of immune responses. *Ann Rev Immunol*, **16**, 225-260.
- Haddad, E.B., Salmon, M., Koto, H., Barnes, P. J., Adcock, I., Chung, K. F. (1996). Ozone induction of cytokine-induced neutrophilic chemoattractant (CINC) and nuclear factor- $\kappa$ B in rat lung: inhibition by corticosteroids. *FEBS Letters*, **379**, 265-268.
- Haefner, B. (2002). NF- $\kappa$ B: arresting a major culprit in cancer. *Drug Discov Today*, **7**, 653-663.
- Hayden, M., Ghosh, S. (2004). Signaling to NF- $\kappa$ B. *Genes and Develop*, **18**, 2195-2224.

- Horwitz, B.H., Scott, M. L., Cherry, S. R., Bronson, R. T., Baltimore, D. (1997). Failure of lymphopoiesis after adoptive transfer of NF- $\kappa$ B-deficient fetal liver cells. *Immunity*, **6**, 765.
- Huang, T.T., Kudo, N., Yoshida, M., Miyamoto, S. (2000). A nuclear export signal in the N-terminal regulatory domain of I $\kappa$ B- $\alpha$  controls cytoplasmic localization of inactive NF- $\kappa$ B/I $\kappa$ B- $\alpha$  complexes. *Proc Natl Acad Sci USA*, **97**, 1014-1019.
- Iwasaki, A., Medzhitov, R. (2004). Toll-like receptor control of the adaptive immune responses. *Nature Immunol*, **5**, 987-995.
- Karin, M., Ben-Neriah, Y. (2000). Phosphorylation meets ubiquitination: the control of NF- $\kappa$ B activity. *Ann Rev Immunol*, **18**, 621-663.
- Kennedy, D.W., Abkowitz, J. L. (1997). Kinetics of central nervous system microglial and macrophage engraftment: analysis using transgenic bone marrow transplantation model. *Blood*, **90**, 986-993.
- Kingman, S.M., Kingman, A. J. (1996). The regulation of human immunodeficiency virus type-1 gene expression. *Eur J Biochem*, **240**, 491-507.
- Klement, J.F., Rice, N. R., Car, B. D., Abbondanzo, S. J., Powers, G. D., Bhatt, P. H., Chen, C. H., Rosen, C. A., and Stewart, C. L. (1996). I $\kappa$ B- $\alpha$  deficiency results in a sustained NF- $\kappa$ B response and severe widespread dermatitis in mice. *Mol Cell Biol*, **16**, 2341-2349.
- Koay, M.A., Gao, X., Washington, M. K., Parman, K. S., Sadikot, R. T., Blackwell, T. S., Christman, J. W. (2002). Macrophages are necessary for maximal NF- $\kappa$ B activation in response to endotoxin. *Am J Respir Cell Mol Biol*, **26**, 572-578.
- Kooguchi, K., Hashimoto, S., Kobayashi, A., Kitamura, Y., Kudoh, I., Wiener-kronish, J., Sawa, T. (1998). Role of alveolar macrophages in initiation and regulation of inflammation in *Pseudomonas aeruginosa* pneumonia. *Infection and Immunity*, **66**, 3164-3169.
- Koransky, M.L., Ip, T. K., Wu, S., Cao, Y., Berry, G., Contag, C. (2001). In vivo monitoring of myoblast transplantation into rat myocardium. *J Heart Lung Transplant*, **20**, 188-189.
- Kretzschmar, M., Meisterernst, M., Schneidereit, C., Li, G., Roeder, R. G. (1992). Transcriptional regulation of the HIV-1 promoter by NF- $\kappa$ B in vitro. *Genes and Develop*, **6**, 761-774.
- Lagasse, E., Weissman, I. L. (1996). Flow cytometric identification of murine neutrophils and monocytes. *J Immunol Meth*, **197**, 139-150.

- Lang, R., Rutschman, R. L., Greaves, D. R., Murray, P. J. (2002). Autocrine deactivation of macrophages in transgenic mice constitutively overexpressing IL-10 under control of the human CD68 promoter. *J. Immunol.*, **168**, 3402-3411.
- Lauzurica, P., Martinez, S., Marazuela, M., el Arco, P. G., Martinez, A. C., Sanchez-Madrid, F., Redondo, J. M. (1999). Pyrrolidine dithiocarbamate protects mice from lethal shock induced by LPS and TNF-alpha. *Eur J Immunol*, **29**, 1890-1900.
- Lentsch, A.B., Czewrmak, B. J., Bless, N. M., Van Rooijen, N., Ward, P. A. (1999). Essential role of alveolar macrophages in intrapulmonary activation of NF-kappa B. *Am J Respir Cell Mol Biol*, **20**, 692-698.
- Linton, M.F., Atkison, J. B., Fazio S. (1995). Prevention of atherosclerosis in apolipoprotein E-deficient mice by bone marrow transplantation. *Science*, **267**, 1034-1037.
- Malek, S., Chen, Y., Huxford, T., Ghosh, G., (2001). Ikb-beta, but not Ikb-alpha, functions as a classical cytoplasmic inhibitor of NF-kB dimers by masking both NF-kB nuclear localization sequences in resting cells. *J Biol Chem*, **276**, 45225-45235.
- McManus, K.J., Hendzel, M. J. (2001). CBP, a transcriptional coactivator and acetyltransferase. *Biochem Cell Biol*, **79**, 253-266.
- Mebius, R.E., Miyamoto, T., Christensen, J., Domen, J., Cupedo, T., Weissman, I. L., Akashi, K. (2001). The fetal liver counterpart of adult common lymphoid progenitors gives rise to all lymphoid lineages, CD45<sup>+</sup>CD4<sup>+</sup>CD3<sup>-</sup> cells, as well as macrophages. *J. Immunol.*, **166**, 6593-6601.
- Medzhitov, R., Preston-Hurlburt, P., Janeway, C. A. Jr. (1997). A human homologue of the *Drosophila* Toll protein signals activation of adaptive immunity. *Nature*, **388**, 394-397.
- Mercurio, R., Zhu, H., Murray, B. W., Shevchenko, A., Bennett, B. L., Li, J., Young, D. B., Barbosa, M., Mann, M., Manning, A., Rao, A. (1997). IKK-1 and IKK-2: cytokine-activated Ikb kinases essential for NF-kB activation. *Science*, **278**, 860-866.
- Mizgerd, J.P., Horwitz, B. H., Quillen, H. C., Scott, M. L., Doershuck, C. M. (1999). Effects of CD18 deficiency on the emigration of murine neutrophils during pneumonia. *J. Immunol.*, **163**, 995-999.
- Mizgerd, J.P., Lupu, M. M., Kogan, M. S., Warren, H. B., Kobzik, L., Topulos, G. P. (2003). Nuclear factor-kB p50 limits inflammation and prevents lung injury during *Escherichia coli* pneumonia. *Am J Respir Crit Care Med*, **168**, 810-817.
- Mizgerd, J.P., Peschon, J. J., Doerschuck, C. M. (2000). Roles of tumor necrosis factor receptor signaling during murine *Escherichia coli* pneumonia. *Am J Respir Cell Mol Biol*, **22**, 85-91.

- Mizgerd, J.P., Scott, M. L., Spieker, M. R., Doerschuk, C. M. (2002). Functions of I $\kappa$ B proteins in inflammatory responses to *E. coli* LPS in mouse lungs. *Am J Respir Cell Mol Biol*, **27**, 575-582.
- Muir, A., Soong, G., Sokol, S., Reddy, B., Gomez, M., van Heeckeren, A., Prince, A. (2004). Toll like receptors in normal and cystic fibrosis airway epithelial cells. *Am J Respir Cell Mol Biol*, **30**, 777-783.
- Nabel, G., Baltimore, D. (1987). An inducible transcription factor activates expression of human immunodeficiency virus in T-cells. *Nature*, **326**, 711-713.
- Ono, K., Takii, T., Onozaki, K., Ikawa, M., Okabe, M., Sawada, M. (1999). Migration of exogenous immature hematopoietic cells into adult mouse brain parenchyma under GFP-expressing bone marrow chimera. *Biochem Biophys Res Commun*, **262**, 610-614.
- Poltorak, A., He, X., Smirnova, I., Liu, M. Y., Huffel, C. V. (1998). Defective LPS signaling in C3H/HeJ and C57BL/10ScCr mice: mutation in *Tlr4* gene. *Science*, 2085-2088.
- Regnier, C.H., Song, H. Y., Gao, X., Goeddel, D. V., Cao, Z., Rothe, M. (1997). Identification and characterization of an I $\kappa$ B kinase. *Cell*, **90**, 373-383.
- Rehemtulla, A., Steman, L. D., Cardozo, S. J., Gupta, S., Hall, D. E., Contag, C. H. (2000). Rapid and quantitative assessment of cancer treatment response using in vivo bioluminescence imaging. *Neoplasia*, **2**, 491-495.
- Rocchetta, H.L., Boylan, C. J., Foley, J. W., Iversen, P. W., Letourneau, D. L., McMillan, C. L. (2001). Validation of a noninvasive, real-time imaging technology using bioluminescent *Escherichia coli* in the neutropenic mouse thigh model of infection. *Antimicrobial Agents and Chemotherapy*, **45**, 129-137.
- Rothwarf, D.M., Zandi, E., Natoli, G., Karin, M. (1998). IKK-gamma is an essential regulatory subunit of the I $\kappa$ B kinase complex. *Nature*, **395**, 297-300.
- Royo, C., Touraine, J. L., Veyron, P., Aitouche, A. (1987). Survey of experimental data on fetal liver transplantation. *Thymus*, **10**, 5-12.
- Saccini, S., Pantano, S., Natoli, G. (2001). Two waves of nuclear factor  $\kappa$ B recruitment to target promoters. *J Exp Med*, **193**, 1351-1359.
- Schmitz, M.L., Steizer, G., Altmann, H., Meisterernst, M., Baeuerle, P. A. (1995). Interaction of the COOH-terminal transactivation domain of p65 NF- $\kappa$ B with TATA-binding protein, transcription factor IIB, and coactivators. *J Biol Chem*, **270**, 7219-7226.
- Sen, R., Baltimore, D. (1986). Multiple nuclear factors interact with the immunoglobulin enhancer sequences. *Cell*, **46**, 705-716.

- Sha, W.C., Liou, H., Toumanen, E. I., Baltimore, D. (1995). Targeted disruption of the p50 subunit of NF-kB leads to multifocal defects in immune responses. *Cell*, **80**, 321-330.
- Shenkar, R., Schwartz, M. D., Terada, L. S., Repine, J. E., McCord, J., Abraham, E. (1996). Hemorrhage activates NF-kappa B in murine lung mononuclear cells *in vivo*. *Am J Physiol Lung Cell Mol Physiol*, **14**, L729-L735.
- Sheppard, K.A., Rose, D. W., Hague, Z. K., Kurokawa, R., McInerney, E., Westin, S., Thanos, D., Rosenfeld, M. G., Glass, C. K., Collins, T. (1999). Transcriptional activation by NF-kB requires multiple coactivators. *Mol Cell Biol*, **19**, 6367-6378.
- Siebenlist, U., Franzoso, G., Brown, K. (1994). Structure, regulation and function of NF-kB. *Ann Rev Cell Biol*, **10**, 405-455.
- Takeda, K., Akira, S. (2004). TLR signaling pathways. *Sem in Immunol*, **16**, 3-9.
- Tang, Y., Shah, K., Messerli, S. M., Snyder, E., Breakefield, X., Weissleder, R. (2003). In vivo tracking of neural progenitor cell migration to glioblastomas. *Human Gene Therapy*, **14**, 1247-1254.
- Turpin, P., Hay, R. T., Dargemont, C. (1999). Characterization of Ikb-alpha nuclear import pathway. *J Biol Chem*, **274**, 6804-6812.
- van Rooijen, N., Sanders, A. (1994a). Liposome mediated depletion of macrophages: mechanism of action, preparation of liposomes and applications. *J Immunol Meth*, **174**, 83-93.
- van Rooijen, N., Sanders, A. (1994b). Liposome mediated depletion of macrophages: mechanism of action, preparation of liposomes and applications. *J. Immunol. Methods.*, **174**, 83-93.
- Vanden Berghe, W., Bosscher, K. D., Boone, E., Plaisance, S., Maegeman, G. (1999). The nuclear factor-kB engages CBP/p300 and histone acetyltransferase activity for transcriptional activation of the interleukin-6 gene promoter. *J Biol Chem*, **274**, 32091-32098.
- Verma, I.M., Stevenson, J. K., Schwarz, E. M., Van Antwerp, D., Miyamoto, S. (1995). Rel/NF-kB/IkB family: intimate tales of association and dissociation. *Genes & Develop*, **9**, 2723-2735.
- Wadgaonkar, R., Phelps, K. M., Hague, Z., Williams, A. J., Silverman, E. S., Collins, T. (1999). CREB-binding protein is a nuclear integrator of nuclear factor-kB and p53 signaling. *J Biol Chem*, **274**, 1879-1882.
- Wang, D., Baldwin, A. S. (1998). Activation of nuclear factor-kB-dependent transcription by tumor necrosis factor-alpha is mediated through phosphorylation of RelA/p65 on serine 529. *J Biol Chem*, **273**, 29411-29416.

- Yull, F.E., Han, W., Jansen, E. D., Everhart, M. B., Sadikot, R. T., Christman, J. W., Blackwell, T. S. (2003). Bioluminescent detection of endotoxin effects on HIV-1 LTR-driven transcription in vivo. *J Histochem Cytochem*, **51**, 741-749.
- Zandi, E., Rothwarf, D. M., Delhase, M., Hayakawa, M., Karin, M. (1997). The I $\kappa$ B kinase complex (IKK) contains two kinase subunits, IKK-alpha and IKK-beta, necessary for I $\kappa$ B phosphorylation and NF-kB activation. *Cell*, **91**, 243-252.
- Zhong, H., May, M. J., Jimi, E., Ghosh, S. (2002). The phosphorylation status of nuclear NF-kappa B determines its association with CBP/p300 or HDAC-1. *Mol Cell*, **9**, 625-636.
- Zhong, H., Voll, R. E., Ghosh, S. (1998). Phosphorylation of NF-kB p65 by PKA stimulates transcriptional activity by promoting a novel bivalent interaction with the coactivator CBP/p300. *Mol Cell*, **1**, 661-667.